THESIS FOR THE DEGREE OF DOCTOR OF PHILOSOPHY

# Electric Grid Resilience

*Possibility of households and buildings to contribute to a resilient network*

Sindhu Kanya Nalini Ramakrishna

Department of Electrical Engineering
Chalmers University of Technology
Gothenburg, Sweden, 2025

**Electric Grid Resilience**

*Possibility of households and buildings to contribute to a resilient network*

Sindhu Kanya Nalini Ramakrishna
ISBN 978-91-8103-341-0

Acknowledgements, dedications, and similar personal statements in this thesis, reflect the author's own views.



Doktorsavhandlingar vid Chalmers tekniska högskola
Ny serie nr 5798
ISSN 0346-718X

Department of Electrical Engineering
Chalmers University of Technology
SE-412 96 Gothenburg, Sweden
Phone: +46 (0)31 772 1000

Cover:
Single family houses equipped with heat pumps helping to balance the electricity grid during power shortages

Printed by Chalmers Digital Printing
Gothenburg, Sweden, December 2025

*"Greatest glory lies not in never falling,*
*but in rising after every fall."*

***-Confucius***

---

*To everyone who has wished me well and believed in me. Your kindness and encouragement have been the quiet force behind my journey so far.*

**Electric Grid Resilience**

*Possibility of households and buildings to contribute to a resilient network*

Sindhu Kanya Nalini Ramakrishna
Department of Electrical Engineering
Chalmers University of Technology

# Abstract

To reinforce resilience in power systems during severe power shortage conditions, the flexibility of heat pump-equipped heating systems in single-family houses is quantified. To quantify this potential, physics-based models involving a heat pump with space and water heating systems are developed.

The Swedish power system with a maximum consumption of 20-25 GW is used as a reference case. Houses built after the 1960s in southern Sweden, representing 54% of the total single-family houses, are considered. The flexibility levels found range between 2.1 and 0.5 GW, for outdoor temperatures varying between -10°C and 10°C, respectively. These estimates are independent of the degree of thermal compromise. However, the duration for which the above flexibility can be provided is dependent on the degree of thermal compromise. An example result shows that the power system could be relieved of 2.1 GW for 5 hours and 0.8 GW as long as flexibility is required, at -10°C outside temperature, with the consequence that indoor and water temperatures reduce to 15°C and 44°C, from 20°C and 55°C, respectively.

A modified Nordic-32 bus system with a high share of renewable power installations is proposed. Here, the role of flexibility in limiting the instantaneous frequency deviation during the loss of a major generation is demonstrated.

Thus, the flexibility of heating systems from a group of houses has the potential to reinforce resilience in a large-scale power grid from seconds to several hours.

The rebound effect of using flexibility has large negative cold load pick-up effects while restoring indoor temperatures to normal conditions. Hence, an adaptive heat pump controller design is proposed to limit this effect. At -5°C outdoor temperature, approximately 1.9 GW is found to maintain indoor temperatures at 20°C, in 44% of the houses. The power system could be relieved of 1.9 GW for 7 hours and 650 MW for the next 10 hours, with

the consequence that the indoor temperatures drop to 15°C. During indoor temperature recovery to 20°C, over 20 hours using the proposed controller, the peak rebound power was found to be limited to 2.6 GW compared to 3.9 GW using the standard controller.

**Keywords**: heat pumps, flexibility, space heating, water heating, multi-room house, rebound power, cold load pick-up effects

# List of Publications

This thesis is based on the following publications.

[I] **S. K. Nalini Ramakrishna**, T. Thiringer, C. Markusson, "Quantification of electrical load flexibility offered by an air to water heat pump equipped single-family residential building in Sweden," in $14^{th}$ *IEA, Heat pump conference,2023.*

[II] **S. K. Nalini Ramakrishna**, T. Thiringer, "Domestic hot water heat pump: Modelling, analysis and flexibility assessment," $15^{th}$ *Asia-Pacific Power and Energy Engineering Conference (APPEEC), Chiang Mai, Thailand, 2023*, pp. 1-5, doi: 10.1109/APPEEC57400.2023.10562015.

[III] **S. K. Nalini Ramakrishna**, H. Björner Brauer, T. Thiringer, M. Håkansson, "Social and technical potential of single family houses in increasing the resilience of the power grid during severe disturbances," *Energy Conversion and Management*, vol. 321, p.119077, ISSN 0196-8904.

[IV] **S. K. Nalini Ramakrishna**, T. Thiringer, P. Chen, "Potential of single family houses to reinforce resilience in a large scale power system during severe power deficit conditions," *Submitted for second-round review, Energy Conversion and Management: X, 2025.*

[V] **S. K. Nalini Ramakrishna**, T. Thiringer, P. Chen, "Power system resilience support from heat-pump equipped houses – thermal comfort consequence for various room priority strategies" *Energy Conversion and Management: X*, Volume 29, 2026, 101436, ISSN 2590-1745.

[VI] **S. K. Nalini Ramakrishna**, T. Thiringer, P. Chen, "Limiting the rebound effects when utilising flexibility from heat pumps using an adaptive heat pump controller," *Accepted, Energy Conversion and Management, 2025.*

## Authorship Contributions

[I] Sindhu Kanya Nalini Ramakrishna : Conceptualisation, literature review, scoping, methodology, simulation, investigation, formal analysis, visualisation, writing, and manuscript management. Torbjörn Thiringer: Conceptualisation, funding acquisition, supervision, and writing-review and editing. Caroline Markusson: Co-supervision.

[II] Sindhu Kanya Nalini Ramakrishna : Conceptualisation, literature review, scoping, methodology, simulation, investigation, formal analysis, visualisation, writing, and manuscript management. Torbjörn Thiringer: Conceptualisation, funding acquisition, supervision, and writing-review and editing.

[III] Sindhu Kanya Nalini Ramakrishna : Conceptualisation, literature review (Engineering science), scoping, methodology, simulation, investigation, formal analysis, visualisation, writing, and manuscript management. Hanna Brauer Björner : Conceptualisation, literature review (social science), scoping, methodology, interviews, and writing. Torbjörn Thiringer: Conceptualisation, funding acquisition, supervision, and writing-review and editing. Maria Håkansson: Conceptualisation, supervision, and writing- review and editing.

[IV] Sindhu Kanya Nalini Ramakrishna : Conceptualisation, literature review, scoping, methodology, simulation, investigation, formal analysis, visualisation, writing, and manuscript management. Torbjörn Thiringer: Conceptualisation, funding acquisition, supervision, and writing-review and editing. Peiyuan Chen: Co-supervision, writing-review and editing.

[V] Sindhu Kanya Nalini Ramakrishna : Conceptualisation, literature review, scoping, methodology, simulation, investigation, formal analysis, visualisation, writing, and manuscript management. Torbjörn Thiringer: Conceptualisation, funding acquisition, supervision, and writing- review and editing. Peiyuan Chen: Co-supervision, writing-review and editing.

[VI] Sindhu Kanya Nalini Ramakrishna : Conceptualisation, literature review, scoping, methodology, simulation, investigation, formal analysis, visualisation, writing, and manuscript management. Torbjörn Thiringer: Conceptualisation, funding acquisition, Supervision, and writing- review and editing. Peiyuan Chen: Co-supervision, writing-review and editing.

# Acknowledgments

This PhD work is the result of an enriching and rewarding journey of 5 years. I take this opportunity to express my gratitude for the support received from many people during this journey.

First of all, I would like to thank my main supervisor Torbjörn Thiringer for providing me the opportunity to pursue this PhD. Torbjörn thanks for guiding and, most importantly, for always believing and supporting me during the challenging times. Many thanks for creating a friendly and safe environment in which I could freely express my thoughts. Your wisdom has helped me grow both personally and professionally.

Thanks to my co-supervisor Peiyuan Chen for lightening challenging situations with humour and for the constant encouragement. I would also like to thank Maria Håkansson, from RISE (Research Institutes of Sweden) for always being warm and friendly during project meetings.

I also take a moment to thank the members of the reference group involved in this PhD project. Special thanks to Anders Mannikoff from Herrljunga Elektriska AB for sharing the operational data of the heat pump. Many thanks to Caroline Haglund Stignor from RISE for dedicating extra time to answer my questions on heat pumps and for the valuable feedback.

I also thank Huijuan Chen from RISE for sharing the data related to buildings and also for answering my questions regarding modelling the buildings.

Special thanks to Forskarskola Energisystem (FoES) and the Swedish Energy Agency for funding and supporting this project. It has been a pleasure to get to know my fellow PhD students from FoES and to share experiences during various meetings. So thanks to Sairam, Celeste, Emma, Janneke, Alexandra, Charlotte, Emily, and Hanna. Alexandra, thank you for taking the time to share your experience in modelling heat pumps during the early days of my PhD journey and for being inclusive.

I thank all my colleagues at the division of Electric Power Engineering for providing a good working environment. Tatiana, it was great to collaborate with you. Kristoffer thank you for the interesting discussions on heating systems. Meng-Ju, Lluc, and Daniel thank you for all the friendly interactions. Amir, Kavian, Surya, I had a good time with you while teaching various courses. Dimitrios and Chetan, it was fun playing darts and chatting during various after-works. Reza and Maryam, thanks for being the go to colleagues to get insights about publications. Vaishnavi, Moon Moon, Anant, Vineetha,

Lin, Peng Peng, Vidusala, Araavind, Sankar, Ritambhara, Mebtu, Ruonan, Wentao, thank you for creating a jovial environment during lunch.

Qixuan, thank you for being a good friend and for the gifts during your various visits to different places. Meryem, thank you for being the friend in need. It was interesting to get to know the Moroccan culture and the delicious Moroccan desserts.

To Prateebha, thanks for cooking South Indian food. I enjoyed the long walks along with some interesting conversations and your insights on research. It was a pleasure to get to know you.

Last but not least, thanks to my family. I would like to thank my father-in-law and mother-in-law, Chayya and Srinidhi, for being supportive. Shruthi, Shilpa, Srivatsa, Dakshayani, and Avani, it is always a lot of fun to spend time with you and thanks for always encouraging me. Dakshayani, as you said before, I did not forget to include you !!

I would like to thank my grandmother and my parents for always believing in me. To my grandmother, Ajji, I cannot thank you enough for taking care of me and for many wonderful trips. The three of you have always stood by me during the various walks of my life. I am very grateful for everything you have given me. The latest addition to this list is my husband. Srikanth, thanks for supporting, tolerating, and keeping me grounded during various ups and downs in our life. Thanks for actively listening and giving suggestions to improve both professionally and personally. You are the best friend I could ever ask for.

# Nomenclature

| | |
|---|---|
| $A_{ext}$ | External surface area of the building envelope $\left(\mathrm{m}^2\right)$ |
| $A_{floor}$ | Heated floor area $\left(\mathrm{m}^2\right)$ |
| $A_x$ | Area of the building's component $\left(\mathrm{m}^2\right)$ where $x \in \{\text{external walls}, \text{roof}, \text{internal walls}, \text{floor}\}$ |
| $C_{air}$ | Thermal mass of the indoor air and furnishings $\left(\frac{\mathrm{J}}{\mathrm{K}}\right)$ |
| $C_{ext}$ | Thermal mass of a room's external envelope $\left(\frac{\mathrm{J}}{\mathrm{K}}\right)$ |
| $C_{floor}$ | Thermal mass of a room's floor $\left(\frac{\mathrm{J}}{\mathrm{K}}\right)$ |
| $C_{int\ wall}$ | Thermal mass of a room's internal walls $\left(\frac{\mathrm{J}}{\mathrm{K}}\right)$ |
| $C_{overall}$ | Overall thermal capacitance of a house $\left(\frac{\mathrm{J}}{\mathrm{K}}\right)$ |
| $C_{p,air}$ | Specific heat capacity of air $\left(\frac{\mathrm{J}}{\mathrm{KgK}}\right)$ |
| $C_{p,\mathrm{water}}$ | Specific heat capacity of water $\left(\frac{\mathrm{J}}{\mathrm{KgK}}\right)$ |
| $C_{pi}$ | Specific heat capacity of the construction material 'i' in each building component $\left(\frac{\mathrm{J}}{\mathrm{kgK}}\right)$ |
| $C_{tank}$ | Thermal mass of the water in the water tank $\left(\frac{\mathrm{J}}{\mathrm{K}}\right)$ |
| $G_i$ | Thermal conductivity of the construction material 'i' in each building component $\left(\frac{\mathrm{W}}{\mathrm{m}^\circ\mathrm{C}}\right)$ |
| $N_{comp}$ | Compressor speed (Hz) |
| $P_{comp}$ | Electric power consumed by the compressor (W) |
| $Q_{cond,Li}$ | Heat transfer due to conduction in the layer 'Li' of the water tank (W) |
| $Q_{flow,Li}$ | Heat transfer due to water extraction in the layer 'Li' of the water tank (W) |
| $Q_{heat}$ | Actual value of the heat delivered considering the limitations in the heat emitters and the heat pump (W) |
| ${Q_{heat}}^*$ | Reference value of the heat considering limitations in heat emitters (W) |
| ${Q_{heat}}^{**}$ | Reference value of the desired heat (W) |
| $Q_{heat,\ watercoil}$ | Heat delivered by the hot water coil (W) |

| | |
|---|---|
| $Q_{heat,Zp}$ | Actual value of the heat delivered considering the limitations in the heat emitters and the heat pump in zone 'Zp' (W) |
| $Q_{heat,Zp}{}^{*}$ | Reference value of the heat considering limitations in heat emitters in Zone 'Zp' (W). |
| $Q_{heat,Zp}{}^{**}$ | Reference value of the desired heat in zone 'Zp' (W) |
| $Q_{inv,Li}$ | Heat transfer due to temperature inversion in the layer 'Li' of the water tank (W) |
| $Q_{inv,gain}$ | Heat gain due to inversion mixing (W) |
| $Q_{inv,loss}$ | Heat loss due to inversion mixing (W) |
| $Q_{rad}$ | Heat delivered by the radiators (W) |
| $Q_{room,Li}$ | Heat transfer to the room from the layer 'Li' of the water tank (W) |
| $Q_{std}$ | Heat delivered by the radiators at standard conditions (W) |
| $Q_{Withdrawl}$ | Heat loss in the water tank due to water withdrawal (W) |
| $R_{air,ext}$ | Thermal resistance due to convection and radiation from a room's external wall's surface exposed to outdoor ambient air $\left(\frac{^{\circ}\mathrm{C}}{\mathrm{W}}\right)$ |
| $R_{ext}$ | Thermal resistance of a room's external envelope $\left(\frac{^{\circ}\mathrm{C}}{\mathrm{W}}\right)$ |
| $R_{ext\ air,in}$ | Thermal resistance due to convection and radiation from a room's external wall's surface exposed to indoor air $\left(\frac{^{\circ}\mathrm{C}}{\mathrm{W}}\right)$ |
| $R_{floor}$ | Thermal resistance of a room's floor $\left(\frac{^{\circ}\mathrm{C}}{\mathrm{W}}\right)$ |
| $R_{floor\ air,in}$ | Thermal resistance due to convection and radiation from a room's floor surface $\left(\frac{^{\circ}\mathrm{C}}{\mathrm{W}}\right)$ |
| $R_{int\ wall}$ | Thermal resistance of a room's internal wall $\left(\frac{^{\circ}\mathrm{C}}{\mathrm{W}}\right)$ |
| $R_{int\ wall\ air,\ in}$ | Thermal resistance due to convection and radiation from a room's internal wall's surface $\left(\frac{^{\circ}\mathrm{C}}{\mathrm{W}}\right)$ |
| $R_{overall}$ | Overall thermal resistance of a house $\left(\frac{^{\circ}\mathrm{C}}{\mathrm{W}}\right)$ |

| | |
|---|---|
| $R_{ventilation,infiltration}$ | Thermal resistance to infiltration, sanitary ventilation accounting for, heat recovery from a heat recovery unit $\left(\frac{^{\circ}\mathrm{C}}{\mathrm{W}}\right)$ |
| $R_x$ | Thermal resistance of the building's components $\left(\frac{^{\circ}\mathrm{C}}{\mathrm{W}}\right)$ where $x \in \{\text{external walls}, \text{roof}, \text{internal walls}, \text{floor}\}$ |
| $t_i$ | Thickness of the construction material 'i' in each building component (m) |
| $T_{amb}$ | Outdoor ambient temperature (°C) |
| $T_c$ | Temperature of the condenser (°F) |
| $T_{cond}{}^*$ | Estimated condenser temperature (°C) |
| $T_e$ | Temperature of the evaporator (°F) |
| $T_{in}$ | Temperature of the cold water at the inlet of the water tank (°C) |
| $T_{inj}$ | Temperature in the vapour injection line (°F) |
| $T_{Li}$ | Temperature of the water in the layer 'Li' of the water tank (°C) |
| $T_{return}$ | Water return temperature (°C) |
| $T_{room}$ | Room temperature (°C) |
| $T_{room}{}^*$ | Reference value of room temperature (°C) |
| $T_{room,Zp}$ | Room temperature in zone 'Zp' (°C). |
| $T_{room,Zp}{}^*$ | Reference room temperature in zone 'Zp' (°C) |
| $T_{source}$ | Source temperature of the heat pump (°C) |
| $T_{supply}$ | Water supply temperature (°C) |
| $\hat{T}_{return}*$ | Estimated value of return temperature after delivering required heat (°C) |
| $\hat{T}_{supply}*$ | Estimated value of the desired supply temperature in the heat emitters (°C) |
| $\hat{T}_{supply,max\ heat}*$ | Estimate of supply temperature for delivering maximum heat considering limitations in radiators and the heat pump (°C) |
| $\hat{T}_{supply,rad}*$ | Estimated value of supply temperature desired in the radiators (°C) |
| $T_{water,average}$ | Average water temperature in the location where the hot water coil is placed inside the domestic hot water tank (°C) |

| | |
|---|---|
| $T_{water,Li}$ | Water temperature in the layer 'Li' where the sensor is placed in the domestic hot water tank (°C) |
| ${T_{water}}^*$ | Reference value of water temperature (°C) |
| $U_{Li}$ | Heat conduction coefficient of the tank in each layer of water in the domestic hot water tank $\left(\frac{\mathrm{W}}{^\circ\mathrm{C}}\right)$ |
| $U_{overall}$ | Total heat transfer coefficient of a house $\left(\frac{\mathrm{W}}{^\circ\mathrm{C}}\right)$ |
| $U_{value}$ | Average heat transfer coefficient of a house's envelope per heated floor $\left(\frac{\mathrm{W}}{\mathrm{m}^2\ ^\circ\mathrm{C}}\right)$ |
| $U_{vent,infil}$ | The heat transfer coefficient due to infiltration, sanitary ventilation accounting for, heat recovery from a heat recovery unit $\left(\frac{\mathrm{W}}{^\circ\mathrm{C}}\right)$ |
| $UA_{water\ coil}$ | Heat transfer coefficient of the hot water coil $\left(\frac{\mathrm{W}}{^\circ\mathrm{C}}\right)$ |
| $V_{dis}$ | Compressor displacement volume $\left(\frac{cc}{rev}\right)$ |
| $V_{infil}$ | Air infiltration rate $\left(\frac{\mathrm{l}}{\mathrm{s\ m^2}}\right)$ |
| $V_{room}$ | Volume of air in the room $\left(\mathrm{m}^3\right)$ |
| $V_{vent}$ | Sanitary ventilation rate $\left(\frac{\mathrm{l}}{\mathrm{s\ m^2}}\right)$ |
| $\dot{m}$ | Refrigerant's mass flow rate in the evaporator $\left(\frac{\mathrm{Kg}}{\mathrm{s}}\right)$ |
| $\dot{m}_{inj}$ | Refrigerant's mass flow rate of injected vapour $\left(\frac{\mathrm{Kg}}{\mathrm{s}}\right)$ |
| $\dot{m}_{water}$ | Mass flow rate of the water being extracted $\left(\frac{\mathrm{Kg}}{\mathrm{s}}\right)$ |
| $\Delta T_{std}$ | Temperature difference between the radiators and the indoor temperature at standard conditions (°C) |
| $\eta_{isent}$ | Isentropic efficiency of the compressor |
| $\eta_{vent}$ | Efficiency of the heat recovery unit |
| $\eta_{vol}$ | Volumetric efficiency of the compressor |
| $h_p$ | Enthalpy of the refrigerant at a given state 'p' |
| $m_{Li}$ | Mass of the water in the layer 'Li' of the water tank (Kg) |
| $n$ | Exponent characteristic of the radiators (W) |
| $\rho_{air}$ | Air density $\left(\frac{\mathrm{Kg}}{\mathrm{m}^3}\right)$ |
| $\rho_i$ | Density of the construction material 'i' in each building component $\left(\frac{\mathrm{Kg}}{\mathrm{m}^3}\right)$ |
| $\rho_s$ | Density of the refrigerant at suction $\left(\frac{\mathrm{Kg}}{\mathrm{m}^3}\right)$ |

# Contents

# CHAPTER 1

# Introduction

## 1.1 Background

In order to reduce greenhouse gas emissions, conventional fossil fuel-based power plants are today being replaced by renewable power plants. In addition, electricity demand is increasing due to the electrification of the industrial and transportation sectors. Hence, to meet this growing demand for clean energy, the share of renewable power installations is continuously increasing. Consequently, a future renewable-dominated power system would mainly consist of hydro, wind, and solar power installations. And, with hydro being a limited resource, the share of non-dispatchable production originally from wind and solar power will be increasing.

Currently, the power system is being digitalised. Although digitalisation of the power system has significant advantages, it also increases the risk of cyber attacks. Furthermore, since solar and wind power plants will most likely dominate the power system, the variability and uncertainty in electricity supply will increase. Even in areas with geographical possibilities, the amount of controllable power from hydroelectric power plants may be limited by operational constraints [1]. Consequently, threats to the power system are increasing, as

envisioned by the International Energy Agency [2].

In northern European countries, winter represents a critical period for the power system as it is sometimes operated close to its limits. Colder weather conditions coupled with a loss of a major power plant or cyber attacks on the control system of power plants and transmission systems could lead to severe power deficit conditions [3]. During such a scenario, the lack of preparedness for a major power crisis can lead to blackouts, an example being the Texas power outage in 2021 [4].

To prevent the collapse of the power system during such power deficit situations, the available electric power could have to be rationed in Sweden [5]. In such a scenario, identifying the loads with the highest electric power consumption, as well as the loads that could contribute to resilience, would be a key knowledge for the network operators to take appropriate actions to manage such dramatic power-deficit situations.

In Sweden, the residential and service sector accounts for the highest total energy use and electric energy consumption [6]. In the residential sector, the total consumption of electric energy in single-family houses is approximately 4.5 times higher compared to multifamily buildings [7]. Approximately 1.3 million out of 2 million single-family houses use electricity for heating [8] and the majority of them are equipped with heat pumps [9]. In these houses, about 50% of the total electricity use is attributed to space heating and water heating [10]. In addition, energy efficiency measures are an important ongoing process with a significant impact on the power system. Hence, traditional fixed speed heat pumps are being replaced with new variable speed heat pumps, which have high controllability. Thus, a group of single-family houses equipped with variable speed heat pumps could serve as valuable flexible resources to reduce the electric power consumption during severe power deficit conditions. The consequence of this action is a drop in thermal comfort. Of course, this resource could also be used for traditional demand-side management.

However, using the flexibility of heating systems equipped with heat pumps to support the grid in severe power deficit conditions will have rebound effects [11], while restoring thermal comfort. Reference [12] confirms that participation of thermostatically controlled loads (TCL) in dynamic pricing schemes leads to cold load pickup effects (CLPU). These effects are typically witnessed during network restoration after extended periods of outages. CLPU is a phenomenon where loads, typically related to heating, need to consume a power

higher than the steady-state consumption level [13]. Thus, heat pumps after providing flexibility during thermal comfort restoration have significant CLPU effects.

This means that quantifying this flexibility potential with associated rebound effects, during various operating conditions, would be a very valuable information for network operators to make informed decisions during severe power deficit conditions.

#### Heating system equipped with heat pumps in single-family houses

In Swedish single-family houses, the heat pump typically provides both space and water heating. The representation of this heating system is shown in Figure 1.1. The heat delivered is used to heat water, which in turn is used for either space or water heating, with a priority set for the latter. If the heat delivered is insufficient to provide space heating, additional heating will be provided by the electric heater built in the heat pump. In addition, for water heating, additional heating is sometimes provided by the electric heater inside the water tank.

## 1.2 Aim

With this background, the main aim of this thesis is to quantify the load reduction potential when using the flexibility of space and water heating systems equipped with variable speed heat pumps, under various operating conditions. Secondly, the aim is to reduce the rebound effects of using the flexibility of heating systems equipped with heat pumps while restoring thermal comfort. Thirdly, to quantify the thermal comfort impact in relation to the electric power savings.

## 1.3 Previous work

To address the stated goals, in this section, a brief review of previous work is presented.

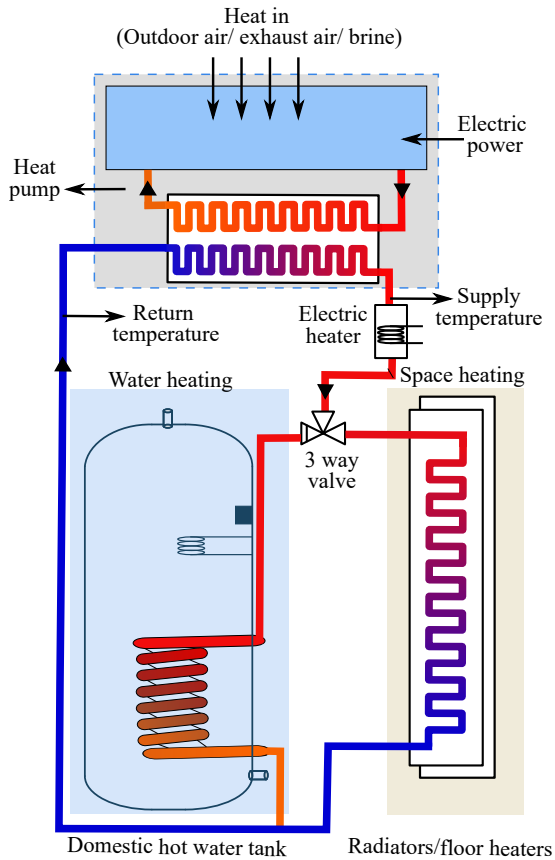


**Figure 1.1:** Heating system in typical Swedish single-family houses.

## Modelling of heat pumps in flexibility studies

A review of the modelling of heat pumps is undertaken in flexibility studies. Typically, the coefficient of performance (COP) is a key parameter used in the literature to estimate the electric power consumption of heat pumps.

The frequency reserve services offered by variable speed hydronic[1] heat pumps in commercial buildings are investigated in [14]. [15] involves experimental study of demand response from electric and heat pump water heaters. In articles [14], [15], it is assumed that COP is a constant value. Consequently, the flexibility potential cannot be adequately estimated as the COP changes under different operating conditions.

The coordination of small- and large-scale variable speed heat pumps to provide primary frequency support is dealt with in [16]. Furthermore, the dynamic frequency response of domestic fixed speed heat pumps, dedicated for space heating, is studied in [17]. In [16], [17], the on-off operation of the heat pumps is considered and the electric power consumption of the heat pumps is constant. Consequently, the flexibility potential cannot be adequately estimated as electric power consumption changes under different operating conditions.

[18] deals with demand response by aggregating fixed speed domestic hydronic heat pumps. Here, COP is modelled based on the operation data. [19] assess domestic fixed speed air source heat pumps as flexible loads, considering a buffer tank in addition to a domestic hot water tank. [20] involves quantifying flexibility in residential buildings, equipped with heat pumps, considering significant wind penetration. In articles [19], [20], explicit mathematical models of COP or the heat pump to estimate the electricity consumption under various operating conditions are missing.

To provide demand response, the optimal control of solar photovoltaic, fixed speed air source heat pumps, thermal energy storage, and electric vehicles in residential buildings, is dealt with in [21]. [22] deals with the flexibility assessment of a residential heat pump pool with air and ground source heat pumps. Separate tanks and separate heat pumps are used for space and water heating in [22] and [21], respectively. Here, COP of heat pumps is obtained using an empirical formula based on the source and sink temperatures of heat pumps. The space and water heating setups do not represent the typical setup in Swedish single-family houses, where a single heat pump is used for both

[1] water based heating

space and water heating, with no storage tank for space heating.

[23] deals with the participation of variable speed heat pump systems and electric vehicles, to provide flexibility in the electricity markets. In [23], the COP model is a function of outdoor and indoor temperatures. [24] deals with demand response from air to water heat pumps and electric vehicles, with the heat pumps exclusively dedicated to water heating. Here, the COP of the heat pump is obtained from an empirical formula involving atmospheric temperature. In articles [23], [24], the empirical expressions that are used to model COP are system-specific.

[25] deals with primary frequency control in a microgrid using air conditioners, electric water heaters, and ground source heat pumps, dedicated solely for space heating. Here, COP is obtained by empirical fitting. [26] and [27] deals with the use of a pool of domestic variable speed air to water heat pumps to reduce peak electricity use. Here, COPs are modelled based on performance maps provided by the manufacturer in one case and an empirical formula involving outdoor ambient air temperature and supply water temperature in a latter case. In articles [25]–[27], the empirical expressions that are used to model COP are system-specific.

[28] deals with the improvement of energy flexibility in residential buildings using variable speed air source heat pumps, typically used in Swedish single-family houses. Here, COP is modelled as a black box based on the experimental results and performance maps of heat pumps. Articles [29],[30] deal with grid frequency regulation through a variable speed heat pump. Here, the actual performance of the heat pump is taken into account by considering different operating conditions. The COP model is data-driven (based on outdoor ambient temperature and the water supply temperature in the former and based on the evaporator and condenser temperature in the latter case) and the values of coefficients in the regression equation are not mentioned. In articles [28]–[30], the empirical expressions that are used to model COP are system-specific and data demanding.

Thus, in the articles [14]–[20], the mathematical models for the estimation of COP are not discussed. Moving to [21]–[30], empirical expressions are used to estimate the COP. These models are system-specific, data-demanding, and therefore cannot be used for any heat pump.

In summary, lacking in the scientific literature, has been an effort to construct a reproducible and adaptable physics-based model of a heat pump con-

sidering operational limitations, to estimate the consumption of electric power under various conditions. In addition, the COP depends on the water supply temperature. Estimates of these water supply temperatures for space and water heating to satisfy various heating requirements are missing in the literature. In recent years, heat pump operation at low source temperatures has developed and performance has improved using enhanced vapour injection technology [31] and this is not explicitly considered in the above literature. Finally, all of the above studies focus on supporting the power system during normal conditions and not during emergency periods with severe power shortages.

The summary of heat pump modelling in flexibility studies is shown in Table 1.1.

**Table 1.1:** Summary of modelling heat pumps in flexibility studies.

| Reference | Heat pump type | COP |
|---|---|---|
| [14] | ✗ | Constant |
| [15] | ✗ | Constant |
| [16] | ✗ | ✗ |
| [17] | ✗ | ✗ |
| [18] | Air source | Empirical (Explicit model missing) |
| [19] | Air source | ✗ |
| [20] | ✗ | around 3,5 |
| [21] | Air source | Empirical |
| [22] | Air source/ Ground source | Empirical |
| [23] | ✗ | Empirical |
| [24] | Air source | Empirical |
| [25] | Ground source | Empirical |
| [26] | Air source | Empirical |
| [27] | Air source | Empirical |
| [28] | Air source | Empirical |
| [29] | Air source | Empirical |
| [30] | Air source | Empirical |

## Modelling of domestic hot water tank

The domestic hot water tanks in Swedish single-family houses are heated by passing hot water through a coil placed inside the tank, as seen in Figure 1.1. The water in the tank is stratified, which means that the layer of water with the highest temperature occupies the highest position, followed by other layers with temperatures in descending order. Stratification plays a key role in flexibility studies, as the control action for heating will be based on the location of the temperature sensor.

[32] deals with the use of residential water heaters for flexibility services. However, the models of the tank and the heat pump are not in detail. In addition, the heat pump used is of the fixed speed type and not a variable speed heat pump.

To obtain demand response from residential electric water heaters, a physics-based model of an electrically heated domestic hot water tank with stratification is modelled in detail in [33]. Reproducing this model provided a higher water temperature in the bottom portion of the tank compared to the top portion, which is physically not realisable.

[34] deals with the grey box modelling of an electrically heated domestic hot water tank considering stratification. Black and grey box models are system specific and would be challenging to adapt the model if parameters change. Furthermore, such models are data demanding, and having specific experimental data is crucial.

Thus, missing in the scientific literature related to flexibility studies [14]–[30], [32]–[34] with [26] as an exception, is a physics-based model of a domestic hot water tank with stratification, which is heated by passing hot water through a coil placed in the tank.

## Modelling multi-room house equipped with a heat pump

A literature review dealing with thermal modelling of multi-room buildings equipped with heat pumps is undertaken. This is to investigate and quantify the flexibility potential considering different indoor temperatures in various rooms of a house.

Article [35] deals with the modelling of a heat pump and a physics-based multi-zone model of a building to generate the profiles of electric power consumption by heat pumps. In [35], heat pumps are of the traditional fixed

speed type, while today, as mentioned earlier, variable speed heat pumps are becoming dominant. Reference [36] presents a hierarchical model-based scheme to offer flexibility, considering a multi-zone building model to control temperatures in different zones of a building. In this article, non-hydronic heating systems are used, as opposed to water-based heating systems which are typical in Sweden.

Reference [37] involves modelling and temperature control in multiple rooms according to occupancy, to optimise the electric power consumption of a heat pump. Article [38] also deals with unlocking the flexibility potential based on occupancy, by accounting for thermal dynamics in multiple rooms of a Danish test house, using an economic model predictive control. The flexibility potential in a single family house in Norway is investigated by modelling and controlling temperatures in multiple rooms, using predictive rule-based control in [39]. The annual savings in electric energy using a heat pump compared to the boiler system is quantified by simulating a terraced house in Wales with multiple temperature zones in article [40]. In the above articles, a buffer tank is used in space heating, which is typically absent in Swedish single-family houses. Furthermore, in these studies, a detailed model of a heat pump is missing.

Reference [41] presents an integrated demand response method, to reduce operational cost by selecting various indoor temperature set points for different rooms, for a space heating system involving an air source heat pump and district heating in an educational building. Articles [42] and [43] deal with the operational optimisation of the heat pump, battery, and rooftop solar to reduce peak electricity demand and operational costs, while ensuring thermal comfort in different rooms of a building, respectively. Reference [44] presents a multi-zone price storage control, to reduce the operating cost of a space heating system equipped with a heat pump, by accounting for the thermal satisfaction of the occupants, without the need for a building model. Article [45] deals with controlling temperatures in different rooms with the objective of reducing operational costs for a microgrid involving heat pumps and battery storages. In the articles dealt with above, even though buildings with multiple rooms are modelled, heat pump models are not dealt with in detail despite the fact that the electric power consumption by heat pumps at various operating conditions had a significant role in the respective studies.

In the above articles [35]-[45], the thermal models of multi-room houses are

not fully transparent and reproducible. For example, in article [41], the thermal model of the house is not described in detail. In references [39], [45] the values of the thermal mass associated with the different components of the building are missing. Articles [36]–[38], [43], [44] use grey box modelling to identify building parameters. Furthermore, the heat pump models incorporated in these studies [35]-[45] lack information on operating limitations under various operating conditions.

Missing in the scientific literature is a detailed model of a multi-room house equipped with a variable speed heat pump. In addition, all the above articles deal with either reducing the operational cost or with flexibility studies for normal demand side management. They do not deal with supporting a power system with severe power deficit conditions, which then leaves a research gap to fill.

The summary of modelling a multi-room house equipped with a heat pump in the above literature is shown in Table 1.2.

**Table 1.2:** Summary of modelling a multi-room house equipped with a heat pump.

| Reference | Thermal model of building | Heat pump model |
|---|---|---|
| [35] | 2R3C model-floor, walls and roof | Empirical |
| [36] | Grey box | ✗ |
| [37] | Grey box | ✗ |
| [38] | Grey box | ✗ |
| [39] | IDA ICE | ✗ |
| [40] | TRANSYS | Empirical |
| [41] | Carnot tool box | Empirical |
| [42] | Grey box | ✗ |
| [43] | Grey box | ✗ |
| [44] | Grey box | ✗ |
| [45] | Each zone- 3R1C model | ✗ |

## Reducing the rebound effect of using the flexibility

Heat pump systems after providing flexibility during the indoor temperature restoration have significant CLPU effects. With this background, previous

work on CLPU effects is presented.

There are several valuable articles dealing with the characterisation of the CLPU phenomenon to make informed decisions while restoring distribution feeders after power outages. For example, article [46] presents a method for evaluating the CLPU effects of heat pumps using multi-state models. Reference [47] proposes a data-driven approach to estimate CLPU demand at the feeder level as well as at the customer level. A computationally efficient analytical method to quantify the CLPU demand is proposed in [48]. A general load modelling expression to estimate the CLPU demand is presented in [49]. Article [50] demonstrates the consistency of different mathematical models used to study CLPU effects, through simulations.

There are also beneficial articles on the restoration of load in distribution systems, involving CLPU loads. For example, reference [51] deals with time-dependent CLPU effects, by accounting for the operating state evolution of TCLs. Article [52] deals with minimising the total restoration time, taking into account the loading limits of the transformer and the CLPU effects. The significance of including CLPU effects in load restoration actions, leading to improved reliability of the distribution system, is demonstrated in [53]. Article [54] proposes a stochastic decision-dependent service restoration, accounting for the relationship between the duration of the outage and the CLPU effect. A new variant of the typical CLPU model is proposed in [55]. A multiobjective algorithm including CLPU effects is presented in [56]. In [57], a data-driven approach for load restoration is proposed for a system involving distributed energy resources and CLPU loads. Reference [58] deals with the resilience-driven restoration scheme using an improved situational awareness tool. This tool, among many other aspects, includes the estimation of CLPU demand.

In the articles dealt with in [46]–[58], exponential, delayed-exponential and time-dependent models are used to represent CLPU effects. These models are based on the fact that fixed speed heat pumps or the on-off type of TCLs is accounted for, as the CLPU effect is a consequence of losing the load diversity among TCLs. Today, modern variable speed heat pumps dominate new installations strongly and will soon dominate accumulated installations. Thus, the rebound effect following a power system support event using variable speed heat pumps is yet to be investigated.

Furthermore, in the literature, the focus is mainly on staggered load restoration involving loads with CLPU characteristics, in a distribution network after

power outages. Additionally, the thermal dynamics involving the heat pump and indoor temperature is rarely addressed in the literature except in [46]. In [46] although the dynamics of indoor temperature is taken into account, the heat pump model is of fixed speed type and the heat pump model is not discussed in detail. Consequently, a proposal for a controller to limit rebound power at the component level of a heat pump, considering the dynamics of indoor temperature, is missing in the literature today and forms an important research gap to fill.

The summary of literature review on CLPU effects is shown in Table 1.3.

**Table 1.3:** Summary of literature review on CLPU effects.

| Reference | Staggered load restoration | Indoor temperature dynamics | TCL model description | Type of TCL | Limiting rebound effect at a component level |
|---|---|---|---|---|---|
| [46] | - | ✓ | ✗ | Heat pump | ✗ |
| [47] | - | ✗ | ✗ | ✗ | ✗ |
| [48] | - | ✓ | ✗ | Electric heating | ✗ |
| [49] | - | ✗ | ✗ | ✗ | ✗ |
| [50] | - | ✓ | ✗ | Air conditioner | ✗ |
| [51] | ✓ | ✓ | ✗ | ✗ | ✗ |
| [52] | ✓ | ✗ | ✗ | ✗ | ✗ |
| [53] | ✓ | ✓ | ✗ | Air conditioner | ✗ |
| [54] | ✓ | ✗ | ✗ | ✗ | ✗ |
| [55] | ✓ | ✗ | ✗ | ✗ | ✗ |
| [56] | ✓ | ✗ | ✗ | ✗ | ✗ |
| [57] | ✓ | ✗ | ✗ | ✗ | ✗ |
| [58] | ✓ | ✗ | ✗ | ✗ | ✗ |

## 1.4 Identified research gaps

The following are the research gaps identified based on the review of previous work undertaken in section 1.3

I. The scientific literature is missing a reproducible and adaptable physics-based model of a variable speed heat pump to estimate electric power consumption under various operating conditions.

II. Furthermore, the operation of heat pumps at low source temperatures using vapour injection technology is often overlooked in the literature.

III. Studies rarely reflect the typical setup in Swedish single-family houses, where a heat pump is used for both space heating and water heating without a storage tank for space heating.

IV. Methods for estimating water supply temperatures for space and water heating are largely missing. Article [22] is an exception, which presents empirical models for only space heating. However, the corresponding information on indoor temperature is missing.

V. Existing studies rarely include physics-based models of domestic hot water tanks with thermal stratification, where heating is carried out by circulating hot water through a coil inside the tank.

VI. A detailed model of a multi-room house equipped with a variable speed heat pump is missing.

VII. The rebound effect following a power system support event involving variable speed heat pumps remains an open research area. Furthermore, the literature lacks control strategies on a component-level, to limit this effect.

## 1.5 Contributions

The following are the contributions of this thesis :

I. A reproducible and adaptable physics-based model of a variable speed heat pump is developed, and its performance is demonstrated under various operating conditions. [see Chapter 5, based on articles I and III]

II. A variable speed heat pump with vapour injection is modelled, and its performance is presented under various operating conditions. [see Chapter 6, based on article IV]

III. A physics-based model of a space and water heating system with a heat pump is presented. The system has no storage tank for space heating and has priority set for water heating. The effect of setting this priority on the indoor temperature is also demonstrated. [see Chapter 6 , based on articles II and IV]

IV. Controllers for space and water heating systems involving dynamic estimation of the water supply temperatures are proposed to meet different heating requirements under various operating conditions. [see Chapters 5 and 6, based on articles I, III and IV]

V. A physics-based model of a domestic hot water tank with thermal stratification is developed, where the heating is performed by passing hot water through the coil placed in the tank. In addition, the significance of using this stratified model in flexibility studies is demonstrated. [see Chapter 6, based on articles II and IV]

VI. A detailed model of a multi-room house equipped with a variable speed heat pump is developed. The model also includes a controller to control the indoor temperatures in different rooms of a house. The ability of the model to maintain different temperatures in various rooms is demonstrated. [see Chapter 7, based on article V]

VII. A new heat pump control strategy is proposed to limit the rebound effect associated with using flexibility and its advantage over the standard controller is demonstrated. [see Chapter 8, based on article VI]

# CHAPTER 2

# Theories and key concepts

This chapter provides an overview of the basic concepts of heat pumps.

## 2.1 Introduction

Heat pumps are widely adopted for space heating, space cooling, and water heating applications due to an increasing emphasis on decarbonisation and energy efficiency.

The main components of a heat pump are an evaporator, a compressor, a condenser, and an expansion valve. This is shown in Figure 2.1.

The operation of a heat pump is based on the vapour compression heat pump cycle. In this cycle, the refrigerant in the evaporator absorbs heat from a low temperature source such as outdoor air, ground, or exhaust air. This is followed by the compressor compressing the refrigerant to a high temperature and a high pressure, using electric power. Later, the refrigerant releases heat in the condenser. Finally, the refrigerant undergoes expansion in the expansion valve and the cycle repeats.

A comprehensive analysis of the vapour compression heat pump cycle is presented in the following section.

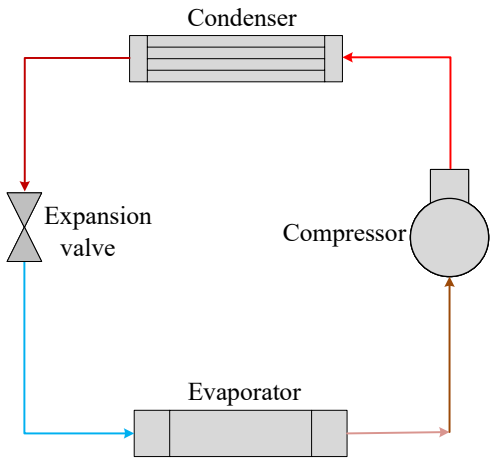


**Figure 2.1:** Main components in a heat pump.

## 2.2 Vapour compression heat pump cycle

In the analysis of the vapour compression heat pump cycle, the properties of the specific internal energy ($u$), pressure ($P$) and specific volume ($v$) of the refrigerant are significant. In this regard, these properties are combined from a simplification point of view as follows.

$$h = u + P \cdot v \tag{2.1}$$

This property is termed specific enthalpy ($h$) and has the unit in $\left(\frac{\text{kJ}}{\text{kg}}\right)$.

### Pressure-enthalpy diagram

The pressure-enthalpy ($P-h$) diagram plays an important role in understanding and analysing the vapour compression heat pump cycle. The refrigerant 'R134a' is taken as an example and its $P-h$ diagram is shown in Figure 2.2.

The vapour dome indicated by the black outline filled with green lines represents the region in which the refrigerant exists as a mixture of vapour and liquid. The black line on the left-hand side of the vapour dome represents

saturated liquid and that on the right-hand side represents saturated vapour. The region towards the left and right of the vapour dome indicates the liquid and vapour states of the refrigerant, respectively. The green lines represent quality, indicating the percentage of vapour present in the liquid-vapour mixture. The temperature of the refrigerant is indicated by the blue lines. It is observed that both temperature and pressure are constant inside the vapour dome.

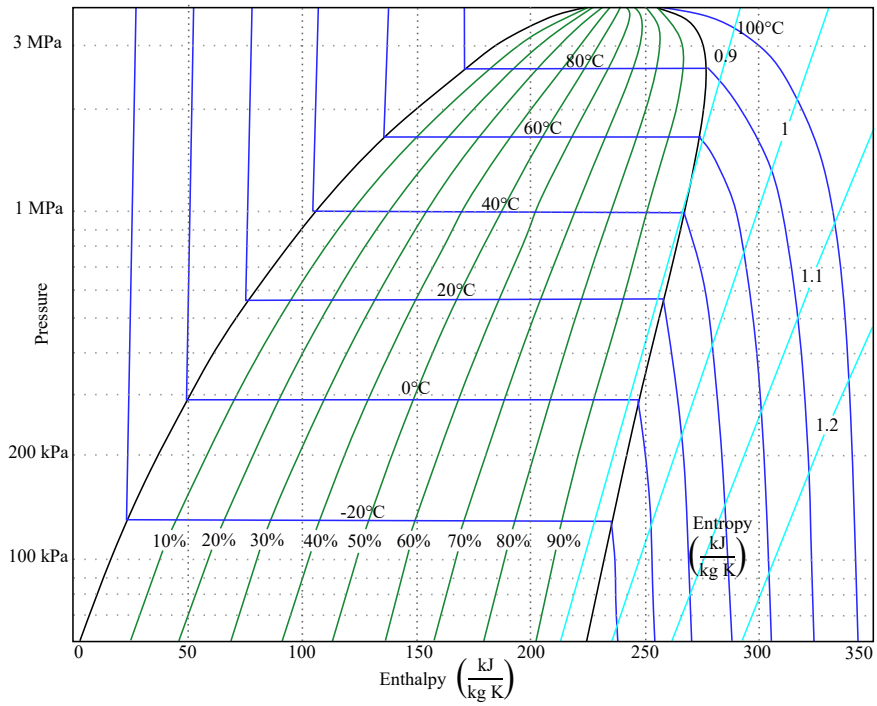


**Figure 2.2:** Pressure enthalpy diagram of refrigerant R134a [59].

In addition to enthalpy, another thermodynamic property of interest in entropy. It indicates the measure of disorderly behaviour of a substance during different states or the kinetic energy lost or the energy unavailable to do useful work $\left(\frac{\text{kJ}}{\text{kg}}\right)$. In Figure 2.2, the entropy is represented by the aqua lines.

Given two properties such as pressure and temperature for a refrigerant

outside the vapour dome, other properties can be estimated. These properties are tabulated for different refrigerants at various states, and these tables are known as thermodynamic tables.

## Thermodynamic analysis of the components in a heat pump

The vapour compression heat pump cycle is shown in Figure 2.3. The subsequent explanation will be based on this figure and $\dot{m}$ corresponds to the mass flow rate.

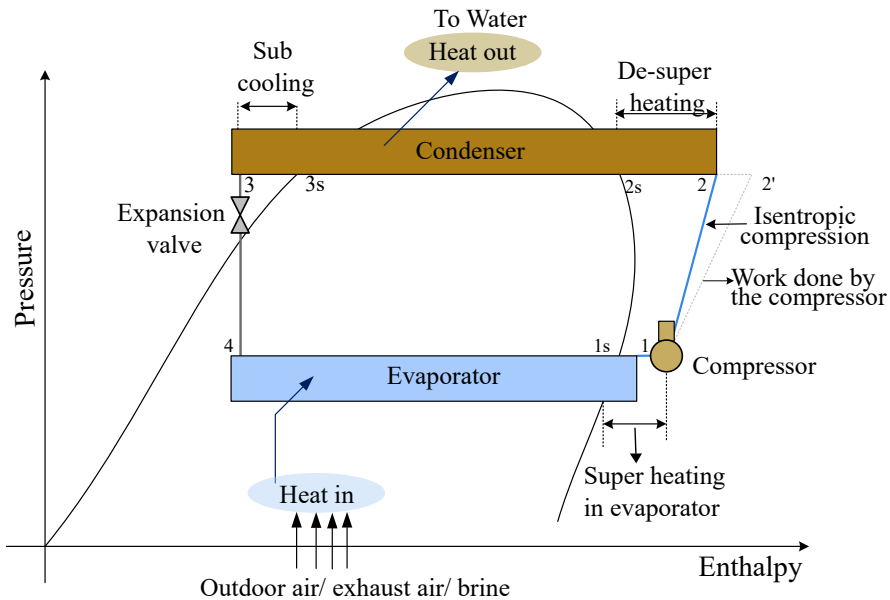


**Figure 2.3:** Vapour compression heat pump cycle [60].

- **Evaporator**: In the evaporator, the refrigerant with low boiling point absorbs heat from the source in the surrounding medium, until it reaches the saturated vapour state. This state is represented as '1s' on the vapour dome. Until this point, the process is isothermal. Practically, it is challenging to precisely control the state of saturated vapour, and

hence the refrigerant is slightly superheated. This also ensures that the refrigerant is completely vaporised.

In the evaporator, there is only heat injection and no work is done. The state of the refrigerant at the inlet and outlet of the evaporator is represented by '4' and '1', respectively.

- **Compressor**: The superheated refrigerant at the outlet of the evaporator enters the compressor. Here, the refrigerant is compressed to obtain a high temperature and a high pressure vapour. The compressor performs this operation by consuming electric power. In this stage, there is only work done and no heat addition. Thus, the process is adiabatic. The states of the refrigerant at the inlet and outlet of the compressor are represented by '1' and '2', respectively.

  The actual power consumption for this process is indicated by the dotted line connecting states 1 and 2' as the input electric power should overcome the mechanical losses, leakage losses, and the motor losses. The electric power consumed by the compressor is given by

$$P_{comp} = \frac{\dot{m}(h_2 - h_1)}{\eta_{isent}} \tag{2.2}$$

  Here, $\eta_{isent}$ represents the overall isentropic efficiency, $h_2$ and $h_1$ represents the enthalpy of the refrigerant at the outlet and inlet of the compressor in $\left(\frac{\text{kJ}}{\text{kg}}\right)$.

- **Condenser**: High pressure and high temperature refrigerant at the compressor outlet enter the condenser. In the condenser, the refrigerant rejects the heat by initially undergoing de-superheating. '2s' represents the state of a saturated vapour at high pressure and high temperature. This is followed by heat rejection at constant temperature. This process occurs when the refrigerant state changes from '2s' to '3s'. The state '3s' represents the state of saturated liquid. Furthermore, the refrigerant is sub-cooled. The condenser does not perform any work and only heat is rejected. The heat rejected by the condenser is given by

$$\dot{Q}_{out} = \dot{m}(h_2 - h_3) \tag{2.3}$$

Here, $h_2$ and $h_3$ represent the enthalpy at the inlet and outlet of the condenser in $\left(\frac{\text{kJ}}{\text{kg}}\right)$

- **Expansion valve**: The refrigerant enters the expansion valve at state '3'. Here, the refrigerant undergoes expansion and enters the evaporator. This process is represented by the line connecting the states 3 and 4. During this process, no heat addition or rejection takes place and no work is done. This process is adiabatic and isenthalpic i.e., the enthalpy of the refrigerant remains same at the inlet and outlet of the expansion valve. Again, the refrigerant enters the evaporator and the cycle continues.

## 2.3 Vapour compression heat pump cycle with vapour injection

Enhanced Vapour Injection (EVI) technology in heat pumps has gained attention in recent years, with the objective of improving the performance, especially in cold climates. Thus, it is important to consider this new feature in studies related to electric power consumption.

The operation and COP of a heat pump at low source temperatures can be increased by incorporating vapour injection into the vapour compression heat pump cycle. This is realised using an economiser, which is a combination of a heat exchanger and an expansion valve. The representation of vapour injection with the associated components in a heat pump is shown in Figure 2.4.

The heat pump cycle with vapour injection is similar to the vapour compression cycle explained in Section 2.2, with vapour injected at an intermediate temperature between the evaporator and the condenser.

In a vapour compression heat pump cycle with vapour injection, a part of the liquefied refrigerant with amount $\dot{m}$ after sub-cooling in the condenser flows into the heat exchanger of the economiser. The other part of the refrigerant with amount $\dot{m}_{inj}$ initially flows through an expansion valve (undergoing a reduction in pressure and also temperature) and then enters the heat exchanger of the economiser as shown in Figure 2.4. In the heat exchanger of the economiser, $\dot{m}$ undergoes sub-cooling and the corresponding heat released is absorbed by $\dot{m}_{inj}$. Subsequently, as $\dot{m}_{inj}$ is superheated, it is injected into the

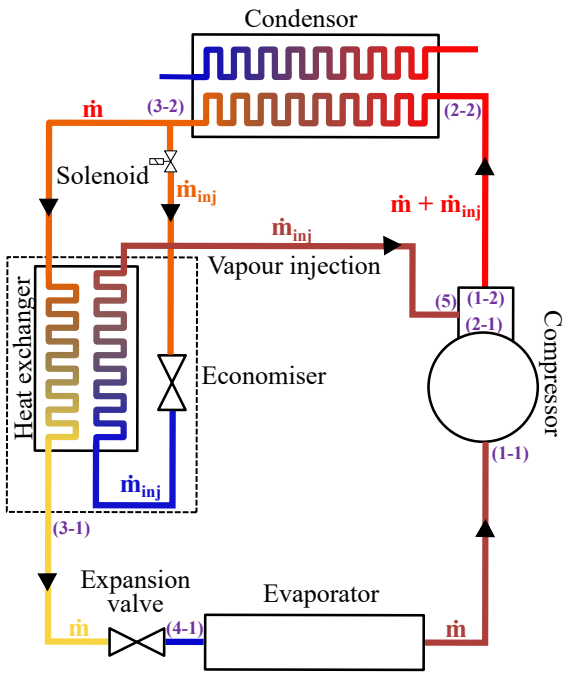


**Figure 2.4:** Heat pump with vapour injection technology [61].

compressor through an intermediate injection port. Thus, the compressor will compress the vapour twice. The first compression is the compression of the superheated vapour at the outlet of the evaporator. The second compression is the compression of the sum of superheated injected vapour and the vapour compressed from the first compression.

Hence, the work performed by the compressor will be higher compared to the work performed by the compressor in the normal vapour compression cycle.

## 2.4 Compressors

The compressor is the heart of a heat pump. The manufacturers provide operating envelopes, indicating the conditions within which the compressors can operate safely and performance is guaranteed.

An example operating envelope of a compressor is shown in Figure 2.5. The envelope indicates the limitations of the compressor's operation in terms of maximum condensing temperature and minimum speed for a given evaporating temperature. For example, the innermost blue envelope indicates that the compressor should run at a minimum speed of 900 RPM for a given set of condenser and evaporator temperatures.

Depending on the speed, there are two types of compressors, fixed speed and variable speed compressors. In variable speed compressors, the speed is adjusted to deliver appropriate heat to maintain the temperature set by the users. However, this is subject to the constraints provided by the operating envelope of the compressor.

### Mass flow rate estimation

The refrigerant mass flow rate $\left(\frac{\text{kg}}{\text{s}}\right)$ is estimated as

$$\dot{m} = \frac{V_{dis}\rho_s N_{comp}\eta_{vol}}{10^6} \tag{2.4}$$

Here, $V_{dis}$ is the compressor displacement volume in $\left(\frac{cc}{rev}\right)$, $\rho_s$ is the density of the refrigerant at suction $\left(\frac{Kg}{m^3}\right)$, $N_{comp}$ is the compressor speed in Hz, and $\eta_{vol}$ is the volumetric efficiency [62].

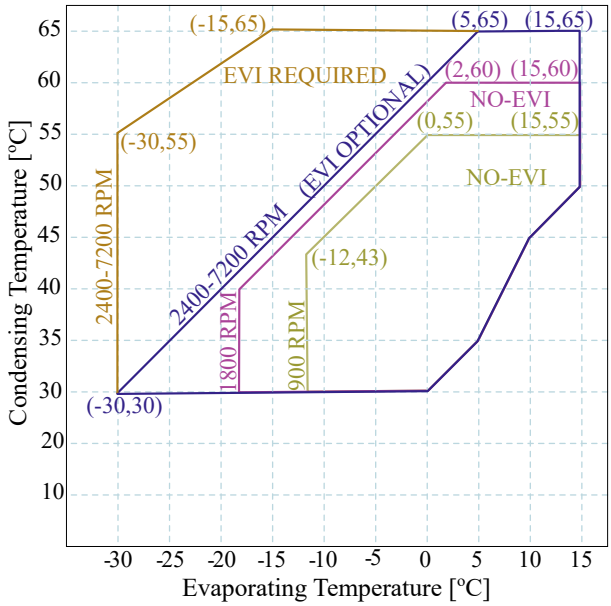


**Figure 2.5:** An example compressor operating envelope [31].

## 2.5 Performance indicator of heat pumps

The performance of a heat pump is indicated in terms of COP. The COP for any heat pump cycle is given by

$$COP = \frac{\text{Heat delivered}}{\text{Electric power consumed by compressor}} \tag{2.5}$$

The maximum theoretical COP for any heat pump operating between the source and sink temperatures of $T_C$ and $T_H$ (both in K), respectively, is formulated as

$$COP = \frac{T_H}{T_H - T_C} \tag{2.6}$$

# CHAPTER 3

# Modelling of heating systems equipped with heat pumps

This chapter describes the mathematical models used to quantify the flexibility potential of a heating system equipped with a heat pump, typically found in Swedish single-family houses. It also deals with modelling of a heat pump controller to limit the rebound effects associated with using flexibility.

## 3.1 Modelling of heat pumps

The modelling of a heat pump, with and without vapour injection technology, is dealt with in this section.

The COP of a heat pump at different operating conditions can be estimated through the analysis of vapour compression heat pump cycle, by using the thermodynamic tables of refrigerants.

### Modelling of heat pumps without vapour injection

The procedure for modelling the heat pump is given below and is based on Figure 2.3 :

1. The pressure in the evaporator is determined by using information on the

temperature at which evaporation occurs and the corresponding quality of saturated vapour.

2. In the evaporator, the increase in refrigerant temperature due to superheating is set to 5 K (evaporating temperature + 5 K) as recommended in Copeland's application guidelines [63]. The enthalpy '$h_1$' is obtained using the details of the temperature at which the refrigerant is superheated and the pressure in the evaporator. In addition, the entropy and density of the refrigerant are obtained under the same conditions (state: 1). This is followed by the calculation of the mass flow rate using (2.4).
3. As the compression process is assumed to be isentropic, the entropy of compressed vapour is the same as that of the vapour at the outlet of the evaporator(state: (1)).
4. The pressure in the condenser is obtained by using information on the temperature at which condensation occurs and the quality of the saturated liquid.
5. The temperature of the compressed vapour is obtained using the details of the pressure in the condenser and the entropy of the compressed vapour.
6. Using the details of the entropy and temperature of the compressed vapour, the enthalpy '$h_2$' is obtained. The work carried out by the compressor to perform compression is calculated using (2.2).
7. In the condenser, the reduction in refrigerant temperature due to subcooling is set to 5 K (condensing temperature - 5 K), as recommended in Copeland's application guidelines [63].
8. The enthalpy '$h_3$' is obtained using the details of the temperature at which the refrigerant is completely sub-cooled and the pressure in the condenser .
9. The heat delivered by the condenser and the COP is calculated using (2.3) and (2.5), respectively.

## Modelling of heat pumps with vapour injection

The vapour compression heat pump cycle with vapour injection operates at three pressures corresponding to the pressures of evaporator, vapour injection, and condenser. The vapour compression heat pump cycle with vapour injection on a pressure-enthalpy diagram is shown in Figure 3.1. The subsequent explanation will be based on figures 2.4 and 3.1. With this background,

the procedure used for modelling with appropriate reasoning is listed below [61][64] :

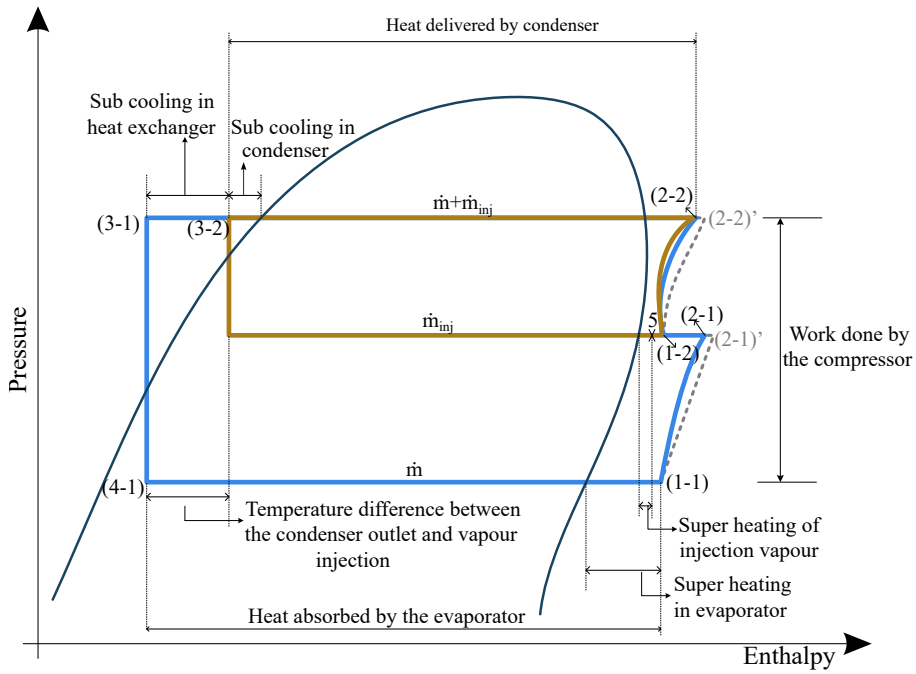


**Figure 3.1:** Vapour compression heat pump cycle with vapour injection [61].

1. The enthalpy '$h_{1-1}$' followed by entropy and density of the refrigerant are obtained at state 1-1, as described previously. This is followed by the calculation of mass flow rate using (2.4).
2. The temperature of vapour injection line (saturated temperature at an intermediate pressure) is approximated using the expression

$$T_{inj} = 0.8T_e + 0.5T_c - 21 \tag{3.1}$$

The terms $T_e$ and $T_c$ correspond to evaporator and condenser temper-

atures in °F. This is experimentally derived for vapour injection scroll compressor models by Emerson climate technologies with an accuracy of ± °5 [61].

3. From an optimal system performance point of view, a temperature difference of 5 K is set in the following cases as recommended in Copeland's application guidelines [63]:
   - Condenser sub-cooling
   - The temperature of the sub-cooled liquid at the outlet of economiser's heat exchanger (state:(3-1)) and the temperature of vapour injection line ($T_{inj}$).
   - The temperature of vapour injection at the outlet of injection port (state:5) and the temperature of vapour injection line ($T_{inj}$).
4. The pressure in the vapour injection line is obtained using the temperature of the vapour injection line ($T_{inj}$) and the corresponding quality of the saturated vapour.
5. The enthalpy '$h_5$' of the superheated vapour to be injected is obtained using the temperature of injection vapour at the outlet of the injection port ($T_{inj}$+5) and the pressure in the vapour injection line.
6. The pressure in the condenser is obtained using the details of the temperature in the condenser and the quality of saturated liquid.
7. The enthalpy '$h_{3-2}$' at state (3-2), is obtained using the details of the condenser temperature considering sub-cooling and the pressure in the condenser.
8. The enthalpy '$h_{3-1}$' at state (3-1) is obtained using the details of the temperature of the subcooled liquid at the outlet of economiser ($T_{inj}$+5) and the pressure in the condenser.
9. The mass flow rate of vapour injected is calculated based on the energy balance equation in the economiser and is given by

$$\dot{m}_{inj} = \frac{\dot{m}(h_{3-2} - h_{3-1})}{(h_5 - h_{3-2})} \tag{3.2}$$

10. As the process of compression is isentropic, the entropy of the vapour from the first compression (state: (2-1)) is the same as that of the vapour at the outlet of the evaporator (state: (1-1)).
11. The enthalpy '$h_{2-1}$' at state (2-1), is obtained using the details of entropy at state (2-1) and the pressure in the vapour injection line.

12. The enthalpy '$h_{1-2}$' at state (1-2), is obtained by using the energy balance equation at the vapour injection port of the compressor and is given by

$$\dot{m}_{inj}(h_{1-2} - h_5) = \dot{m}(h_{2-1} - h_{1-2})$$
$$h_{1-2} = \frac{\dot{m}h_{2-1} + \dot{m}_{inj}h_5}{(\dot{m} + \dot{m}_{inj})} \tag{3.3}$$

13. The entropy at state (1-2) is obtained using the information of enthalpy at the same state and pressure corresponding to the vapour injection line.
14. The entropy of state (2-2) is equal to the entropy at state (1-2) due to isentropic compression. The enthalpy at state (2-2) is obtained by using the details of entropy at the same state and condenser pressure.
15. The electric power consumed by the compressor is given by

$$P_{comp} = \frac{(\dot{m}(h_{2-1} - h_{1-1})) + ((\dot{m} + \dot{m}_{inj})(h_{2-2} - h_{1-2}))}{\eta_{isent}} \tag{3.4}$$

16. The COP of the heat pump is given by

$$COP = \frac{(\dot{m} + \dot{m}_{inj})(h_{2-2} - h_{3-2}))}{P_{comp}} \tag{3.5}$$

## 3.2 Thermal modelling of houses

The thermal modelling of houses includes the calculation of heat losses due to infiltration, sanitary ventilation, and the recovery of ventilation heat loss through a heat recovery unit. In addition, heat input from a specific type of heat pump is taken into account via heat emitters such as radiators or floor heaters. Furthermore, heat losses due to conduction based on the construction materials of a house are also considered. The representation of a house considered for modelling is shown in Figure 3.2.

- The heat loss due to sanitary ventilation accounting for, heat recovery from a heat recovery unit and infiltration, $U_{vent,infil}$ in $\left(\frac{\mathrm{W}}{\mathrm{K}}\right)$ is estimated as

$$U_{vent,infil} = \frac{\rho_{air}C_{p,air}}{1000}\left((1 - \eta_{vent})V_{vent}A_{floor} + V_{infil}A_{ext}\right) \tag{3.6}$$

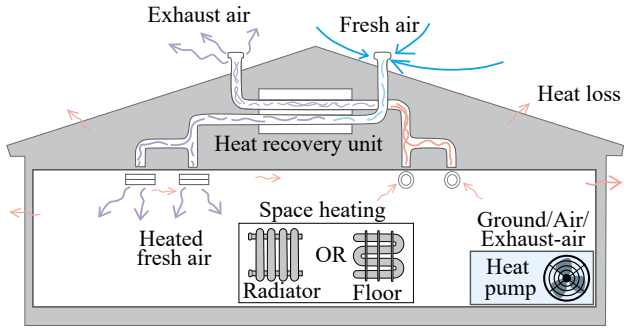


**Figure 3.2:** Representation of a house considered for thermal modelling [65].

where, $\rho_{air}$ is the density of air in $\left(\frac{\text{Kg}}{\text{m}^3}\right)$ and $C_{p,air}$ is the specific heat capacity of air in $\left(\frac{\text{J}}{\text{KgK}}\right)$, $\eta_{vent}$ is the efficiency of the heat recovery unit, $V_{vent}$ and $V_{infil}$ are ventilation rates for sanitary ventilation and infiltration respectively in $\left(\frac{\text{l}}{\text{s}\cdot\text{m}^2}\right)$. $A_{floor}$ is the heated floor area and $A_{ext}$ is the external surface area of the building envelope in $\text{m}^2$ (excluding window and doors). $\eta_{vent}$ is zero, in the absence of a heat recovery unit.

- The overall heat transfer co-efficient of a house $U_{overall}$ is given by

$$U_{overall} = U_{value}A_{floor} + U_{vent,infil} \tag{3.7}$$

here $U_{value}$ represents the average heat transfer coefficient of a house's envelope per heated floor area, considering all construction materials. The total thermal resistance $R_{overall}$ is the reciprocal of $U_{overall}$.

- Based on the time constant $\tau$ in hours and $R_{overall}$ of a house, the thermal capacitance, $C_{overall}$ is obtained as

$$C_{overall} = \frac{\tau}{R_{overall}} 3600 \tag{3.8}$$

- After obtaining $R_{overall}$ and $C_{overall}$, accounting for the heat from the heat pump $Q_{heat}$ via heat emitters, the thermal model is represented as a series resistance-capacitance network as shown in Figure 3.3.

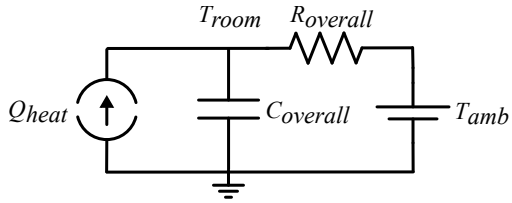


**Figure 3.3:** Thermal model of a building.

- The outdoor ambient temperature $T_{amb}$ is represented as a voltage source. The voltage across the capacitor represents the indoor temperature $T_{room}$. $Q_{heat}$ is modelled as a dependant current source as the heat requirement changes based on the outdoor ambient temperature and a set value of indoor temperature.
- Based on the circuit in Figure 3.3, the indoor temperature is estimated as

$$\frac{dT_{room}}{dt} = \frac{1}{C_{overall}} \left( Q_{heat}(t) - \frac{T_{room}(t) - T_{amb}(t)}{R_{overall}} \right) \tag{3.9}$$

### Thermal modelling of radiators

The thermal output of the radiators is modelled as shown in Figure 3.4 [66]. The terms $T_{supply}$ and $T_{return}$ represent the temperature of the water supplied and the temperature of the water returned from the radiators, respectively. $Q_{std}$ and $\Delta T_{std}$ represent the total heat output of the radiators and the temperature difference between the radiator and the room under standard conditions (i.e., at 55°C supply temperature, 45°C return temperature and 20°C room temperature) respectively. The term '$n$' refers to the exponent characteristic of a radiator.

## 3.3 Thermal modelling of a multi-room house

This section describes the procedure to model a multi-room house. Each component of the building (walls, roof and floor) is composed of several materials. Based on the construction materials of the building, the thermal resistance and thermal capacitance of the external envelope (external walls and roof), internal walls and floor are computed. The total thermal resistance and thermal

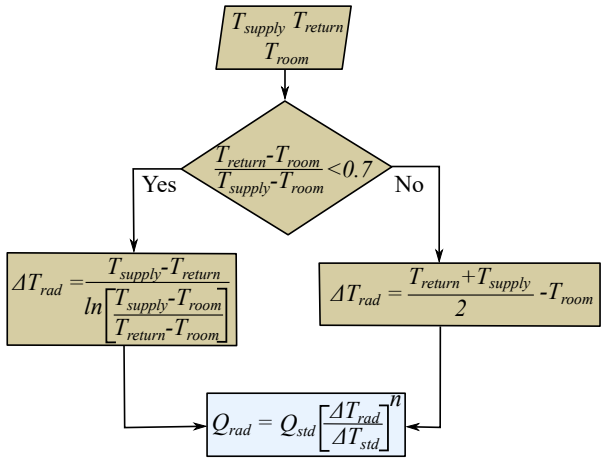


**Figure 3.4:** Radiator model.

capacitance of each component are computed as

$$R_x = \sum_{i=1}^{n} \frac{t_i}{G_i \; A_x} \tag{3.10}$$

$$C_x = \sum_{i=1}^{n} \rho_i \; C_{p_i} \; t_i \; A_x \tag{3.11}$$

where $x \in \{\text{external walls}, \text{roof}, \text{internal walls}, \text{floor}\}$, $i$ corresponds to various materials in each component of the building, $t_i$ is the thickness of the material in (m), $G_i$ is the thermal conductivity in $\left(\frac{\text{W}}{\text{mK}}\right)$, $A_x$ is the area of the building component in $\left(\text{m}^2\right)$, $\rho_i$ is the density in $\left(\frac{\text{Kg}}{\text{m}^3}\right)$ and $Cp_i$ is the specific heat capacity in $\left(\frac{\text{J}}{\text{kgK}}\right)$.

The thermal resistance of the external envelope is obtained from the parallel combination of the thermal resistances of windows, doors, external walls, and the roof. The thermal mass of the external envelope is obtained by summing the associated thermal masses together.

In addition, the heat loss coefficients due to ventilation and infiltration, including heat recovery, are calculated using (3.6).

The thermal mass of the indoor air including the furnishings is computed as

$$C_{air} = ZM\,(\rho_{air}\ C_{in}\ V_{room}) \tag{3.12}$$

where, $ZM$ is the zone capacity multiplier factor. This accounts for the furnishings contributing to the internal thermal mass. $V_{room}$ is the volume of air in the room in $(\mathrm{m}^3)$.

Figure 3.5 shows the thermal model of one zone in a multi-zone model of a house. The external envelope and the internal walls are modelled using a 1R2C network. The heat loss coefficient due to ventilation and infiltration is modelled as a resistance. Thermal resistances ($R_{air,ext}$, $R_{ext\ air,in}$, $R_{floor\ air,in}$, $R_{int\ wall\ air,\ in}$) due to convection and radiation from the surfaces of walls and floors are also taken into account.

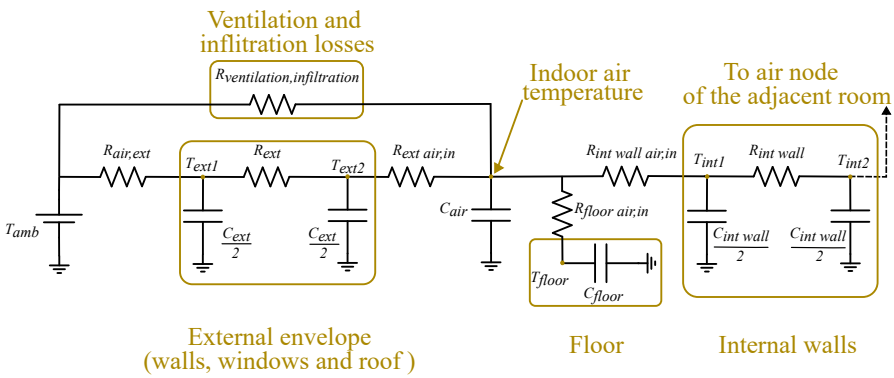


**Figure 3.5:** Thermal model of one zone in a multi-zone thermal model.

## 3.4 Thermal modelling of domestic hot water tank

The domestic hot water tank is stratified, which means that the layer of water with the highest temperature occupies the top position, followed by other layers with temperatures in descending order. Hot water is drawn from the top of the tank. As and when hot water is drawn, it is replaced by an equal amount of cold water from the cold water inlet, typically placed at the bottom of the tank.

Stratification plays a key role in flexibility studies, as the control action for heating will be based on the location of the temperature sensor in the tank.

The temperature of water at different positions in a tank is estimated using a state-space model. From a modelling perspective, it is assumed that the water tank is divided into '$N$' equal volumes and will be further referred to as layers. The temperature is assumed to be uniform within each layer. The upper layer (warmest) and the lower layer (coldest) of the tank are represented by '1' and '$N$' respectively. By setting up an energy balance equation for each layer and solving all the equations simultaneously, the temperature at different positions in the tank can be estimated. The types of heat transfer in the tank are as follows [33] [67]:

- Heat transfer due to conduction ($Q_{cond}$)
- Heat transfer due to flow/water extraction ($Q_{flow}$)
- Heat transfer to the ambient environment or the room in which the tank is placed ($Q_{room}$)
- Heat transfer due to inversion mixing ($Q_{inv}$). This occurs only when a lower layer of water is warmer than the layer above it.
- Heat transfer from the heating element ($Q_{heat}$)

The equation of heat balance in each layer of the water tank is given by

$$m_{Li}\, C_{p,\text{water}}\, \frac{dT_{Li}}{dt} = Q_{cond,Li}+Q_{flow,Li}+Q_{room,Li}+Q_{inv,Li}+Q_{heat,Li} \quad (3.13)$$

where $m_{Li}$, $C_{p,\text{water}}$ and $T_{Li}$ represent the mass, specific heat capacity, and temperature of the water in layer 'i'.

The heat transfer due to conduction at layer '$i$' is given by

$$Q_{cond,Li} = \begin{cases} K_i(T_{L(i+1)} - T_{Li}) & \text{if } i = 1 \\ K_i(T_{L(i-1)} - T_{Li}) & \text{if } i = N \\ K_i(T_{L(i+1)} + T_{L(i-1)} - 2T_{Li}) & \text{otherwise} \end{cases} \quad (3.14)$$

where $K_i$ represents the conductivity coefficient between the layers.

The heat transfer resulting from the flow (during water extraction) in the layer '$i$' is given by

$$Q_{flow,Li} = \begin{cases} \dot{m}_{water}\, C_{p,\text{water}}(T_{in} - T_{Li}) & \text{if } i = N \\ \dot{m}_{water}\, C_{p,\text{water}}(T_{L(i+1)} - T_{Li}) & \text{otherwise} \end{cases} \quad (3.15)$$

where $\dot{m}_{water}$ is the mass flow rate of the water being extracted and $T_{in}$ is the temperature of the cold water at the inlet of the tank.

The heat transfer due to temperature inversion follows the relation

$$Q_{inv,Li} = Q_{inv,gain} + Q_{inv,loss} \tag{3.16}$$

where $Q_{inv,gain}$ and $Q_{inv,loss}$ are the heat gain and heat loss due to inversion mixing in each layer.

The heat gain $Q_{inv,gain}$ due to inversion mixing can be determined as

$$Q_{inv,gain} = \begin{cases} \frac{0.5\ m_{Li}\ C_{p,\text{water}}}{\Delta t}(T_{L(i+1)} - T_{Li}) & \text{if } T_{L(i+1)} > T_{Li} \\ 0 & \text{for } i = N \text{ and otherwise} \end{cases} \tag{3.17}$$

where $\Delta t$ is the time interval considered for inversion mixing.

The heat loss $Q_{inv,loss}$ due to the inversion mixing is found as

$$Q_{inv,loss} = \begin{cases} \frac{0.5\ m_{Li}\ C_{p,\text{water}}}{\Delta t}(T_{L(i-1)} - T_{Li}) & \text{if } T_{L(i-1)} < T_{Li} \\ 0 & \text{for } i = 1 \text{ and otherwise} \end{cases} \tag{3.18}$$

The heat transfer to the ambient environment in which the tank is placed is given by

$$Q_{room,Li} = U_{Li}(T_{room} - T_{Li}) \tag{3.19}$$

where, $U_{Li}$ represents the heat conduction coefficient of the tank in the layer '$i$' and $T_{room}$ is the room temperature in which the hot water tank is placed.

## Modelling of thermal output by the hot water coil

The heat emitted from the hot water coil is modelled as shown in Figure 3.6. The terms $T_{supply}$ and $T_{return}$ represent the temperature of the water supplied and the temperature of the water returned from the hot water coil, respectively. $T_{water,average}$ represents the average temperature of the water in the location where the hot water coil is placed. $UA_{water,coil}$ represents the heat transfer coefficient of the hot water coil.

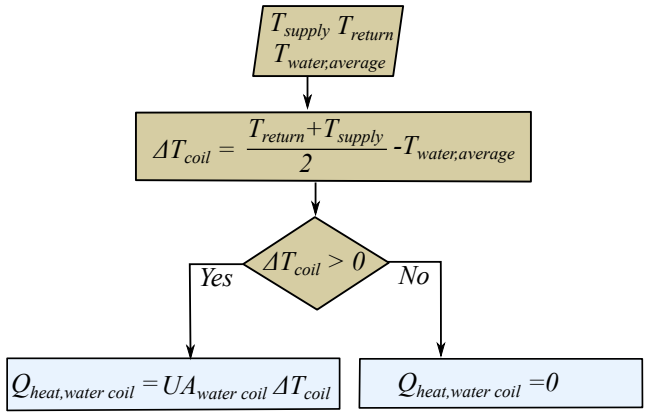


**Figure 3.6:** Model of the hot water coil.

## 3.5 Standard weather compensated heat pump controller

The operation of a heat pump is controlled based on the outdoor ambient temperature. Based on the outdoor temperature, a specific value of the water supply temperature is chosen. This information is transformed into curves and is known as heating curves. The control of a heat pump using heating curves is known as the standard weather-compensated control.

Example heating curves are shown in Figure 3.7 [68]. This provides information on the different water supply temperatures required in houses to meet the space heating requirements at different outdoor ambient temperatures.

Based on the heating requirements of a house, a specific heating curve is selected. For example, in Figure 3.7, assume that the heating curve of 0.8 is selected, which is indicated by the blue dashed line. This curve will be used as a reference to obtain the required supply temperatures at different outdoor ambient temperatures. For example, at an outdoor ambient temperature of -5°C, a supply temperature of about 46°C is maintained. If additional heating is required, the heating curve is shifted up, where a higher supply temperature is selected to deliver a higher heat. This is indicated by the green arrow. Typically for heat pump systems with radiators in Sweden, the maximum supply temperature in the radiators is limited to 55°C and this is indicated

by the solid red line.

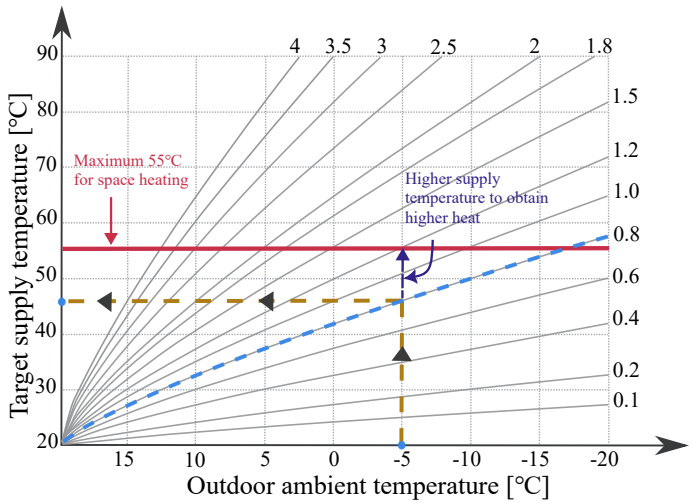


**Figure 3.7:** Example heating curves [68].

## 3.6 Proposed controller design for space heating

A proportional-integral (PI) controller with an anti-wind up and a feed-forward structure is adopted to control the indoor temperature. The control diagram is shown in Figure 3.8.

The transfer function of the thermal model of the house in Figure 3.3, with the output as $T_{room}$ and the inputs as $Q_{heat}$ and $T_{amb}$ can be derived as follows

Applying Kirchhoff's current law (KCL) to the circuit gives

$$Q_{heat}(t) = C_{overall}\frac{dT_{room}}{dt} + \frac{T_{room}(t) - T_{amb}(t)}{R_{overall}} \tag{3.20}$$

Taking the Laplace transform on (3.20) and rearranging the terms, the transfer function is obtained as

$$\frac{T_{room}(s)}{(Q_{heat}(s) + \frac{T_{amb}(s)}{R_{overall}})} = \frac{R_{overall}}{R_{overall}C_{overall}S + 1} \tag{3.21}$$

Since the values in the term $\frac{T_{amb}}{R_{overall}}$ are known, it is modelled as a feed-forward.

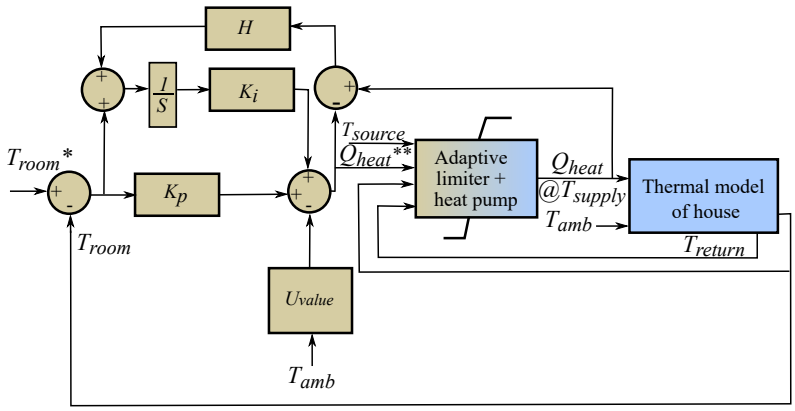


**Figure 3.8:** Block diagram of the controller for space heating. (Here brown blocks refer to controller and blue blocks refer to the plant model).

The heat delivering capacity of the heat pump depends on the source and sink temperatures. Furthermore, the heat provided by the radiators is limited by the supply, return temperature of water, and room temperature. Thus, the saturation block is modelled as an adaptive limiter.

## Details of adaptive limiter

The flow chart of the adaptive limiter is shown in Figure 3.9. The radiator look-up table (LUT) is formulated on the basis of the radiator model presented in Section 3.2. This table is formulated for a given temperature difference $\Delta T$ between $\hat{T}_{supply}*$ and $\hat{T}_{return}*$ in radiators. Based on ${Q_{heat}}^{**}$, $T_{room}$, the radiator LUT provides $\hat{T}_{supply}*$. This is an advanced version of the standard weather-compensated heat pump controller, where the selection of the supply temperature is automated based on the desired heat and the actual room temperature.

Using $\hat{T}_{supply}*$, $\hat{T}_{return}*$, and $T_{room}$, the reference value ${Q_{heat}}^{*}$ consider-

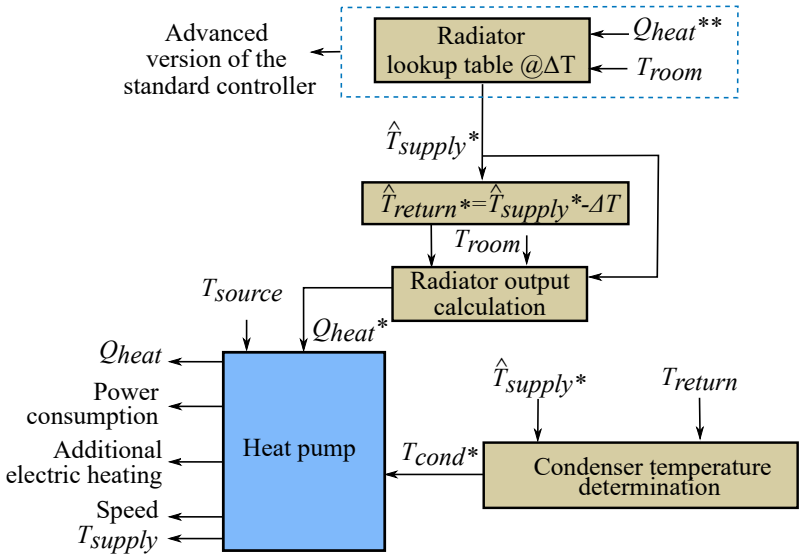


**Figure 3.9:** Flow chart of adaptive limiter.

ing the limitations of the radiators is determined using the radiator model. Furthermore, $T_{cond}{}^*$ is calculated using $\hat{T}_{supply}{}^*$ and $T_{return}$ [69] as

$$T_{cond}{}^* = T_{return} + \frac{\hat{T}_{supply} * - T_{return}}{1 - e^{\frac{-(\hat{T}_{supply}{}^* - T_{return})}{\Delta T_{log.cond}}}} \tag{3.22}$$

$\Delta T_{log.cond}$, is the logarithmic temperature difference of the heat exchanger and is assumed to be 4 K.

Finally, the heat pump model using the values of $T_{cond}{}^*$, $Q_{heat}{}^*$ and $T_{source}$ provides the values of $Q_{heat}$, the total electric power consumption of the heat pump, the compressor speed and $T_{supply}$.

## 3.7 Proposed controller design for water heating

A PI controller with an anti-wind-up and feed-forward structure is chosen for the control of the water heating.

A simple model of a domestic hot water tank without any stratification is

shown in Figure 3.10. Here, $Q_{withdrawl}$ represents the heat loss in the water tank due to water withdrawal, $Q_{heat}$ represents the heat from the heat pump and $C_{tank}$ is the thermal mass of the water in the tank. $T_{room}$ and $T_{water}$ represent the temperature of the room and the water in the tank, respectively.

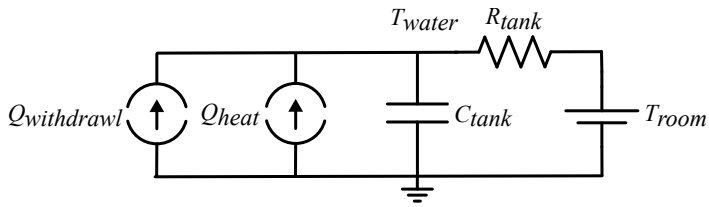


**Figure 3.10:** Simple model for a domestic hot water tank.

Applying KCL to this circuit gives

$$C_{tank}\frac{dT_{water}}{dt} = Q_{heat}(t) + Q_{withdrawl}(t) + \frac{T_{room}(t) - T_{water}(t)}{R_{tank}} \tag{3.23}$$

where, $R_{tank}$ is the reciprocal of the heat transfer coefficient of the water tank. $Q_{withdrawl}$ can be written as

$$Q_{withdrawl}(t) = \dot{m}_{water}(t)\; C_{p,water}(T_{in}(t) - T_{water}(t)) \tag{3.24}$$

Taking the Laplace transform on (3.23) and rearranging the terms, the transfer function is obtained as

$$\frac{T_{\text{water}}(s)}{Q_{\text{heat}}(s) + \frac{T_{\text{room}}(s)}{R_{\text{tank}}} + \dot{m}_{\text{water}}(s)\; C_{p,\text{water}}\; T_{\text{in}}(s)} = \frac{R_{\text{tank}}}{R_{\text{tank}}\,(C_{\text{tank}}S + \dot{m}_{\text{water}}\; C_{p,\text{water}}) + 1} \tag{3.25}$$

The rate at which hot water is drawn, the incoming water temperature at the tank's inlet, and the indoor temperature can be measured. In addition, the heat transfer coefficient of the tank is a known quantity. Thus, the terms involving these parameters is modelled as a feed-forward.

Based on this, the block diagram of the domestic hot water controller is shown in Figure 3.11. A dead band of 1°C is used. Here, $T_{water,average}$

represents the average water temperature in the layers where the hot water coil is placed in the tank. $T_{water,Li}$ represents the temperature of the water in the layer where the temperature sensor is placed.

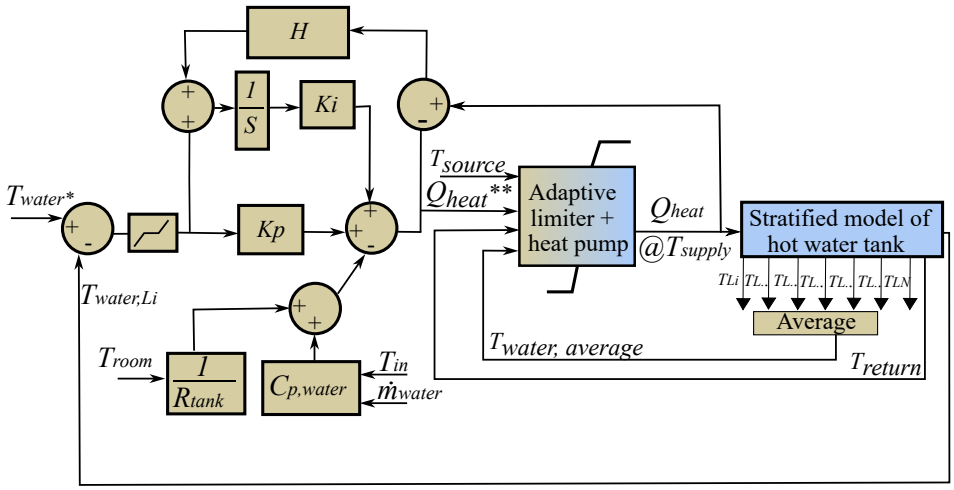


**Figure 3.11:** Controller for water heating. (Here brown blocks refer to controller and blue blocks refer to the plant model).

## Details of adaptive limiter

The flow chart of the adaptive limiter for water heating is shown in Figure 3.12. The LUT for the heat emitted by the hot water coil is formulated based on the model presented in Section 3.4. In addition, the heat capacity of the heat pump at various source temperatures is also taken into account. Based on ${Q_{heat}}^{**}$, $T_{source}$ and $T_{water,average}$, the hot water coil LUT provides the desired $\hat{T}_{supply}*$ and $\hat{T}_{return}*$.

Using $\hat{T}_{supply}*$, $\hat{T}_{return}*$, and $T_{water,average}$, the reference value ${Q_{heat}}^{*}$ is determined considering the limitations in the hot water coil. Furthermore, ${T_{cond}}^{*}$ is calculated using ${\hat{T}_{supply}}^{*}$ and $T_{return}$ using (3.22).

Finally, the heat pump model using the values of ${T_{cond}}^{*}$, ${Q_{heat}}^{*}$ and $T_{source}$ provides the values of $Q_{heat}$, the consumption of electric power by the heat

pump, the compressor speed and $T_{supply}$.

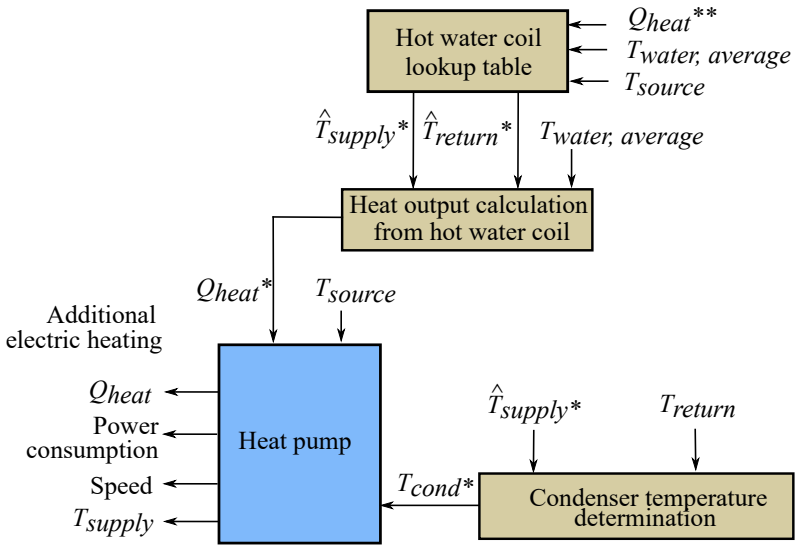


**Figure 3.12:** Flow chart of adaptive limiter for water heating.

## Working principle of the proposed controller for water heating

The explanation in this section is based on the figures 3.11 and 3.12. The input to the controller is the error signal obtained from the reference temperature of water ${T_{water}}^*$ and the actual temperature of water $T_{water,Li}$, read from a sensor placed at a specific location in the domestic hot water tank. Based on the error signal, the controller provides a reference signal for heat ${Q_{heat}}^{**}$. In the adaptive limiter, based on ${Q_{heat}}^{**}$, $T_{source}$, $T_{water,average}$ and finally accounting for the heat pump model, the information regarding the speed, the use of direct heating, the electric power consumed by the compressor and the actual value of heat $Q_{heat}$ delivered is obtained. Based on the value of $Q_{heat}$ released into the water in the tank, the temperature of the water is estimated using the model presented in Section 3.4.

## 3.8 Proposed controller for providing space and water heating

The block diagram of the controller providing space and water heating is shown in Figure 3.13.

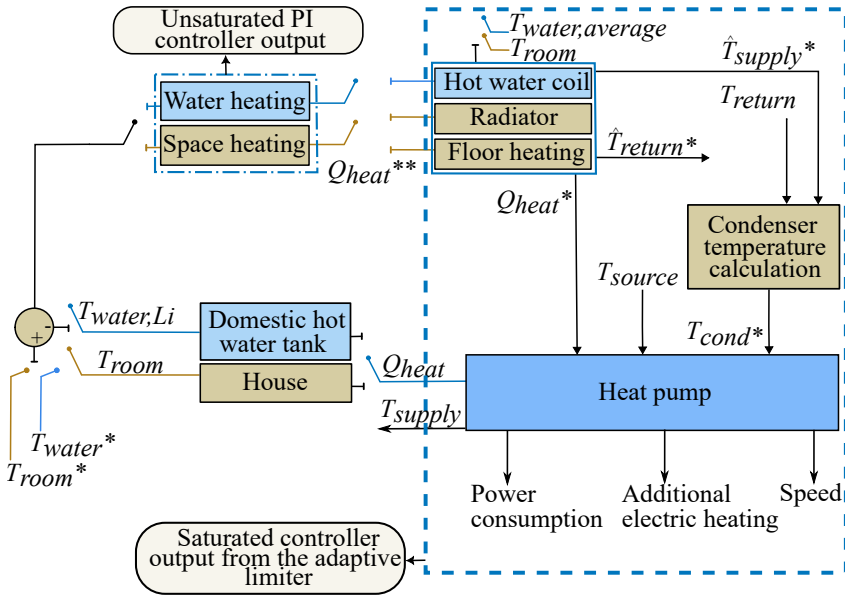


**Figure 3.13:** Flow chart of the controller for providing space and water heating.

Depending on the requirement, an appropriate control mode, that is, space or water heating, is selected. The description of the work flow in each mode of operation is described in sections 3.6 and 3.7, respectively.

## 3.9 Proposed controller design for space heating with multiple rooms

A closed-loop PI controller with an anti-wind up and a feed-forward structure is chosen, to control the main zone's indoor temperature. A rule-based control

structure is adopted to control the indoor temperature of the other zones of the building.

The block diagram of the adopted multi-zone temperature controller structure is shown in Figure 3.14. From a simplicity point of view, only two zones are represented. This structure can be extended to several zones, with a dedicated PI controller in the main zone.

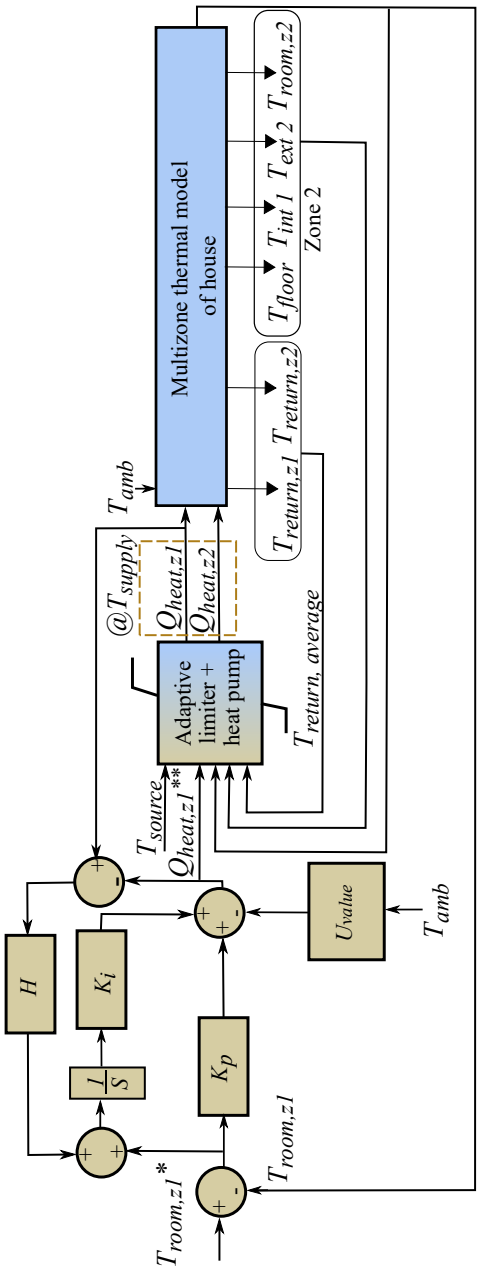


**Figure 3.14:** Multi-zone temperature controller structure. (Here brown blocks refer to controller and blue blocks refer to the plant model).

The flow chart of the adaptive limiter is shown in Figure 3.15. For the rule-based controller, using the thermal model of the zone presented in Figure 3.5 as a reference, the desired heat is calculated using the estimated temperatures of the external envelope, internal walls, floor and the desired indoor temperature as

$$
\begin{aligned}
{Q_{heat,zp}}^{**}(t) = \; & -\left(\frac{T_{amb}(t) - T_{desired\ room\ zp}(t)}{R_{ventilation,infiltration}}\right. \\
& + \frac{T_{ext2}(t) - T_{desired\ room\ zp}(t)}{R_{ext\ air,in}} \\
& + \frac{T_{int1}(t) - T_{desired\ room\ zp}(t)}{R_{int\ wall\ air,in}} \\
& \left. + \frac{T_{floor}(t) - T_{desired\ room\ zp}(t)}{R_{floor\ air,in}}\right)
\end{aligned} \tag{3.26}
$$

Here, '$p$' represents the zone number in the building with multiple zones with a rule-based controller.

The formulation of the LUT of the radiator in each zone is based on the radiator model presented in Subsection 3.2. The radiator LUT provides the required water supply temperature based on the desired heat value to be delivered and the actual indoor temperature. After estimating the temperature of the water supply to the radiator required in various zones, a maximum value is chosen. This is followed by the calculation of the thermal output of the radiators in each zone. Finally, based on the maximum value of the required supply temperature and the average value of return water temperature obtained from different zones, the required condenser temperature is found.

Based on the condenser temperature, the desired value of heat considering the limitations in the radiators and the source temperature of the heat pump, the heat pump model provides the actual value of heat delivered, the water supply temperature, power consumption by the heat pump including the details on additional electric heating and the speed of the compressor.

Finally, in the plant model, the manifolds ensure that water is supplied at the desired temperature and flow rate in each zone.

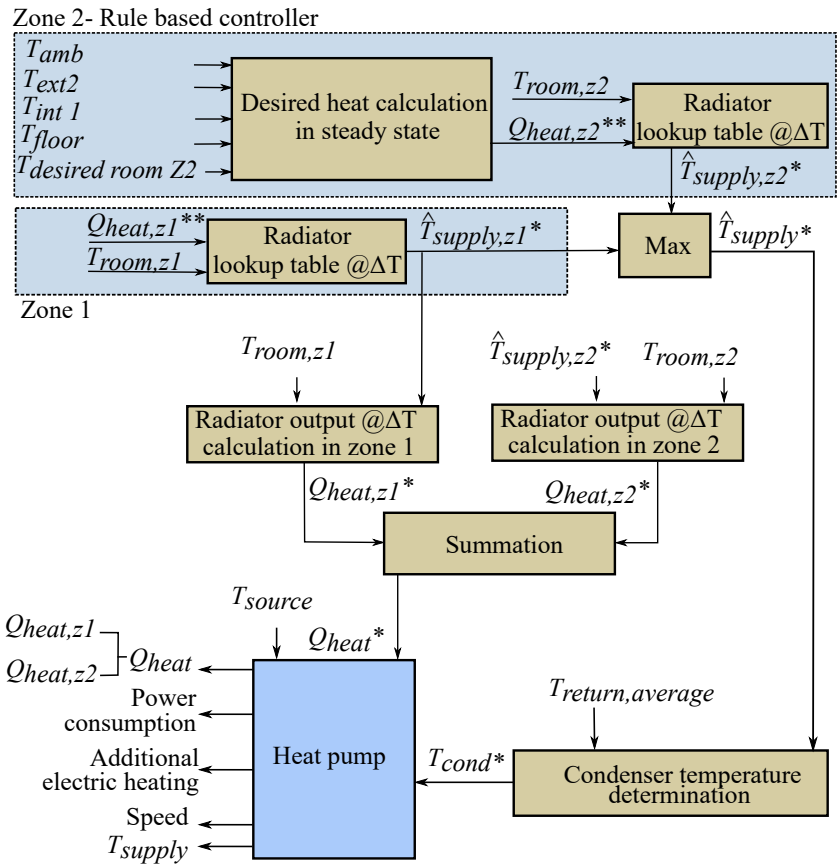


**Figure 3.15:** Flow chart of the adaptive limiter for the proposed multi-zone temperature controller.

## 3.10 Proposed controller for reducing the rebound effect of flexibility

This section describes the concept behind the proposed controller to limit the rebound effect.

### Concept of the proposed controller

The controller design proposed in this study is based on accounting for the maximum heat capacity of the heat pump and the installed radiators in the house. The characteristics of the heat delivering capability of a heat pump

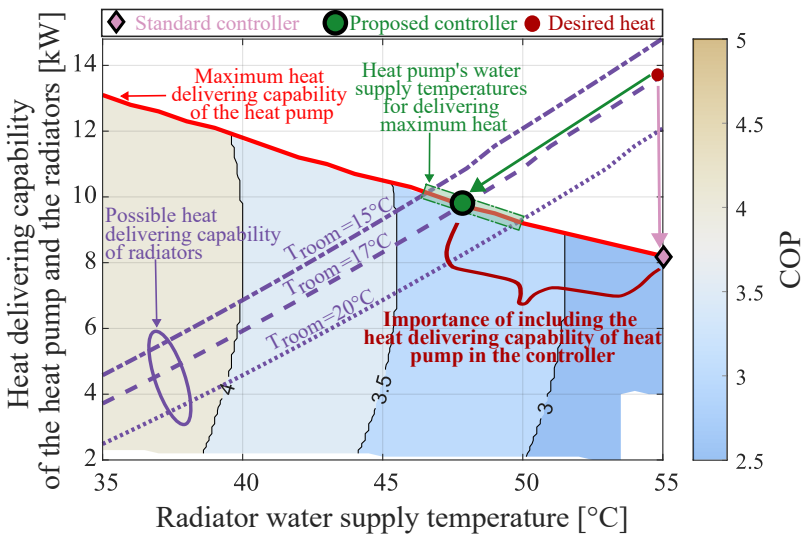


**Figure 3.16:** Concept of the proposed controller.

with possible COP values are shown in Figure 3.16. It is observed that as the temperature of the water supplied to the radiator $T_{supply}$ increases, the heat delivering capability and the COP of the heat pump reduces accordingly.

The characteristics of the heat delivering capability of the radiators based on $T_{supply}$ and $T_{room}$ are also shown. It is observed that as $T_{supply}$ increases, the heat delivering capability of the radiators also increase.

The maximum heat delivered by the heat pump is indicated by the red line. It is interesting to note that even though the radiators have a high heat delivering capability at higher water supply temperatures, the heat delivered will be limited by the maximum heat delivering capability of the heat pump, if electric heating is disabled.

The desired heat is represented using a maroon circle and the heat attained using the standard and proposed controller are represented with a pink diamond and a green circle, respectively.

As the desired heat is typically higher during the recovery period, the standard controller chooses a higher value of the supply temperature to deliver a high heat. However, because of the lack of information regarding the heat delivering capability of the heat pump, a lower heat is obtained instead.

The proposed controller, by accounting for the maximum heat delivering capability of the heat pump and the radiators, can provide the estimates of water supply temperatures to deliver maximum heat at various indoor temperatures. This is highlighted using the green box in Figure 3.16. Thus, the heat delivered by the heat pump using the standard controller will be lower compared to using the proposed controller, with electric heating disabled.

This result becomes very important during the recovery period where maximum heat is required to restore the indoor temperature to pre-disturbance conditions as fast as possible, while ensuring a high COP.

## Proposed heat pump controller

In this section, details of the proposed controller to limit the rebound effect are provided. The structure selected to control the indoor temperature of a house equipped with a heat pump is shown in Figure 3.8. However, the structure of the adaptive limiter is updated, and this is described in detail in the following paragraphs.

The flow chart of the adaptive limiter is shown in Figure 3.17. The main feature of this design is to obtain the estimate of the water supply temperature to be provided by the heat pump, to deliver maximum heat at a given indoor temperature.

The radiator LUT is formulated based on the model of the radiator presented in Section 3.2. This table is formulated for a given temperature difference $\Delta T$ between $\hat{T}_{supply}*$ and $\hat{T}_{return}*$ in radiators. The LUT characteristics of the radiator can be seen in Figure 3.16, represented by purple curves.

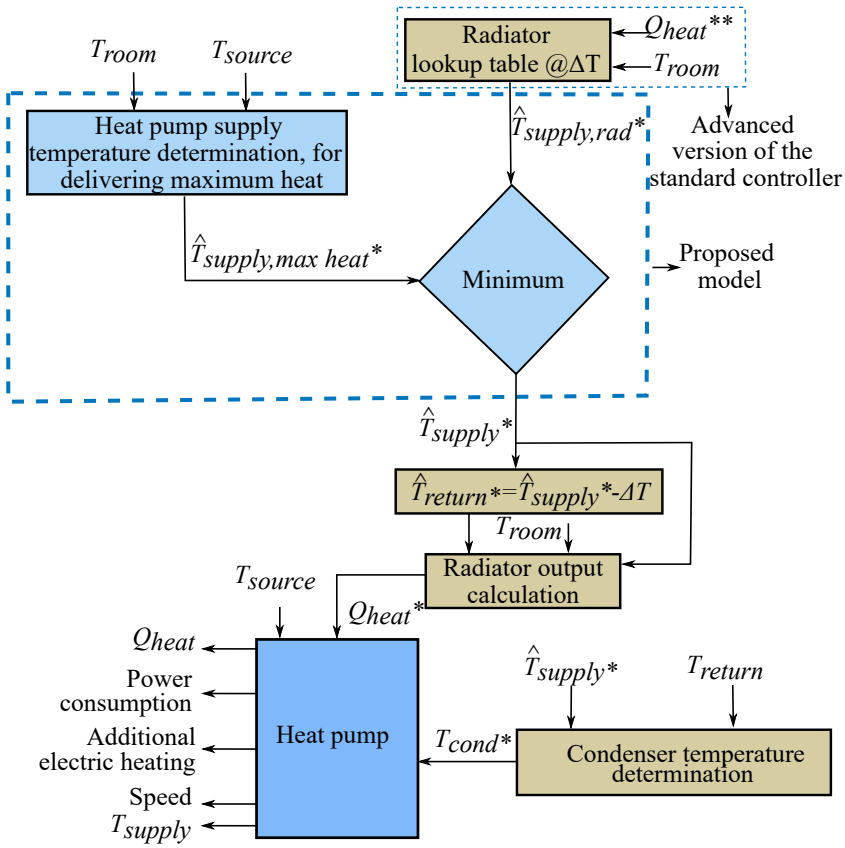


**Figure 3.17:** Flow chart of the adaptive limiter for the proposed heat pump controller.

Based on ${Q_{heat}}^{**}$, $T_{room}$, the radiator LUT provides $\hat{T}_{supply,rad}*$. This is an advanced version of a standard weather-compensated heat pump control, where the selection of supply temperature based on the desired heat and the actual room temperature is automated.

Similarly, based on the values of $T_{room}$ and $T_{source}$, the heat pump supply temperature LUT provides $\hat{T}_{supply,max\ heat}*$, for delivering maximum heat via radiators at a given indoor temperature, without using electric heating. The characteristics of this LUT resemble the area highlighted in the green box in Figure 3.16. This is a very critical feature that needs to be adhered to; otherwise, the rebound effect will be both power and energy intensive. The procedure for determining this is shown in Figure 3.18 and is explained further below. $\hat{T}_{supply,rad}*$ and $\hat{T}_{supply,max\ heat}*$ are compared and the lowest value is chosen.

Now, the estimates of $\hat{T}_{supply}*$ and $\hat{T}_{return}*$ are determined. $\Delta T$ represents the difference between $\hat{T}_{supply}*$ and $\hat{T}_{return}*$. Using the above information followed by using $T_{room}$, the reference value ${Q_{heat}}^{*}$ considering the limitations in radiators is determined using the radiator model. Furthermore, ${T_{cond}}^{*}$ is calculated using $\hat{T}_{supply}*$ and $T_{return}$.

Finally, the heat pump model using the values of ${T_{cond}}^{*}$, ${Q_{heat}}^{*}$ and $T_{source}$ provides the values of $Q_{heat}$, the total electric power consumption by the heat pump, the compressor speed and $T_{supply}$.

#### Algorithm for estimating heat pump's supply temperature for delivering maximum heat via radiators

The algorithm for estimating the supply temperature of the heat pump to deliver maximum heat via the radiators is shown in Figure 3.18. This algorithm is proposed because the heat delivering capability of the heat pump is reduced with an increase in the temperature of the water supplied, as seen in Figure 3.16. This is the key feature of the proposed control structure.

The maximum value of heat delivered by the heat pump ${Q_{HP,max}}^{*}$ corresponding to various values of ${T_{source}}^{*}$ and ${T_{cond}}^{*}$ is obtained using the vapour compression heat pump cycle.

Based on the data available in [70] [71], the temperature difference between $\hat{T}_{supply}*$ and $\hat{T}_{return}*$ vary between 5°C and 10°C ($\Delta T$). Furthermore, by analysing the desired ${T_{cond}}^{*}$ for various values of $\hat{T}_{supply}*$ and $T_{return}$ using (3.14), a temperature difference of 1°C-2°C ($\Delta T_{HX}$) is found between ${T_{cond}}^{*}$

and $\hat{T}_{supply}*$.

For different room temperature values in combination with various values of $\hat{T}_{supply}*$ and $\hat{T}_{return}*$, the heat delivered by the radiators $Q_{rad}*$ is calculated using the radiator model.

This is followed by checking in each case if $Q_{rad}*$ is greater than $Q_{HP,max}*$. In that case, the heat emitted by the radiators is made equal to the heat supplied by the heat pump. Finally, the values obtained for various cases are tabulated. This is followed by data filtering to obtain the maximum value of $Q_{rad}*$ with the corresponding $\hat{T}_{supply}*$ obtained for a given combination of ${T_{source}}^*$ and ${T_{room}}^*$. Thus, $\hat{T}_{supply,max\ heat}*$ is obtained for a given combination of ${T_{source}}^*$ and ${T_{room}}^*$.

The purpose of the procedure presented in this section is to ensure that during the recovery period, COP stays as high as possible.

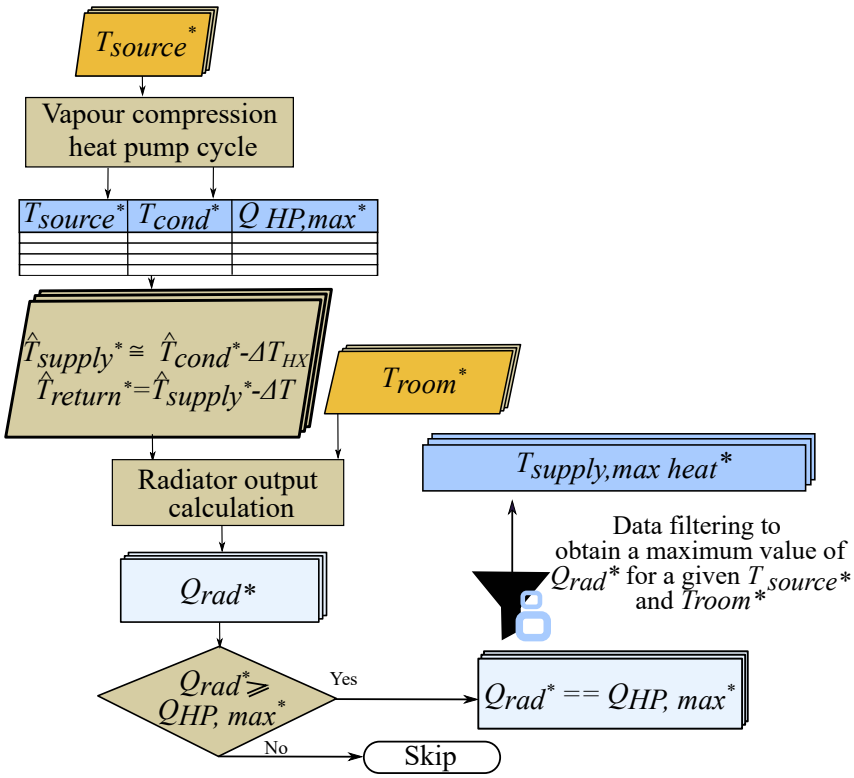


**Figure 3.18:** Flow chart for creating LUT to estimate heat pump's water supply temperature for delivering maximum heat via radiators.

# CHAPTER 4

# Case study setups

This chapter presents the test setups used to analyse the flexibility potential and techniques to reduce the rebound effect associated with using flexibility.

## 4.1 Geographical boundary

In this thesis, Sweden is chosen to be the geographical boundary. The focus is on the southern half of the country, as electricity consumption and population are higher in this region [72].

## 4.2 Power system setup

### Modified Nordic-32 bus system

The original Nordic-32 bus system [73] [74] is a fictitious system with similarities to the actual Swedish power system. It is important to mention that this system is heavily loaded, as it was primarily designed to study voltage instability. As one of the objectives is to study frequency support, using flexibility from single-family houses' heating system, the loading is set to 70% of

the original case. Furthermore, the water time constant in the hydro turbine governor models is set to 1.5 s, which is typical in Sweden [75](In the original system, this value was 1 s).

A future case with an almost sustainable power production is considered. Thus, fossil fuel and nuclear power plants in the central and southern regions have been replaced by wind power plants except for generator G15. This is shown in Figure 4.1. The models 'REGCBU1' and 'REECDU1' are used to model the converter and electrical control modules in wind power plants. The parameter settings of these models are based on the typical range given in [76]. Wind power plants provide only reactive power support during disturbances, and no active power support is assumed.

Furthermore, to account for the impact of the increase in electronic power interface loads, the load characteristics are changed to 60% constant power load and 40% constant current load for active power (originally constant current). The load characteristics for reactive power are changed to 60% constant power load and 40% constant impedance load (Originally constant impedance). Finally, the rating of the G8 hydro generator is changed to 1000 MVA, with active power scheduled at 950 MW, and it is the loss of this unit that is investigated.

## 4.3 Heat pump setup

Scroll compressors are commonly used in residential applications. Hence, compressors in different types of heat pumps are assumed to be equipped with a ZPV030 Emerson Copeland variable speed scroll compressor, having an electrical rating of 3 kW. The compressor displacement volume is 30 $\left(\frac{\text{cc}}{\text{rev}}\right)$. The refrigerant R410a is used. The rating of the electric heater present before the 3-way valve in Figure 1.1 is 3 kW.

The temperature drop set between the source and the evaporator, for different types of heat pumps is shown in Table 4.1. These values are based on references [77] and [78]. The ground temperature is chosen to be 10°C.

The scroll compressor details are as follows:

- The volumetric efficiency $\eta_{vol}$ is set to 83%.
- Based on the data available in references [79] and [80], the isentropic efficiency $\eta_{isent,comp}$ during different compression ratios for the Emerson scroll compressor is shown in Table 4.2.

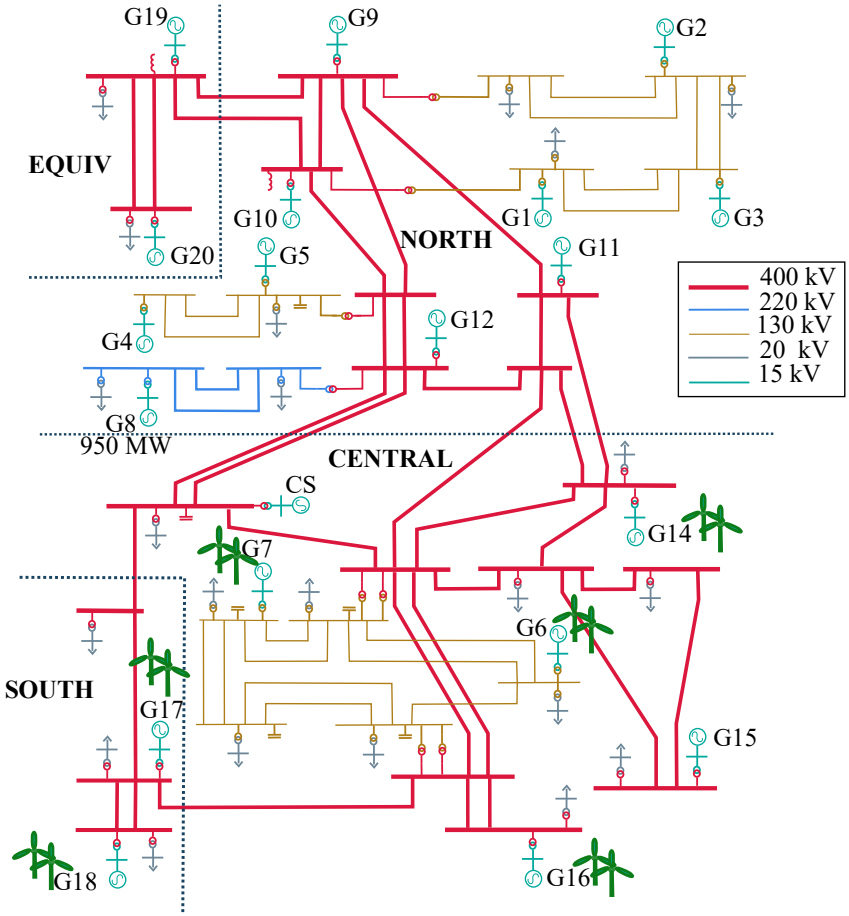


**Figure 4.1:** Modified Nordic-32 bus system.

**Table 4.1:** Temperature drop between source and evaporator.

| Type of heat pump | Source temperature | Temperature drop (°C) |
|---|---|---|
| Ground source | Ground | 10 |
| Air to water | Outdoor ambient air | 8 |
| Exhaust air | Indoor air | 20 |

**Table 4.2:** Variation of isentropic efficiency with respect to compression ratio.

| Compressor ratio | 2.3 | 3 | 3.5 | 4 | 5 | 6 | 7 | 8 | 9 | 11 | 13.9 |
|---|---|---|---|---|---|---|---|---|---|---|---|
| Isentropic efficiency | 0.59 | 0.64 | 0.65 | 0.645 | 0.63 | 0.62 | 0.6 | 0.58 | 0.57 | 0.524 | 0.46 |

- The variation in isentropic efficiency $\eta_{isent}$ with respect to the speed of the compressor ($N_{comp}$) is estimated [81] as

$$\eta_{isent} = \eta_{isent,comp}\left(-0.08\left(\frac{N_{comp}}{N_{comp,60}}\right)^2 + 0.1411\left(\frac{N_{comp}}{N_{comp,60}}\right) + 0.9337\right) \tag{4.1}$$

  where, $N_{comp,60}$ is the speed of the compressor at 60 Hz (3600 RPM).

The operating envelope of the compressor under study is shown in Figure 4.2.

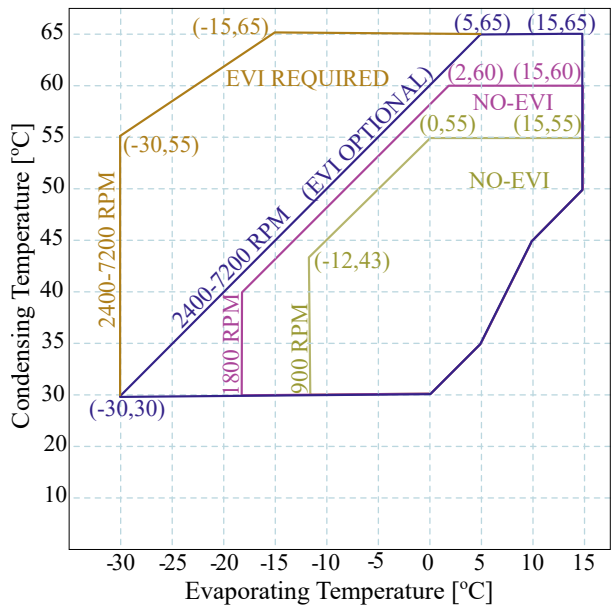


**Figure 4.2:** Operating envelope.

## 4.4 Domestic hot water tank setup

To estimate the temperature at different locations in the hot water tank, the water tank is assumed to be divided into 10 equal volumes. This is shown in Figure 4.3. In the domestic hot water tank, the temperature sensor is assumed

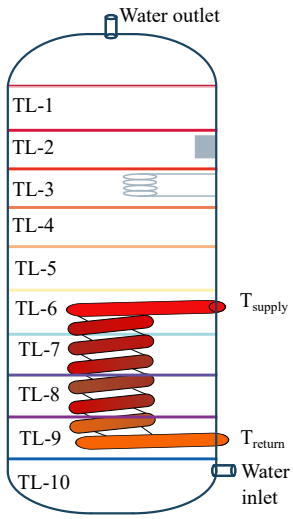


**Figure 4.3:** Domestic hot water tank.

to be placed in layer 2. The electric heater and the hot water coil are assumed to be present in layer 3 and between layers 6 and 9 respectively. The water heated by the heat pump is passed through the coil immersed in the tank. The heat released by the coil is used to heat the water in the tank. The heat released is assumed to be equally distributed among layers 6 to 9. Hot water is extracted from the top and is replaced by an equal volume of cold water at the bottom of the tank.

The thermal and physical properties of the hot water tank used in this study are shown in Table 4.3 [33]. Based on [82], a heat transfer coefficient of $450\left(\frac{\mathrm{W}}{\mathrm{m^2K}}\right)$ is used for the water coil. Furthermore, considering a 35 m long coil with an external diameter of 0.03 m, the heat transfer coefficient of 1484 $\left(\frac{\mathrm{W}}{\mathrm{K}}\right)$ is obtained for the water coil.

The average domestic hot water consumption profile for a day, based on

**Table 4.3:** Parameters of domestic hot water tank model [83].

| Parameter | Value |
|---|---|
| Volume | 180 L |
| Heat conduction co-efficient of tank per layer ($U_i$) | 0.187 $\frac{\mathrm{W}}{\mathrm{K}}$ |
| Electric heater | 3000 W |
| Thermal conductivity of water ($K_i$) | 2.21$\frac{\mathrm{W}}{\mathrm{K}}$ |
| Specific heat capacity of water ($C_p$) | 4180 $\frac{\mathrm{J}}{\mathrm{KgK}}$ |
| Heat transfer co-efficient of the water coil ($UA_{water\ coil}$) | 1484 $\frac{\mathrm{W}}{\mathrm{K}}$ |

time diaries is obtained from [84]. This describes the hot water consumption profiles in Swedish single-family houses. The average number of people living in Swedish single-family houses is 2.7 [85] and the same is considered for the analysis.

## 4.5 Residential buildings setup

### Building parameters for different case setups

The reference [86] deals with the heat transfer coefficient $U_{value}$ of single-family houses in Sweden, according to the year of construction. Following a conservative approach, houses constructed before 1961 are excluded as the source of heating is very mixed. For example, they could be heated with wood, oil, direct electric heating, or heat pumps, and thus the source of the heating is unclear.

The thermal properties of the houses together with the type of heat pump, the type of heat emitter, and the number of houses considered for analysis in different case study setups are shown in Table 4.4. In this study a ventilation rate of 0.35 $\left(\frac{\mathrm{l}}{\mathrm{s}\cdot\mathrm{m}^2}\right)$ is used. The average size of a Swedish single-family house is 122 $\mathrm{m}^2$ [87] and the same is considered. The indoor temperature is set to be 20°C [88].

The radiators in the houses considered for the analysis are assumed to be equipped with Purmo radiators of type PURMO C 33 400x1000 [66]. The difference between the water supply and the return temperature in the radiators is set to 10°C unless otherwise stated.

Due to the lack of data availability, houses with floor heating system are also assumed to be equipped with the same radiator type indicated above. However, the number of radiators considered is high in this case, so it can mimic a floor heating system by producing the desired heat at a low supply temperature of 30°C. This value of the supply temperature is experimentally verified for an under floor heating system in [89]. Furthermore, based on the type and number of radiators considered in the current study, at a water supply temperature of 30°C and a return temperature of 25°C, the radiators provide a desired value of heat, mimicking a typical floor heating system. This is verified using the Purmo heat output calculator [90].

**Table 4.4:** Parameters considered for thermal modelling of houses [86][91][72].

| Case | Year of construction | $U_{value}$ $(\frac{W}{m^2K})$ | Time constant $\tau$ (Hours) | Infiltration $(\frac{l}{sm^2})$ | Efficiency of Heat recovery | Heat emitter | Type of heat pump | No. of radiators | No. of houses (in million) |
|---|---|---|---|---|---|---|---|---|---|
| 1 | 1961–1975 | 1.2 | 34 | 0.00 | 0.00 | Radiators | GSHP | 12 | 0.4455 |
| | 1976–1985 | 0.9 | 38* | 0.60 | 0.60 | Radiators | ASHP | 15 | 0.2743 |
| | 1986–1995 | 0.8 | 42* | 0.00 | 0.60 | Radiators | ASHP | 10 | 0.1474 |
| | 1996–2009 | 0.8 | 48* | 0.00 | 0.00 | Floor heating | EASHP | 28 | 0.1056 |
| | >2010 | 0.6 | 53 | 0.80 | 0.00 | Floor heating | EASHP | 46 | 0.1122 |
| 2 | 1961–1975 | 1.4 | 34 | 0.00 | 0.00 | Radiators | GSHP | 15 | 0.4455 |
| | 1976–1985 | 0.9 | 38* | 0.60 | 0.60 | Radiators | ASHP | 15 | 0.2743 |
| | 1986–1995 | 0.9 | 42* | 0.00 | 0.60 | Radiators | ASHP | 15 | 0.1474 |
| | 1996–2009 | 0.8 | 48* | 0.00 | 0.00 | Floor heating | EASHP | 28 | 0.1056 |
| | >2010 | 0.7 | 53 | 0.80 | 0.00 | Floor heating | EASHP | 46 | 0.1122 |
| 3 | 1961–1975 | 1.06 | 34** | 0.8 | 0.60 | Radiators | GSHP | 14 | 0.4455 |
| | 1976–1985 | 0.82 | 40** | 0.8 | 0.60 | Radiators | ASHP | 15 | 0.2743 |
| | 1986–1995 | 0.72 | 50** | 0.8 | 0.60 | Radiators | ASHP | 12 | 0.1474 |

*Interpolated. The estimates of time constants include furniture.

** These are based on the simulation results from reference [8].

GSHP- Ground source heat pump, ASHP- Air source heat pump, EASHP- Exhaust air source heat pump

## Building parameters of a multi-room house

The floor plan of the house considered for the analysis is based on a study from article [92] and is shown in Figure 4.4. The area of all the doors represented is 2.3 $m^2$. The total area dedicated to windows in each room and the details of the radiators considered for the analysis are shown in Table 4.5. The height of the building is 2.5 m and the roof area is equal to the total floor area of the house.

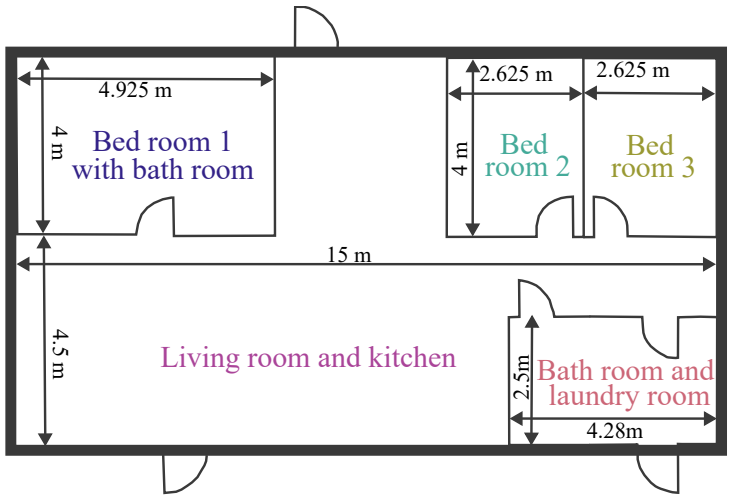


**Figure 4.4:** Floor plan of the house considered for the analysis [92].

**Table 4.5:** Area of the windows and type of PURMO radiators installed in each room.

| Room | Total window area ($m^2$) | Radiator type | Number of radiators |
|---|---|---|---|
| Bedroom 1 | 3.10 | C 33 400x1000 | 2 |
| Bedroom 2 | 1.90 | C 33 400x1200 | 1 |
| Bedroom 3 | 1.90 | C 33 400x1200 | 2 |
| Bath room and laundry | 0.30 | C 33 400x1000 | 2 |
| Living room and kitchen | 9.18 | C 33 400x2000 | 4 |

The specifications and properties of the construction materials used in the exterior walls, roof, internal walls and the floor are shown in tables 4.6 and 4.7, respectively. The thermal resistances for the door and windows are set to 1.4 $\left(\frac{\mathrm{W}}{\mathrm{m^2K}}\right)$.

**Table 4.6:** Specifications of building construction materials used in various building components [92].

| Building component | Material | Thickness (m) |
|---|---|---|
| External Walls | Timber stud | 0.246 |
| | Particle board | 0.013 |
| | Drywall | 0.013 |
| Roof | Mineral wool | 0.35 |
| | Drywall | 0.013 |
| Internal Walls | Drywall | 0.013 |
| | Particle board | 0.07 |
| | Drywall | 0.013 |
| Floor | Concrete | 0.1 |

**Table 4.7:** Properties of the building's construction materials [92].

| Material | Density $\left(\frac{\mathrm{Kg}}{\mathrm{m^3}}\right)$ | Specific heat capacity $\left(\frac{\mathrm{J}}{\mathrm{KgK}}\right)$ | Thermal conductivity $\left(\frac{\mathrm{W}}{\mathrm{m^2K}}\right)$ |
|---|---|---|---|
| Timber stud | 87 | 961 | 0.045 |
| Particle board | 600 | 2300 | 0.14 |
| Drywall | 900 | 1100 | 0.22 |
| Mineral wool | 40 | 800 | 0.042 |
| Concrete | 2300 | 800 | 1.7 |

A ventilation rate of 0.35 $\left(\frac{\mathrm{l}}{\mathrm{s\cdot m^2}}\right)$ and an infiltration rate of 0.6 $\left(\frac{\mathrm{l}}{\mathrm{s\cdot m^2}}\right)$ are used for this multi-room house. Based on reference [93], the thermal resistance due to convection and radiation on the surfaces of the external walls exposed to ambient outdoor air ($R_{air,ext}$) is set at 25 $\left(\frac{\mathrm{W}}{\mathrm{m^2K}}\right)$. The thermal resistance due to convection and radiation on the surfaces of the walls and the floor

facing the indoor air ($R_{int\ wall\ air,in}, R_{floor\ air,in}$) is set to 7.7 $\left(\frac{\mathrm{W}}{\mathrm{m^2K}}\right)$ [93].

Based on the reference [94], [95], the zone capacity multiplier factor is set to 25 for the living room and 15 each for the bedrooms and the bathroom.

## 4.6 Delimitations

The following are the delimitations of the current study:

- The electric power consumption by auxiliary units in a heat pump such as fans and circulation pumps are not included. The electric power consumption of these units is relatively lower compared to the compressor [96].
- The indoor temperature depends on several factors, such as solar irradiation and the activities of the residents. These aspects are excluded from the thermal model of a house to eliminate uncertainty. Internal heat gains and solar heat gains are relatively lower in Swedish residential houses [97].
- The thermal thresholds for quantifying flexibility are based on qualitative interviews conducted in the southern half of Sweden. This study provided a good understanding of the thermal comfort of households and their perspectives on offering flexibility. As the interview results are in limited numbers, statistical generalisations are not possible using a quantitative method such as survey [98].
- Indeed detailed floor plans and interior wall construction materials impact the results. However, in order to keep the result derivation clear and easily reproducible, an entire house is modelled as a one-mass model, as shown in Figure 3.2, in Chapters 5, 6 and 8 . If an entire house is heated to the same temperature, with relatively small internal heat and solar heat gains (which is typical in Sweden), an entire house can be treated as a single thermal zone as described in Section 3.2 [97]. This model is believed to provide a good estimate of indoor temperature based on the input values provided [99] [100].
- Furthermore, in light of detailed knowledge, deterministic models are used to quantify the aggregated flexibility of a million houses. However, it is important to state that five different typical houses equipped with different types of heat pump are considered. Furthermore, a range of

minimum acceptable indoor temperatures stated in interviews is used for flexibility quantification. This helps in obtaining a range of flexibility levels as opposed to a single value.

Using the available data on thermal thresholds and typical thermal properties of houses for simulations can help reflect common operating conditions during different degrees of thermal compromise at various outdoor ambient temperatures. Hence, employing a deterministic approach in this case is beneficial.

## 4.7 Terms used for flexibility quantification

Flexibility is quantified in terms of an instantaneous reduction in power, a duration without electric power consumption, a reduction in electric energy during the flexibility period, and a net reduction in electric energy considering the recovery period with respect to the normal condition. This is shown in Figure 4.5.

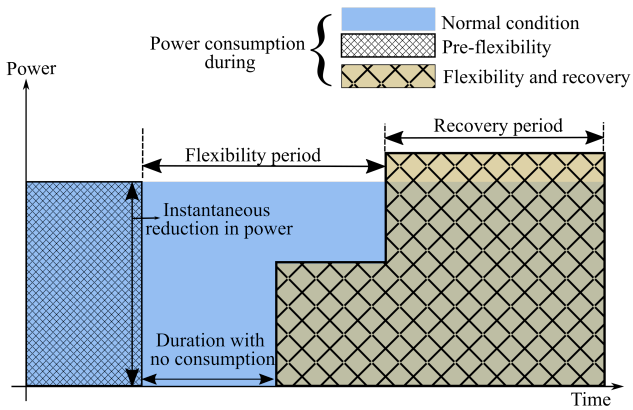


**Figure 4.5:** Terms used for flexibility quantification

The period of time during which the temperatures start to reset to normal conditions is referred to as the recovery period.

# CHAPTER 5

# Flexibility quantification of space heating systems

This chapter is based on the following articles

- **S. K. Nalini Ramakrishna**, T. Thiringer, C. Markusson, "Quantification of electrical load flexibility offered by an air to water heat pump equipped single-family residential building in Sweden," in $14^{th}$ *IEA, Heat pump conference,2023*
- **S. K. Nalini Ramakrishna**, H. Björner Brauer, T. Thiringer, M. Håkansson, "Social and technical potential of single family houses in increasing the resilience of the power grid during severe disturbances," *Energy Conversion and Management*, vol. 321, p.119077, 2024.

## 5.1 Overview

In this chapter, the focus is on quantifying the flexibility of heating systems equipped with heat pumps by blocking water heating. The houses considered for analysis in this study are described in Case 1 of Table 4.4. The setup of the heat pumps is as described in Section 4.3, without vapour injection. An outdoor ambient temperature of -5°C is considered.

## 5.2 Results and discussion

### Indoor temperature range for flexibility quantification

In [98], interviews with residents of single-family houses equipped with heat pumps were conducted. The aim was to study the willingness of residents to compromise thermal comfort, to support the grid in the event of a major power crisis. The result of the interview revealed the willingness of the households to compromise thermal comfort. However, there was no consensus on the minimum acceptable indoor temperature. It was also difficult for some of the respondents to state a temperature drop that they would accept in a power-deficit scenario. Hence, minimum acceptable temperatures varying between 15°C and 18°C are chosen to quantify flexibility, based on the values stated in the interviews.

An advantage of using a range of minimum acceptable indoor temperatures is that a range of flexibility levels is obtained as opposed to a single value.

### Validation of the developed heat pump model

The heat pump model without vapour injection presented in Section 3.1 is validated by comparing the results obtained under standard air conditioning and refrigeration institute (ARI) conditions (i.e., 7.2°C evaporator temperature, 54.4°C condenser temperature, with super heating of 11°C and sub-cooling of 8.3°C) with the data given in [31].

The results are tabulated in Table 5.1 and it is seen that the agreement is good. A discrepancy of 6.7% is observed in the maximum heat delivered. This might be because heat losses in the evaporator are not taken into account. However, the results of the electric power consumption from the model presented agree well with the data provided in [31]. The refrigerant properties at different states are taken from [101].

### Performance comparison of different heat pump types

The performance of three types of heat pumps considered in this study, based on the source temperatures, is shown in Figure 5.1. The source temperatures would be outdoor ambient air, ground temperature, and indoor temperature for ASHP, GSHP, and EASHP respectively. For EASHPs, a water supply temperature of 30°C is chosen as it is mainly used for floor heating in this

**Table 5.1:** Comparison of result obtained with data provided in [31]

| Compressor model | ZPV030 | |
|---|---|---|
| | Given | Obtained |
| Speed (RPM) | 3600 | 3600 |
| Rated Capacity (kW) @ ARI 3600 RPM | 9.7 | 10.35 |
| Electric power input (kW) | 2.98 | 2.94 |
| COP (W/W) | 3.25 | 3.52 |

study. In addition, an indoor temperature varying between 15°C and 20°C is chosen, based on the values stated in the interviews.

As the source temperature for the three different heat pumps is different, the COP as a function of the heat delivered and the water supply temperature is used as a basis of comparison between ASHPs and GSHPs. The COP and heat delivering capability to supply water at 30°C will be used as the basis for comparing ASHPs and GSHPs with EASHPs.

In Figure 5.1, it is observed that the heat delivering capability and COP are higher in EASHPs compared to ASHPs, since the evaporator temperature is higher in the former case, even after considering the temperature drop between the source and the evaporator. The higher the evaporator temperature, the lower the work done by the compressor, thus resulting in a higher COP. However, while EASHPs are compared with GSHPs, the COP and heat delivering capability are relatively closer, because the evaporator temperatures are similar considering the temperature drop between the source and the evaporator.

Upon a comparison of GSHPs and ASHPs, it is noticed that the heat delivering capability and COP are higher in GSHPs because of a higher source temperature. In addition, the capability to supply high water temperatures is greater in GSHPs than in ASHPs.

## Flexibility analysis of a house constructed in 1961-1975

To support the grid during severe power deficit conditions, the space heating is turned off until the indoor temperature drops to 17°C.

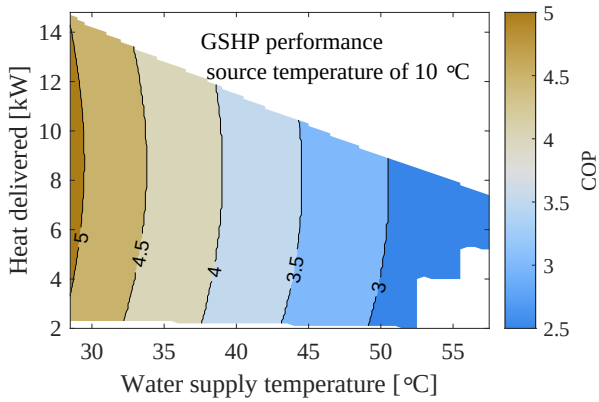


**(a)** Ground source heat pump performance

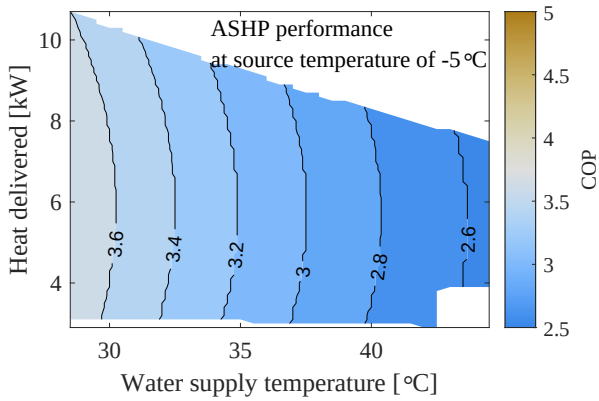


**(b)** Air source heat pump performance

**Figure 5.1:** Performance of ground source, air source and exhaust air heat pumps based on source and sink temperatures.

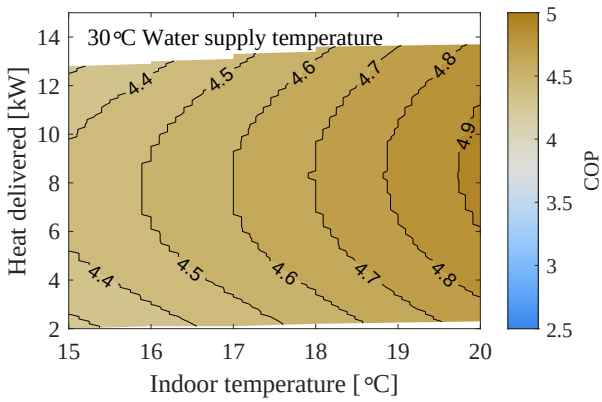


**(c)** Exhaust air heat pump performance with floor heating

**Figure 5.1:** Performance of ground source, air source and exhaust air heat pumps based on source and sink temperatures (continued).

The thermodynamics in the house constructed during 1961-1975, while reducing the indoor temperature to 17°C and during recovery of the same to 20°C, is shown in Figure 5.2. The thermal and physical properties of this house are as indicated in Case 1 of Table 4.4.

From figures 5.2a, 5.2c and 5.2d, it is observed that around 5.1 kW of heat is required to maintain an indoor temperature of 20°C. The supply and return temperature of water to deliver this amount of heat are 43°C and 33°C respectively. The electric power consumption by the GSHP during this condition is 1.4 kW. The corresponding COP and speed of the heat pump are shown in Figure 5.2b.

When the indoor reference temperature reference is changed to 17°C at hour 6.75, in Figure 5.2c it is observed that the consumption of heat and electric power goes to zero for nearly 3.83 hours. This is because the indoor temperature is greater than the reference temperature and, hence, there are no heating requirements. This can also be seen in Figure 5.2d, where the temperature of the water in the radiators eventually decreases and becomes equal to the indoor temperature. Furthermore, in Figure 5.2b, the COP and the speed of the heat pump are zero, indicating that the heat pump is turned off. Thus, during this period, a reduction in electric power of 1.4 kW is offered

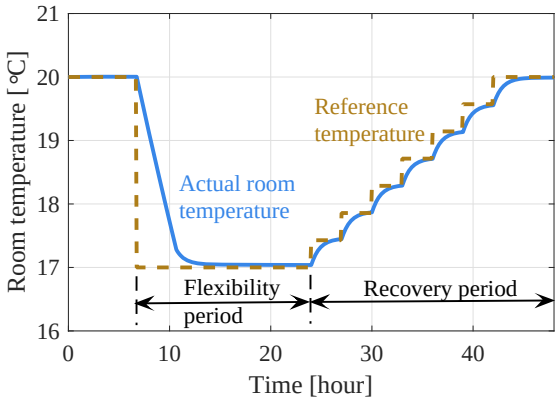


**(a)** Indoor temperature

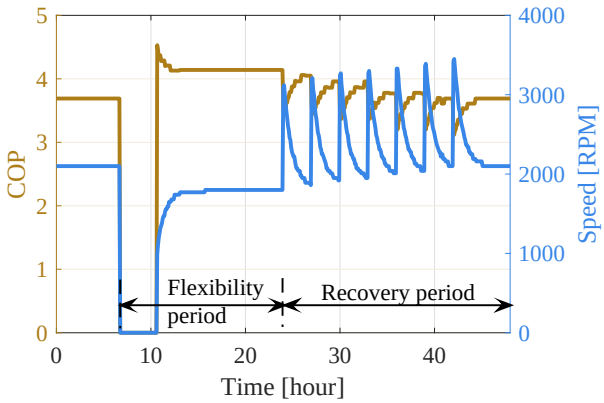


**(b)** COP and speed of the heat pump

**Figure 5.2:** Thermodynamics in a typical house constructed during 1961-1975, equipped with the variable speed ground source heat pump, while offering flexibility and considering slow recovery, at an outdoor ambient temperature of –5°C.

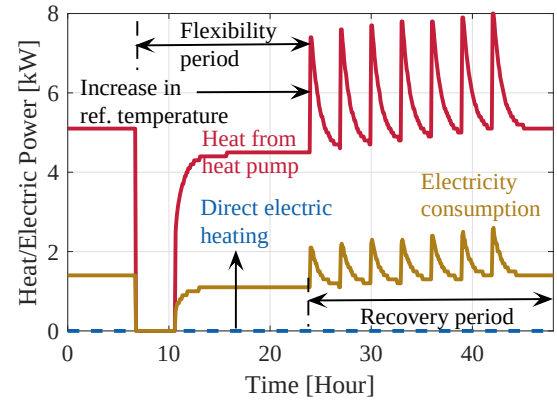


**(c)** Heat and electric power consumption

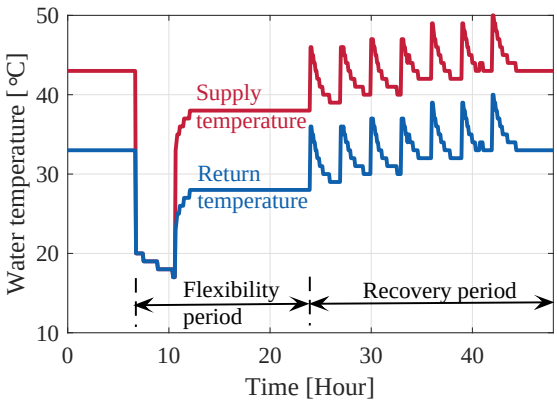


**(d)** Water supply and return temperature

**Figure 5.2:** Thermodynamics in a typical house constructed during 1961-1975, equipped with the variable speed ground source heat pump, while offering flexibility and considering slow recovery, at an outdoor ambient temperature of –5°C (continued).

for a duration of 3.83 hours. Thus, the flexibility in terms of instantaneous reduction in electric power is 1.4 kW. The reduction in electric energy during this period with respect to normal conditions is 5.36 kWh.

When the indoor temperature reaches near the reference temperature at hour 10.6, the indoor temperature controller provides an appropriate signal to the heat pump to produce the required heat, to maintain the indoor temperature at 17°C. During this period, it is observed in figures 5.2d and 5.2b that the COP is initially high and then reduces, since the temperature of the water supply is initially low and then gradually increases until it reaches a steady state value of 38°C. Furthermore, the speed increases gradually and reaches a steady state value of 1800 RPM. During the period between hour 10.6 and hour 24, the consumption of electric power is lower compared to the condition during which the indoor temperature is maintained at 20°C. Consequently, the electric energy consumption is 4.54 kWh lower compared to normal conditions during this period.

The total reduction in electric energy consumption during the flexibility period between hour 6.75 and hour 24 is 9.9 kWh.

During the period after providing flexibility, it is assumed that all the reserves in the power system are restored. The period during which the temperature is gradually brought to 20°C is referred to as recovery period. This is an important aspect to consider, because too high electric energy consumption during this period can strain the power grid, and in Chapter 8 this will be treated in more detail. During this period, the reference temperature is gradually increased in steps. It is noticed that when the reference temperature is increased, there is an increase in the electric power consumption, the heat delivered, water supply temperature, and the speed of the heat pump. As the indoor temperature reaches the reference value, the aforementioned quantities reduce and reach a steady-state value.

The reduction in electric energy until the beginning of the recovery period is 9.9 kWh. During the recovery period, the consumption of electrical energy is 3.55 kWh higher than the consumption of electric energy while maintaining the indoor temperature at 20°C. This means that the net reduction in electric energy consumption is approximately 6.35 kWh.

The flexibility offered in terms of instantaneous reduction in electric power is 1.4 kW and the flexibility in terms of reduction in electric energy is 6.35 kWh compared to the condition, where no flexibility is offered by maintaining

the indoor temperature at 20°C.

If the indoor temperature is directly increased to 20°C at hour 24 by blocking the direct electric heater, the net saving in electric energy would be only 1.15 kWh. This is because the compressor runs at its maximum rating for about 4.67 hours. Also, the water supply temperature is maximum during this condition. This is shown in Figure 5.3. However, it should be noted that the indoor temperature recovers earlier in comparison to resetting the indoor temperature slowly.

An important message is that there is a trade-off between energy savings and compromising thermal comfort. Rapid recovery helps to rapidly recover the indoor temperature. However, the net reduction in electric energy is substantially lower in comparison with slow recovery.

## Validation of the developed thermal model of house

The results obtained from the thermal simulations in Figure 5.3 will be used as a comparison basis for model validation.

The total heat required to maintain an indoor temperature at a given outdoor ambient temperature during a steady state condition is obtained by setting the derivative term in (3.20) to zero.

The value of '$R_{overall}$' is $0.0049\frac{\mathrm{K}}{\mathrm{W}}$, for the house considered for analysis. It is observed that to maintain indoor temperatures at 20°C and 17°C, at an outdoor ambient temperature of -5°C, a heat of 5.1 kW and 4.5 kW are required, respectively. These values obtained using (3.20) are in good agreement with the simulation results in Figure 5.3c. Thus, the model works reasonably well.

The temperature of the water supplied to the radiators, to maintain an indoor temperature of 20°C, is compared to the empirical models defined in [22] and the heating curve defined in [102] to obtain a reasonability check. However, it should be noted that the corresponding information on indoor temperature is missing in the references used for comparison. The comparison results are shown in Table 5.2. The comparison shows that there can be a certain degree of uncertainty in the temperature of the water supplied to the radiators, based on the number of radiators considered for the analysis. Discrepancies of 6% and 8% are found, compared to the empirical models presented in [22]. However, the supply temperature obtained from the simulations in Figure 5.3d perfectly matches the heating curve with a slope of 0.6

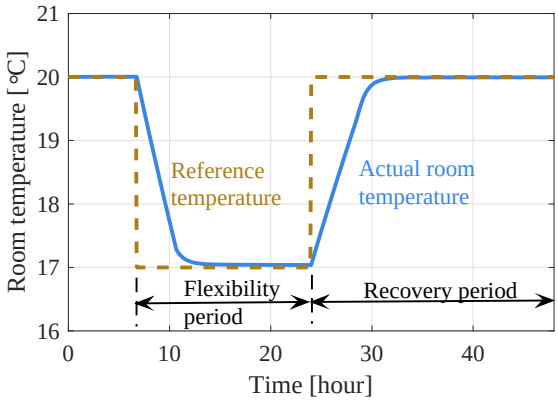


**(a)** Indoor temperature

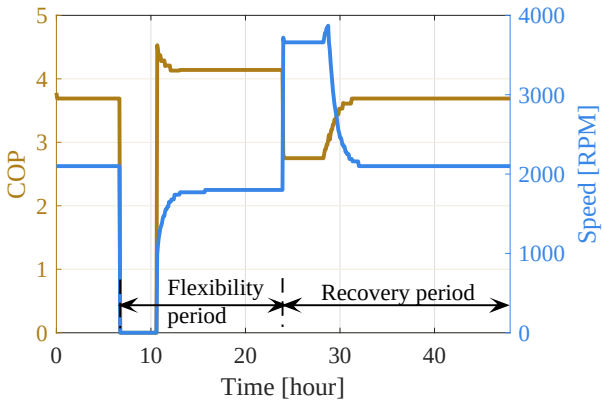


**(b)** COP and speed of the heat pump

**Figure 5.3:** Thermodynamics in a typical house constructed during 1961-1975, equipped with the variable speed ground source heat pump while offering flexibility and considering rapid recovery, at an outdoor ambient temperature of –5°C.

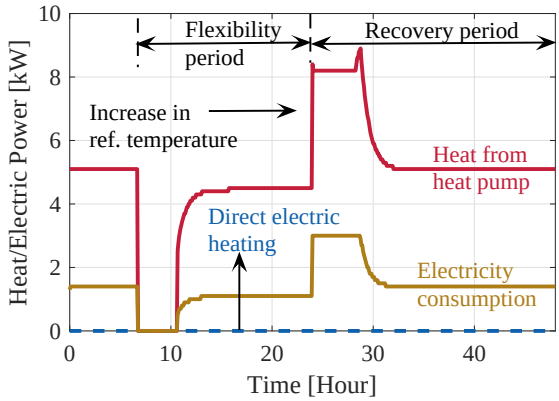


**(c)** Heat and electric power consumption

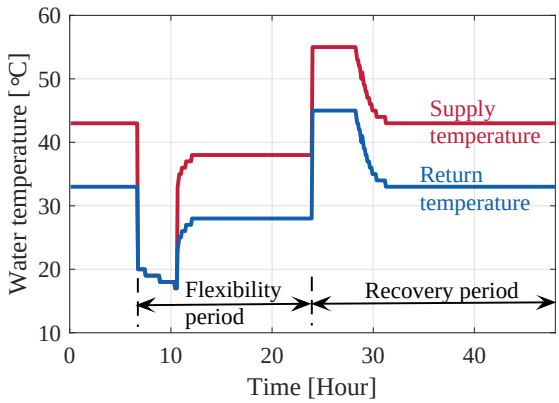


**(d)** Supply and return temperature of water

**Figure 5.3:** Thermodynamics in a typical house constructed during 1961-1975, equipped with the variable speed ground source heat pump while offering flexibility and considering rapid recovery, at an outdoor ambient temperature of –5°C (continued).

**Table 5.2:** Comparison of the expected water supply temperature in radiators at an outdoor ambient temperature of -5°C, available in literature with the current study

| Reference | Heat emitter type | $T_{supply}$[°C] | Discrepancy |
|---|---|---|---|
| [22] | A-10/W51 | 46.8 | 8% |
| | A-10/W44 | 40.5 | 6% |
| [102] | Radiator | 43.0 | 0% |

presented in [102].

The heat emitted by the radiators based on the water supply and return temperature, to maintain an indoor temperature of 20°C and 17°C, can be calculated using the model represented in Figure 3.4. By regulating the mass flow rate at the stated water supply temperature, the heat delivered by radiators matches the value of 5.1 kW and 4.5 kW, respectively. Thus, the integrated model of the house works as desired.

## Fixed speed versus variable speed ground source heat pump

The house constructed during 1961-1975 under Case 1 in Table 4.4 is considered for analysis. This house is assumed to be equipped with the fixed speed GSHP used in [103]. The thermodynamics in the house, while reducing the indoor temperature to 17°C, is shown in Figure 5.4. It is observed that room temperature cannot be controlled exactly at the reference temperature, as in the case of the variable speed heat pump. This is because the heat produced is higher than the desired value. As a result, the heat pump is turned on and off. This can be seen in figures 5.4a, 5.4b and 5.4c.

The electric power consumption by the fixed speed GSHP, when maintaining the indoor temperature around 20°C is 2.3 kW. This is 0.9 kW higher than that of the variable speed heat pump under study. Furthermore, to maintain an indoor temperature of 17°C, the electric power consumption is 1.1 kW and 2.2 kW for the variable and fixed speed heat pumps under study, respectively.

In this case, the average electric power consumption of the traditional fixed speed heat pump is comparable with the variable speed heat pump, while maintaining indoor temperatures at 20°C and 17°C respectively. Typically,

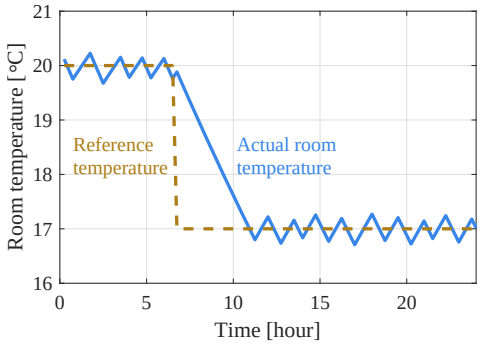


**(a)** Indoor temperature

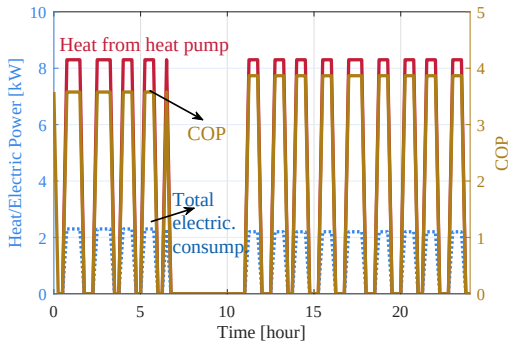


**(b)** Heat and electric power consumption

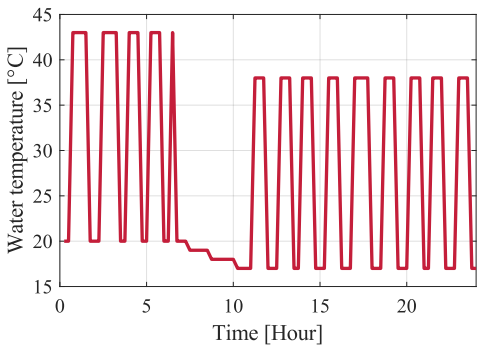


**(c)** Supply temperature of water

**Figure 5.4:** Thermodynamics in a typical house constructed during 1961-1975, equipped with the fixed speed ground source heat pump dealt in [103].

the average electric power consumption for fixed speed heat pumps is higher than that of variable speed heat pumps.

## Quantification of flexibility from space heating systems

The total consumption of electric energy in the houses stated in Case 1 of Table 4.4, when the indoor temperature is maintained at 20°C, is shown in Figure 5.5a. The corresponding flexibility in terms of instantaneous reduction in electric power is shown in Figure 5.5b. This figure indicates the possible instantaneous reduction in electric power by space heating systems in all houses equipped with the heat pumps under study. It should be noted here that the consumption of electric energy and flexibility is also dependent on the number of houses. For example, the number of houses constructed during 1961-1975 is the highest compared to other groups of houses. If these plots are seen on an individual house level, the electric energy consumption and thereby flexibility potential are the highest in the house belonging to the category 1976-1985.

The trend of flexibility in terms of instantaneous reduction in electric power is similar to Figure 5.5a, as it depends on the consumption of electric energy. The higher the consumption, the greater the flexibility potential. However, a low flexibility potential indicates a higher energy efficiency.

The reduction in electric energy during the flexibility period and considering the recovery period with slow and fast recovery are shown in figures 5.6 and 5.7. It is observed that, as the degree of thermal compromise increases, a higher reduction in electric energy is obtained during flexibility, as well as considering the recovery period. It is observed that the net reduction in electric energy is lower in the case of rapid recovery compared to slow recovery. However, indoor temperature recovered earlier with rapid recovery.

## Quantification of temporal flexibility potential

The quantification of the flexibility potential on a system level, during the flexibility and recovery periods, is based on the following assumptions

- The initial indoor temperature in all the houses under study is 20°C.
- The signals for indoor temperature set points during flexibility and recovery periods in all the houses under study are synchronised.

The flexibility potential during the reduction of indoor temperatures from

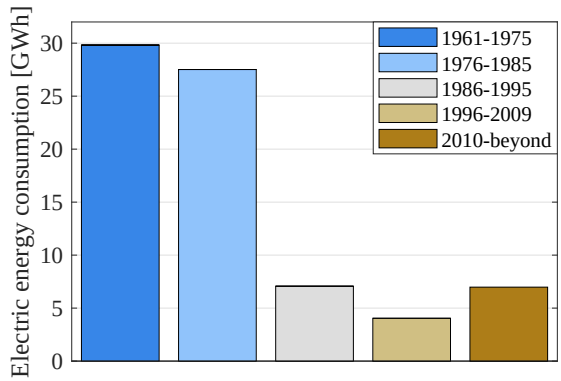


**(a)** Electric energy consumption during normal conditions

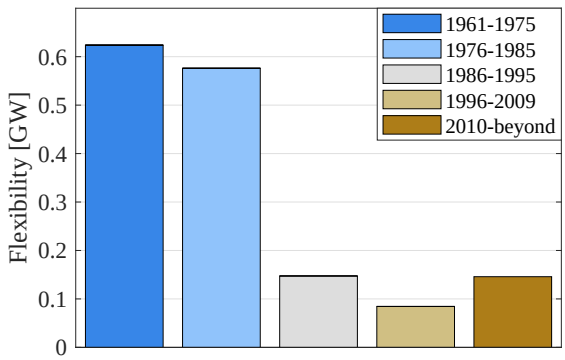


**(b)** Flexibility in terms of instantaneous reduction in electric power

**Figure 5.5:** Total electric energy consumption and flexibility potential of different houses considered in the study, at an outdoor ambient temperature of –5°C.

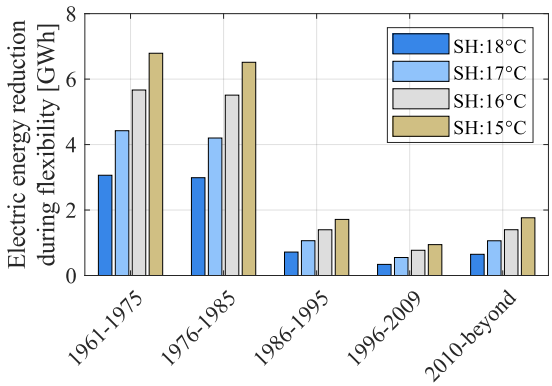


**Figure 5.6:** Electric energy reduction when maintaining various indoor temperatures during flexibility period, at an outdoor ambient temperature of –5°C. (SH:Space heating).

20°C to values between 15°C and 18°C in about a million single family houses, considering the slow and rapid recovery of indoor temperatures, is shown in figures 5.8 and 5.9 respectively. From figures 5.8 and 5.9, it is observed that the flexibility potential from space heating is a function of time, and with time the amount of flexibility reduces. If all houses considered in the study agree to have an indoor temperature of 18°C, the flexibility in terms of instantaneous reduction in electric power is 1.6 GW and this can be offered for 2.33 hours. If the indoor temperature is reduced to 17°C, 16°C and 15°C, flexibility of 1.6 GW can be offered for 3.83 hours, 5.42 hours and 7.1 hours, respectively. The value of 1.6 GW represents about 7% of the total plannable power in Sweden [104]. Thus, the Swedish power system has the potential to be resilient toward a power deficit condition of almost 1.6 GW by temporarily compromising the indoor temperature and in addition with fairly moderate reductions.

During the recovery period, it is observed that flexibility becomes negative, indicating high electric power consumption compared to normal conditions. However, towards the end of the recovery period, the flexibility level goes again to zero. During the recovery period, it is important to note that the trend in flexibility changes for slow and rapid recovery. During a slow recovery, the duration of time for which the flexibility is negative is shorter than that of a fast recovery. Thus, the savings in electric energy are greater considering

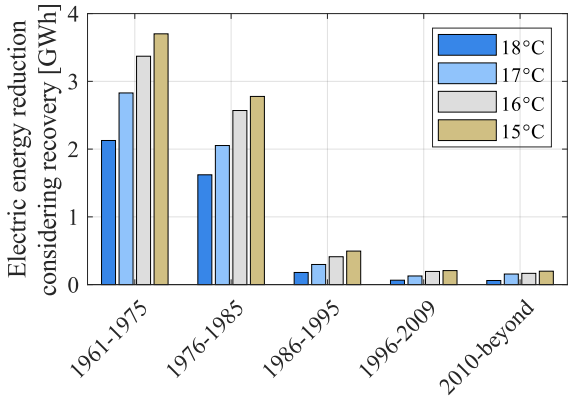


**(a)** Net electric energy reduction with slow recovery

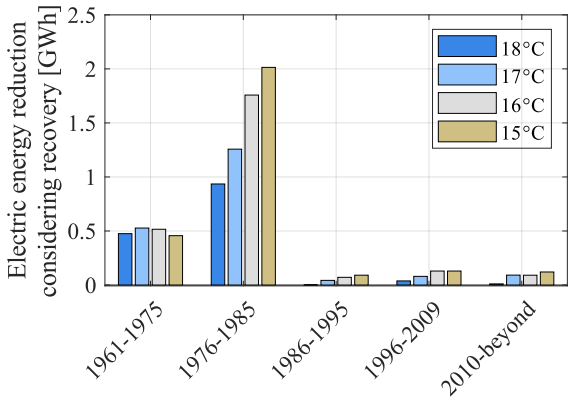


**(b)** Net electric energy reduction with rapid recovery

**Figure 5.7:** Net reduction in electric energy considering various indoor temperatures during flexibility period, along with slow and rapid indoor temperature recovery, at an outdoor ambient temperature of –5°C.

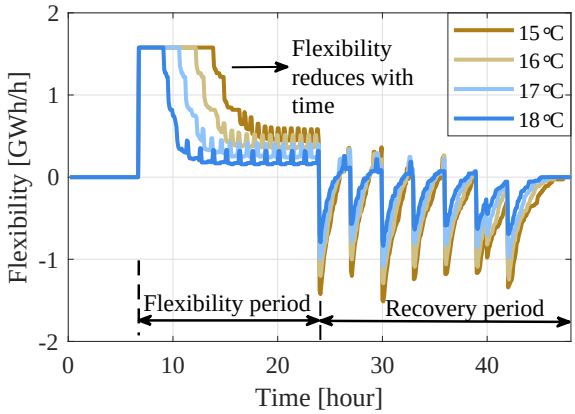


**Figure 5.8:** Estimated flexibility potential considering slow recovery, at an outdoor ambient temperature of –5°C.

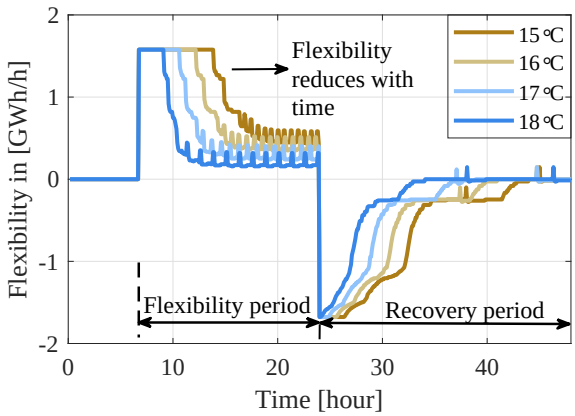


**Figure 5.9:** Estimated flexibility potential considering rapid recovery, at an outdoor ambient temperature of –5°C.

a slow recovery. These flexibility quantification plots can serve as valuable information for power system planning and operation to make informed decisions during severe power shortage conditions. However, it should be noted that these plots are obtained by an aggregation of one million houses. Recovery in these houses should be coordinated so that there are no additional disturbances in the grid due to power peaks.

## 5.3 Conclusions

A reproducible and adaptable model of a variable speed heat pump without vapour injection is developed. This model accounts for the limitations posed by the compressor's operating envelope.

The electric power consumption of the heat pump is estimated to maintain the indoor temperature at a set value. This is realised by integrating the thermal model of a house with the heat pump model and the radiator model.

The flexibility potential is quantified based on the minimum acceptable indoor temperatures stated in the interviews presented in [98]. As a range of minimum acceptable indoor temperature is used for simulations, a flexibility range is obtained as opposed to a single value.

The flexibility potential in terms of instantaneous reduction in electric power is estimated to be 1.6 GW (7% of the total plannable power in Sweden) in about a million single family houses in the southern half of Sweden, at an outdoor ambient temperature of -5°C. This potential is independent of the degree of thermal compromise. Thus, the Swedish power system has the potential to be resilient to a power deficit condition of almost 1.6 GW for a duration between 2.33 and 7.1 hours by temporarily compromising the indoor thermal comfort between 18°C and 15°C respectively.

# CHAPTER 6

# Flexibility quantification of space and water heating systems

This chapter is based on the following articles

- **S. K. Nalini Ramakrishna**, T. Thiringer, "Domestic hot water heat pump: Modelling, analysis and flexibility assessment," $15^{th}$ *Asia-Pacific Power and Energy Engineering Conference (APPEEC), Chiang Mai, Thailand, 2023*, pp. 1-5, doi: 10.1109/APPEEC57400.2023.10562015.
- **S. K. Nalini Ramakrishna**, T. Thiringer, P. Chen, "Potential of single family houses to reinforce resilience in a large scale power system during severe power deficit conditions," *Submitted for second-round review, Energy Conversion and Management: X, 2025.*

## 6.1 Overview

In this chapter, the focus is on quantifying flexibility of space and water heating systems equipped with heat pumps, in Swedish single-family houses. The houses considered for analysis in this study are described in Case 2 of

Table 4.4. The setup of the heat pumps and domestic hot water tank is as described in sections 4.3 and 4.4 respectively.

## 6.2 Results and discussion

In this study, flexibility is quantified for outdoor ambient temperatures varying between -10°C and 10°C, as this represents typical autumn-winter-spring situations in the Nordics. The indoor and water temperature in the tank is set at 20°C and 55°C, respectively, under normal conditions. The interview study revealing the willingness of residents to compromise thermal comfort in the event of a major power crisis to avoid blackouts exists [98]. Thus, the flexibility potential is estimated by turning off the heating, until the indoor temperature of 20°C reaches 18°C, 17°C, 16°C and 15°C respectively. Correspondingly, the water temperature in the tank is reduced from 55°C to 50°C, 48°C, 46°C, and 44°C respectively. At hour 6.75, an event occurs in the power system that requires emergency power support and thus the temperatures for space and water heating are reduced to support the grid.

### Heat pump

The performance of the air source heat pump with EVI operation is shown in Figure 6.1. Higher condenser temperatures can be achieved with this mode, in particular at low outdoor temperatures compared to operating in the non-EVI mode [98]. The water supply temperature depends on whether the heat pump provides space or water heating. Furthermore, in space heating, it depends on the type of heating, i.e., floor heating or radiator heating. The condenser temperature should be higher than the desired water supply temperature.

As the outdoor ambient temperature falls, the COP also reduces accordingly, resulting in an increase in the electric power consumption. This is important since, typically it is under cold conditions that the power system could be operated with small margins.

From the representation point of view, water supply temperatures of 60°C, 45°C and 30°C are selected. COP as a function of the heat delivered and outdoor ambient temperature, during above conditions is shown in Figure 6.2. The heat delivering capacity increases with an increase in the outdoor ambient temperature. Furthermore, for a given outdoor ambient temperature, the heat

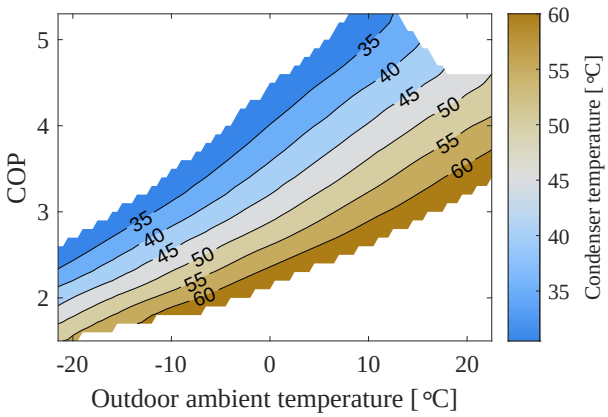


**Figure 6.1:** Condenser temperature as a function COP and outdoor ambient temperature for the air source heat pump.

delivering capacity increases as the water supply temperature decreases.

## Fixed speed versus variable speed air source heat pump

The house constructed during 1976-1985 with the properties dealt with in Case 2 of Table 4.4, is assumed to be equipped with the fixed speed heat pump described in reference [21], in one case. In the second case, it is assumed that the same house is equipped with the variable speed heat pump, described in Section 6.2. The outdoor ambient temperature is set to -10°C.

The performance comparison between the fixed speed heat pump and the variable speed heat pump, when the reference indoor temperature is at 20°C and when changed to 17°C, is shown in Figure 6.3.

Figures 6.3a and 6.3b show that the indoor temperature can be accurately maintained at 20°C, using the variable speed heat pump as opposed to the fixed speed heat pump. This is because the heat delivered by the variable speed heat pump can be adjusted as per the requirements, by modulating the speed of the heat pump. As a result, the heat pump does not need to be turned on and off, as in the case of the fixed speed heat pump. This can be observed in figures 6.3c, 6.3d and 6.3e, 6.3f. It is observed that even though the water supply temperature is the same in both cases, the electric power

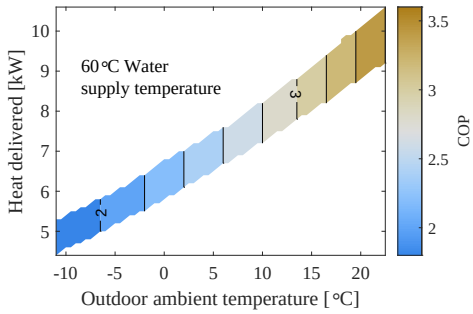


**(a)** Water supply temperature at 60°C

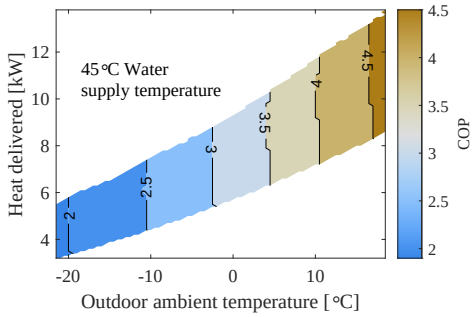


**(b)** Water supply temperature at 45°C

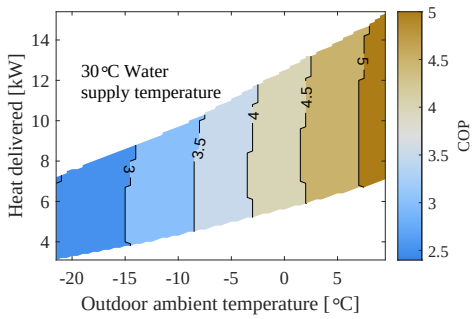


**(c)** Water supply temperature at 30°C

**Figure 6.2:** Heat delivering capability of the air source heat pump with EVI, while supplying water at 60°C, 45°C and 30°C.

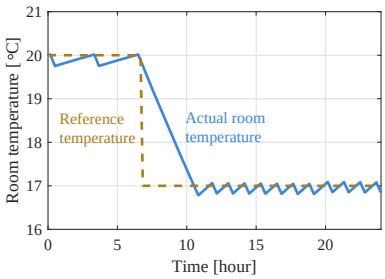


**(a)** Indoor room temperature variation, when equipped with the fixed speed heat pump

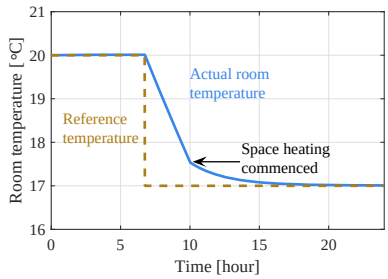


**(b)** Indoor room temperature variation, when equipped with the variable speed heat pump

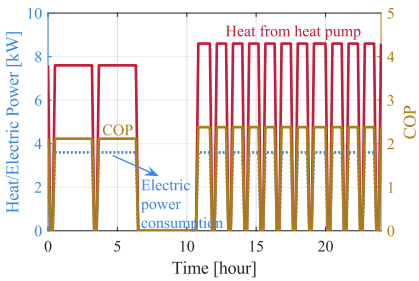


**(c)** Heat delivered, electric power consumption and COP of the fixed speed heat pump

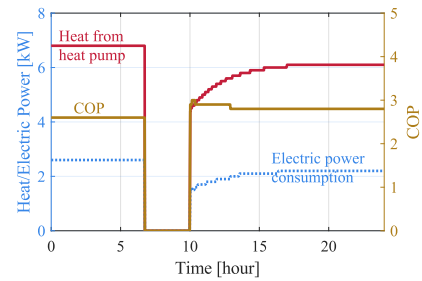


**(d)** Heat delivered, electric power consumption and COP of the variable speed heat pump

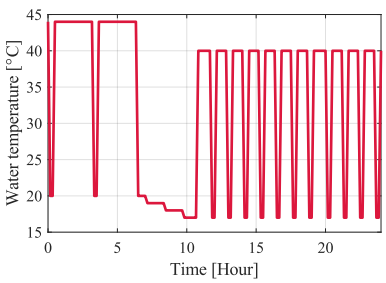


**(e)** Water supply temperature, when equipped with the fixed speed heat pump

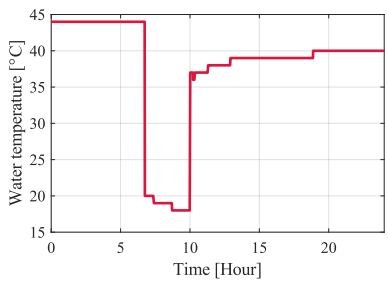


**(f)** Water supply temperature, when equipped with the variable speed heat pump

**Figure 6.3:** Performance comparison between the fixed speed heat pump in [21] and the variable speed heat pump under study.

consumption of the variable speed heat pump is 1 kW lower than that of the fixed speed heat pump. The average electric power consumption of the fixed speed heat pump is 19% higher compared to the variable speed heat pump.

When the reference value of indoor temperature is changed to 17°C, the electric power consumption of both heat pumps is zero, only until the controller output is zero. Later, in the case of the variable speed heat pump, the electric power consumption is reduced as the heating requirements are lower compared to maintaining the indoor temperature at 20°C. However, this is not the case with the fixed speed heat pump. The electric power consumption remains the same as while maintaining the indoor temperature at 20°C.

This comparison shows that the quantification of flexibility in terms of power would be higher for fixed speed heat pumps compared to variable speed heat pumps.

A very important conclusion is thus that, since variable speed heat pumps are expected to take over in the future, the flexibility potential will be overestimated if fixed speed heat pumps are used in these types of studies.

## Flexibility analysis of a typical house constructed in 1976-1985

With the objective of supporting the power system with severe power deficit conditions, the heating is turned off until the indoor temperature and the water temperature in the domestic hot water tank reaches 17°C and 48°C, in the house under study.

The thermodynamics in the house at -10°C outdoor temperature, while providing flexibility, by reducing the indoor temperature to 17°C and the water temperature in the tank to 48°C is shown in Figure 6.4. Before changing the reference temperatures, it is observed in Figure 6.4b, that the indoor temperature is not exactly maintained at 20°C, although a variable speed heat pump is used. This is because the variable speed heat pump can only provide either space or water heating at a time. When the variable speed heat pump is in water heating mode, there is a slight decrease in indoor temperature with respect to the reference value, and this is seen in figures 6.4a, 6.4b and 6.4c. In Figure 6.4c, it is observed that there is a spike in the condenser temperature, supply, and return temperature of water during the water heating mode, as higher temperatures are required for heat transfer.

Furthermore, it is observed that the water temperature in the tank is not

uniform as a stratified model of the domestic hot water tank is considered. All layers in the tank follow a similar trend except for the temperature in layer 'TL-10', since cold water enters this layer every time hot water is extracted. In addition, there is no heating element in this layer. The period of time during which there is no withdrawal of hot water (at night between hour 0 and hour 4), temperature in layer 'TL-10' increases mainly because of heat transfer from the top layers in the tank, and accordingly the temperature of the water in the top layers reduces.

When the reference temperature of space and water heating is reduced at hour 6.75, there is no electric power consumption for nearly 3.2 hours, due to the thermal inertia of the building and the hot water tank. This can be seen in Figure 6.4d. Furthermore, it is observed that there is no water heating provided as the temperature in layer 'TL-2' (temperature sensor is placed in this layer) is above the reference temperature, although the temperature of water is lower in the subsequent layers. This shows the significance of using a stratified model for a domestic hot water tank in flexibility studies. Thus, the house provides a flexibility of 2.68 kW, in terms of an instantaneous reduction in power for nearly 3.2 hours.

After 3.2 hours, the variable speed heat pump starts again to maintain the temperatures at the reference levels. It is observed that the supply temperature of the water is reduced when the reference temperatures for space and water heating are reduced. This is because of the reduced heating requirements. Consequently, the corresponding electric power consumption is also reduced. Furthermore, in Figure 6.4e, it is seen that COP reduces with increasing condenser temperature because the compressor has to do more work and this is evident especially during water heating. The speed of the variable speed heat pump corresponding to the COP is shown in Figure 6.4f. Compared to the normal condition, the electric energy consumption is 20 kWh lower during the flexibility period starting from hour 6.75 until hour 24.

An important aspect to account for is the power needed to restore the situation to a fully normal state. During the recovery period, if the objective is to limit the electric power and energy consumption, the reference temperature should preferably be increased in steps. The reason is that, at an outdoor ambient temperature of -10°C, the heat delivering capability is lower, as seen in Figure 6.2. Thus, if there is a higher heating requirement, additional electric heating must be used. However, despite gradually increasing the reference

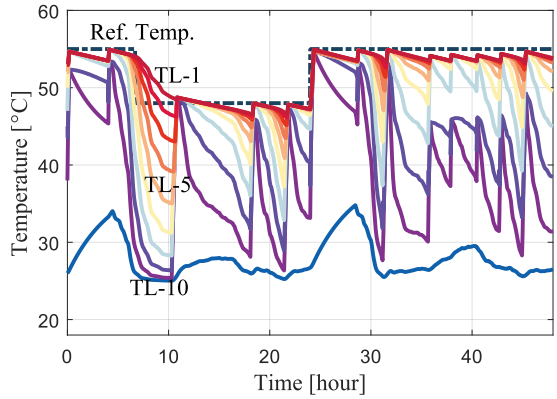


**(a)** Temperature of water in different layers of the hot water tank

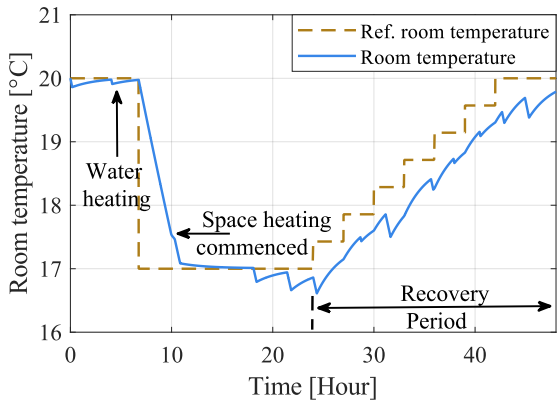


**(b)** Variation in indoor room temperature and reference temperature

**Figure 6.4:** Thermodynamics in the house constructed during 1976-1985 equipped with the air source heat pump at an outdoor ambient temperature of –10°C.

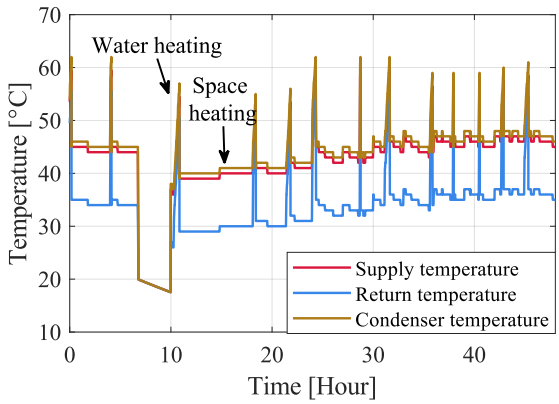


**(c)** Condenser, supply, and return temperature of water

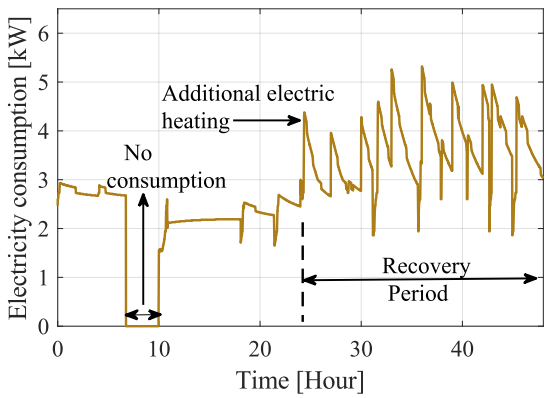


**(d)** Electric power consumption

**Figure 6.4:** Thermodynamics in the house constructed during 1976-1985 equipped with the air source heat pump at an outdoor ambient temperature of –10°C (continued).

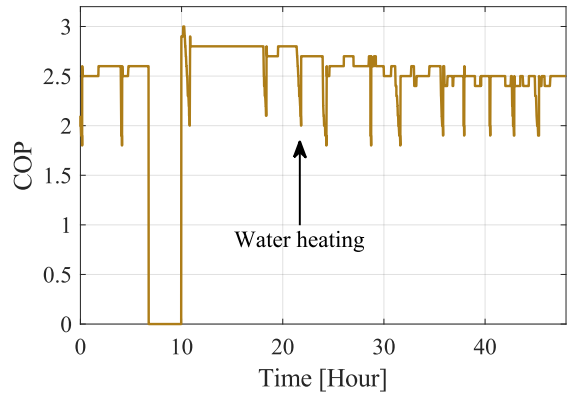


**(e)** COP of the heat pump

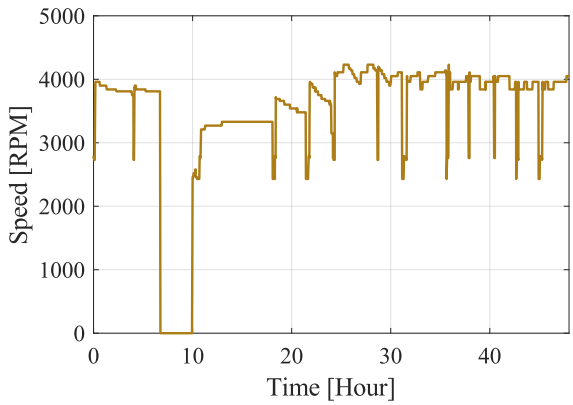


**(f)** Speed of the heat pump

**Figure 6.4:** Thermodynamics in the house constructed during 1976-1985 equipped with the air source heat pump at an outdoor ambient temperature of –10°C (continued).

temperature, additional electric heating is used as seen in Figure 6.4d. However, in this case, the peak value of the power consumed is lower, compared to the case when the reference temperature is increased directly to 20°C.

Until the beginning of the recovery period, the electric energy consumption is 20 kWh lower compared to the normal condition. During the recovery period, the electric energy consumption is 16.48 kWh higher than in normal conditions. Thus, the net reduction is around 3.5 kWh.

If the reference temperature is directly increased to 20°C, an additional electric energy use of 11.5 kWh occurs with respect to the normal condition and, instead of energy savings, energy loss is obtained.

The reference temperature for water heating is not increased in steps as the heating energy requirements are not as high compared to space heating.

## Performance comparison with empirical heat pump models

Figures 6.5a and 6.5c show the comparison of COP and electric power consumption of the variable speed air to water heat pump under study (excluding the recovery period) with the empirical models described in [22],[27]. Empirical models are based on outdoor ambient temperatures and water supply temperatures. However, it should be noted that the heat pump parameters described in Section 4.3 are missing in the empirical models.

It is observed that the COP obtained from [22], matches well with the current study, as opposed to the COP obtained from [27]. However, while looking at the electric power consumed, it is observed that the actual consumption in [22] is lower compared to the current study, as the heat delivering capability at an outdoor ambient temperature of -10°C is limited to 4.5 kW. This can be seen in figures 6.5b and 6.5c. The reason for the limitation in the capacity to deliver heat [22] and the COP values obtained from the empirical models used in [22] and [27] are unknown.

Thus, using physics-based models makes flexibility quantification clear and transparent as opposed to empirical modelling.

## Flexibility quantification

Flexibility is analysed and quantified for all houses described in Case 2 of Table 4.4, by reducing the temperatures of space and water heating. The quantification of flexibility at the individual house level is shown in Table

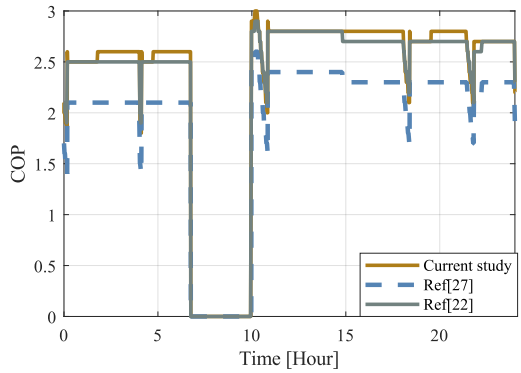


**(a)** Comparison of COP

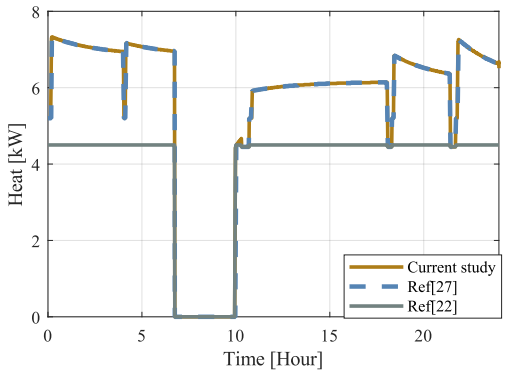


**(b)** Comparison of heat delivered

**Figure 6.5:** Comparison of COP, heat delivered and electricity consumption by the heat pump in the study with the heat pumps in [22] and [27].

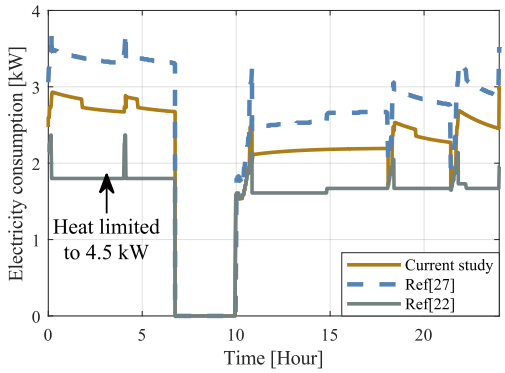


**(c)** Comparison of electricity consumption

**Figure 6.5:** Comparison of COP, heat delivered and electricity consumption by the heat pump in the study with the heat pumps in [22] and [27]. (continued).

6.1. As expected, the flexibility potential in terms of power is observed to be higher in houses that are less energy efficient. Among the houses constructed during 1996 and 2010, the latter has a high value of flexible power due to high infiltration loss. In addition, among the houses constructed during 1961 and 1976, the latter has a high value of flexible power, as it is equipped with the air to water heat pump, which is less efficient compared to the ground source heat pump.

In all categories of houses under study, a positive net reduction in electric energy is observed. The reduction in electric energy during the flexibility period increases with an increase in the degree of thermal compromise. However, the net reduction in electric energy depends on the electric energy consumption during the recovery period. In the case of houses with high efficiency, where the use of direct electric heating is lower during the recovery period, the net reduction in electric energy increases with a higher compromise in thermal comfort, for instance, in houses constructed during 1986-2009. In contrast, if there is a higher utilisation of direct electric heating (typically in houses with limited heating capacity from the heat pump), for instance, in houses constructed during 1976, the net reduction in electric energy decreases with an increase in the compromise of thermal comfort. Thus, the net reduc-

tion in electric energy in a specific house category during different degrees of thermal compromise varies from case to case.

**Table 6.1:** Flexibility quantification in the houses under study. (SH:Space heating, WH:Water heating).

| Construction year of house | Electric energy reduction (kWh) including recovery period, at -10°C outdoor temperature | | | | Flexibility (kW) |
|---|---|---|---|---|---|
| | SH:18°C, WH: 50°C | SH:17°C, WH: 48°C | SH:16°C, WH: 46°C | SH:15°C, WH: 44°C | |
| 1961-1975 | 3.9 | 6.1 | 5.9 | 6.1 | 1.8 |
| 1976-1985 | 3.8 | 3.5 | 2.8 | 0.7 | 2.7 |
| 1986-1995 | 4.0 | 6.1 | 7.3 | 8.2 | 1.6 |
| 1996-2009 | 0.8 | 1.5 | 2.3 | 3.0 | 1.0 |
| 2010- beyond | 1.3 | 2.4 | 2.8 | 0.7 | 1.6 |

The quantification of the electric power consumption by heat pumps on a system level, during the flexibility and recovery periods, is based on the following assumptions

- The initial indoor temperature in all the houses under study is 20°C.
- The signals for indoor temperature set points during flexibility and recovery periods in all the houses under study are synchronised.

The average consumption of electric power at the system level, during the pre-flexibility, flexibility and recovery period, respectively, for two example cases with respect to the normal condition, at an outdoor ambient temperature of -10°C, is shown in Figure 6.6. During the flexibility period, the average consumption is obtained from the instant the electric power consumption starts until the beginning of the recovery period. The average consumption is considered due to the aggregation effect of one million houses. These plots serve as valuable information for power balancing. As anticipated, it is observed that the duration of time for which there is no electric power consumption increases with an increase in the reduction of temperatures for space and water heating. The same holds true when considering the reduction in electric power consumption while offering flexibility. The average consumption of electric power during the recovery period increases in cases with a higher reduction

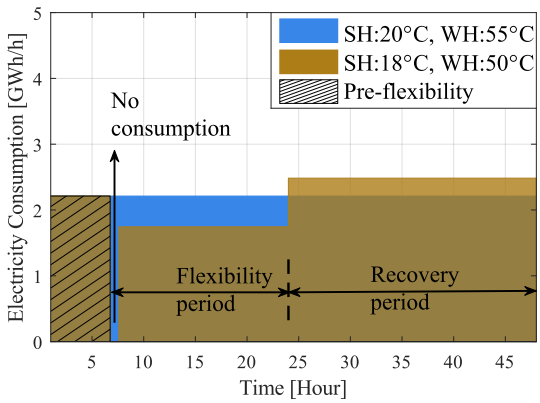


**(a)**

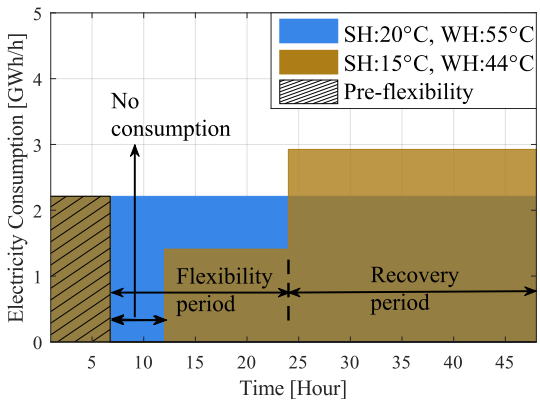


**(b)**

**Figure 6.6:** Electricity consumption on a system level during different set point temperatures at an outdoor ambient temperature of -10°C. (SH:space heating, WH: water heating).

in temperature during the flexibility period. This is because the amount of work done by the heat pump, when recovering the indoor and water temperatures to normal conditions within a period of 24 hours, is higher in the above case. However, flexibility in terms of an instantaneous reduction in power is the same in all cases and is independent of the reference temperatures set for space and water heating during the flexibility period.

## Flexibility quantification during different conditions

The results of the flexibility analysis with respect to the normal case are consolidated and shown in Figure 6.7. In Figure 6.7a, it is seen that for a normal case, the consumption of electric energy for space heating and water heating is reduced with increasing outdoor ambient temperature. Accordingly, the amount of flexibility that can be offered in terms of instantaneous reduction in electric power decreases. The reduction in electric energy, while offering flexibility and considering recovery period, increases with an increase in the degree of thermal compromise, in the majority of the cases. This is observed in Figure 6.7b.

The duration of time with zero electric power consumption during the flexibility period, for various degrees of thermal compromise, at outdoor ambient temperatures ranging between -10°C and 10°C is shown in Figure 6.7c. The flexibility in terms of an instantaneous reduction in electric power is also shown in this figure. According to data in [105] and Figure 6.7c, it is inferred that from the perspective of endurance and flexibility volume, single-family houses in Sweden have the potential to contribute to frequency containment and restoration reserves.

## Frequency support using flexibility from heat pumps

The total flexibility of heating systems equipped with heat pumps in houses built after the 1960s in the southern half of Sweden is quantified. This represents 54.25% of the total single-family houses in Sweden. The flexibility potential at -10°C outdoor temperature is estimated to be 2.1 GW. As the Nordic-32 bus system is a down-scaled version of the actual Swedish power system, the flexibility also needs to be scaled down accordingly. The peak demand in Sweden during the years 2022-2023 was 25 GW and the peak load in the modified Nordic-32 bus system is 7.74 GW. The corresponding flexibility

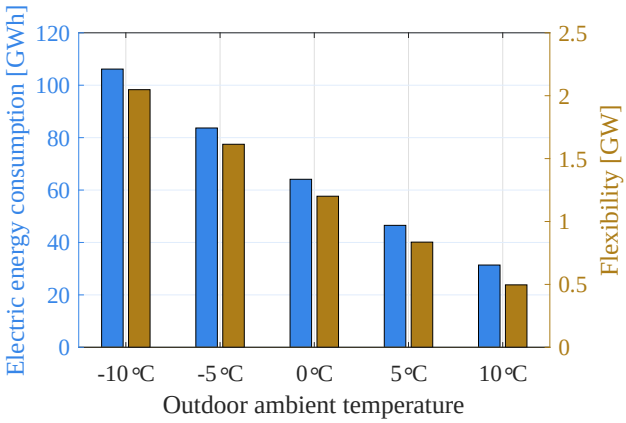


**(a)** Energy consumption for normal case with associated flexibility levels

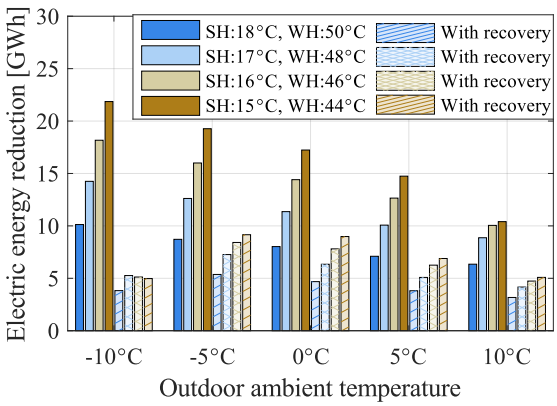


**(b)** Electric energy reduction

**Figure 6.7:** Consolidated results from flexibility analysis (SH: space heating, WH: water heating).

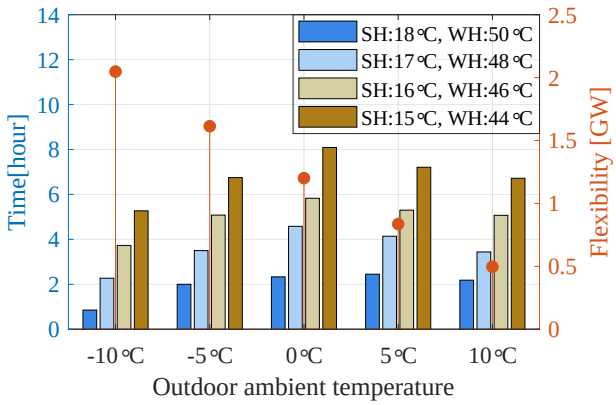


**(c)** Duration of time with zero electric power consumption

**Figure 6.7:** Consolidated results from flexibility analysis.(SH: space heating, WH: water heating) (continued).

level for this modified test system would be approximately 650 MW, which is about 8.4% of the total load in the system.

In the modified Nordic-32 bus system explained in Section 4.2, during the loss of the generating unit G8, producing 950 MW, the frequency deviation reaches below 48 Hz as seen in Figure 6.8. To study the impact of flexibility in improving frequency nadir, it is assumed that local frequency sensors with a filter time constant of 0.1 $\frac{\text{sec}}{\text{rad}}$ are present in all heat pumps. The heat pumps are disconnected from the power supply when a frequency of 49.5 Hz is sensed. The impact of flexibility at different levels, ranging from 50% to 100% on the frequency nadir, is shown in Figure 6.8. It is observed that by using at least 70% of the estimated flexibility, it is possible to limit the frequency nadir to stay above 48.8 Hz, else the under-frequency load shedding scheme is triggered. 70% of the estimated flexibility corresponds to about 5.9% of the total load in the system.

## 6.3 Conclusions

A flexible physics-based model of the heat pump with vapour injection technology is developed to obtain the electric power consumption under various op-

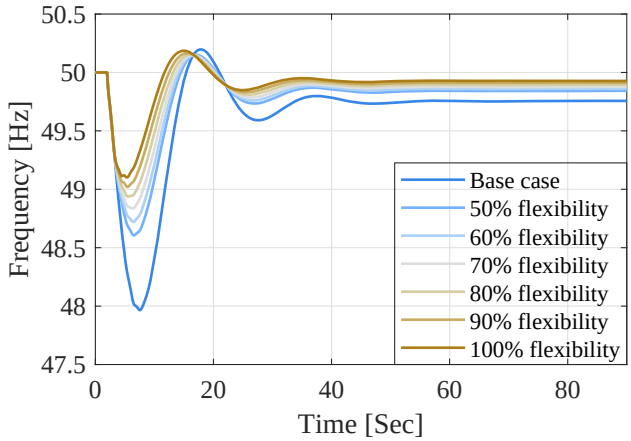


**Figure 6.8:** Impact of flexibility on frequency nadir.

erating conditions considering operational limitations. This is a reproducible and adaptable physics-based model that is not data-demanding and can be conveniently adapted to any operational condition. In addition, an integrated model is developed that involves detailed representations of the heat pump, space heating, and water heating to estimate the electricity consumption under various operating conditions.

It is demonstrated that the flexibility potential will be overestimated if fixed speed heat pumps are used. In addition to this, it is also shown that using physics-based models makes flexibility quantification transparent and clear compared to empirical models. Furthermore, this study reveals that slow recovery aids in energy savings by gradually increasing the reference temperature for space heating, to minimise the use of direct electric heating.

The houses built after the 1960s in southern Sweden, representing 54.25% of the total single-family houses, are considered for the analysis. For the power system with a dimensioning fault of 1.45 GW, the flexibility estimation ranges between 2.1 GW and 0.5 GW, for outdoor ambient temperatures varying between -10°C and 10°C respectively. These estimates are independent of the degree of thermal compromise. However, the duration for which the above flexibility values can be provided is dependent on the degree of thermal compromise.

By reducing indoor and water temperatures from 20°C and 55°C, to 15°C and 44°C, the power system is relieved with 2.1 GW for 5 hours and 0.8 GW for the next 12 hours, at -10°C outdoor temperature. As a consequence of offering flexibility, the electric power consumption increases to 2.9 GW during the recovery of indoor temperatures over 24 hours.

Quantification of electric power consumption as a function of time serves as a valuable information for power balance. It is also shown that a cluster of single-family houses in Sweden has the potential to contribute to frequency containment and restoration reserves. Furthermore, it is shown that during the loss of a major generation in a system with a high share of renewable power installations, active control of heating systems equipped with heat pumps provides a great flexibility, helping to prevent the frequency nadir becoming too low, causing undesirable load disconnections.

Thus, a cluster of single family houses that uses house heating flexibility has the potential to reinforce resilience in a large-scale power grid for a duration varying between seconds and several hours.

# CHAPTER 7

# Flexibility quantification of a multi-room house

This chapter is based on the article,

- **S. K. Nalini Ramakrishna**, T. Thiringer, P. Chen, "Power system resilience support from heat-pump equipped houses – thermal comfort consequence for various room priority strategies" *Energy Conversion and Management: X*, Volume 29, 2026, 101436, ISSN 2590-1745.

## 7.1 Overview

In this chapter, the objective is to quantify the flexibility potential by maintaining different temperatures in various rooms of a house, equipped with a variable speed heat pump.

The details of the house considered for analysis in this study are described in Section 4.5. The house is equipped with an air source heat pump and the setup of this heat pump is described in Section 4.3. The heating of domestic water is blocked and an outdoor ambient temperature of -5°C is considered.

An interview study was conducted by RISE (Research Institutes of Sweden) with single-family home owners equipped with heat pumps [98]. The main aim

was to obtain nuanced information regarding the households' perspective of offering flexibility by compromising the thermal comfort, to support the power system under severe power deficit conditions.

The lowest indoor temperature stated in the interviews was 15°C. Furthermore, the study revealed that households had different preferences for indoor temperatures, while offering flexibility to support the grid in conditions of severe power shortages. Most of the interviewees preferred to have colder bedrooms and a warmer living room. In addition, some of them were positive about shutting down the heating system in storage rooms, garages, and bedrooms while having a warmer living room.

Thus, the cases for quantifying the flexibility potential considering multiple rooms in a house are defined based on the interviews described above [98]. In addition to the interviews, other cases are defined to obtain insight into the flexibility potential and compare the quantified flexibility while maintaining various indoor temperatures.

With this background, the cases defined to study the flexibility potential are listed below.

- Case 1: Reduction of indoor temperature from 20°C to 15°C in the entire house.
- Case 2: Maintain 20°C in the living room and turn off the heating in the other rooms.
- Case 3: Reduction of the temperature of Bedroom 2 from 20°C to 17.5°C and in the other rooms, the minimum acceptable temperature is set to 10°C.
- Case 4: Uniform heating of the entire house versus heating a well-insulated smaller room (Bedroom 2) versus heating a larger room (Living room), to various temperatures ranging between 19°C and 15°C.

In all cases, a power deficit situation occurs at hour 6.75 in the power system that is heavily dependent on a reduction in the electric power consumption. At this time, the indoor temperatures in the house are reduced to support the power system. Later, at hour 24, the recovery of the indoor temperatures is initiated, assuming that the reserve power plants are restored.

In this study, flexibility is defined as a reduction in the electric power consumption of the heat pump, relative to the electric power consumption, while maintaining 20°C in the house.

## 7.2 Thermal model of multi-room house

Based on the floor plan of the house presented in Figure 4.4, five thermal zones are modelled. Three zones dedicated to three bedrooms and one each for the living room and the bathroom. The living room is set to be the main zone as it is larger in area compared to the other zones, and hence a PI controller is used in this zone to control the indoor temperature. The indoor temperature in the other four zones is controlled using rule-based controllers as explained in Subsection 3.9.

The thermal model of the house with five zones is shown in Figure 7.1. The heat output from the radiators is injected into the indoor temperature node in each zone.

## 7.3 Results and discussion

### Heat pump

The heat delivering capacity of the air source heat pump under study, at an outdoor ambient temperature of -5°C, is shown in Figure 7.2. It is observed that as the water supply temperature increases, the heat delivered and the COP reduces. When the water supply temperature reaches 46°C, there is an increase in the heat delivering capacity and the COP value increases to 2.7. The reason for this is that to supply higher water temperatures at low outdoor temperatures, the heat pump must operate with vapour injection, as indicated in the operating envelope in Figure 4.2. As a result, the performance of the heat pump improved. In addition, it is interesting to note that the minimum value of heat delivered with vapour injection is higher in comparison to the heat-delivering capability at low water supply temperatures.

The result on the minimum heat-delivering capability becomes important in flexibility studies. For instance, if the required heat is lower than the minimum heat provided by the heat pump, it leads to an on-off operation, like fixed-speed heat pumps even for a variable-speed heat pump.

### Case 1: 15°C in the entire house

With the objective of supporting the power system under severe power deficit conditions, the indoor temperature is allowed to reduce until 15°C, in the

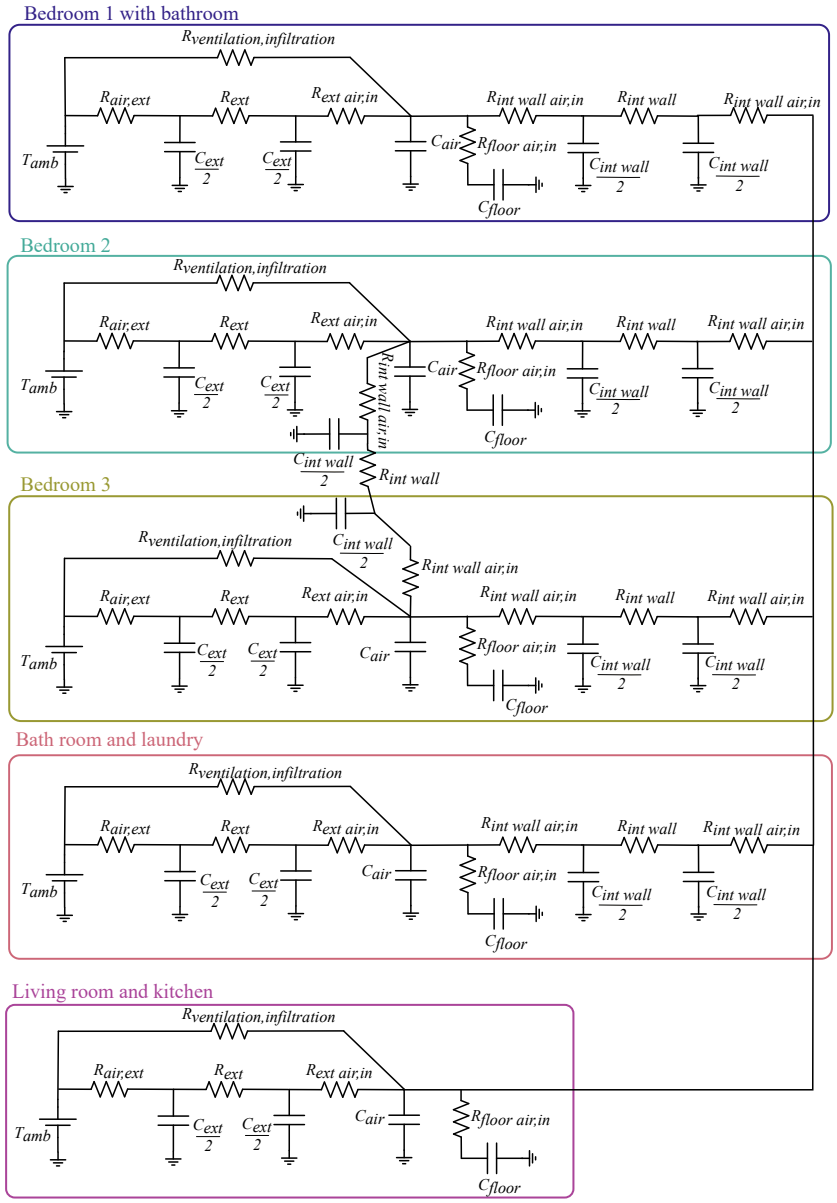


**Figure 7.1:** Thermal model of the house.

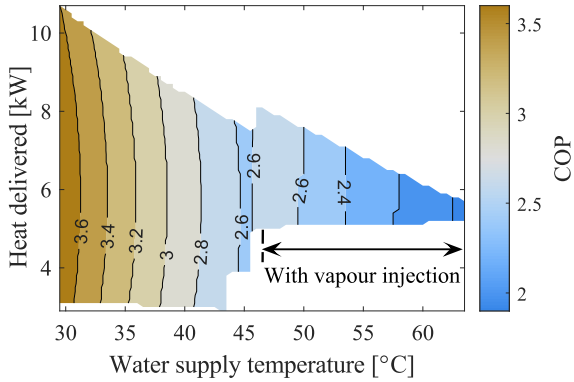


**Figure 7.2:** Performance of the air source heat pump at an outdoor ambient temperature of -5°C.

house under study. This case is chosen based on the lowest acceptable thermal threshold stated in the interviews.

During normal conditions, when the indoor temperature is maintained at 20°C throughout the house, it is observed that around 6 kW of heat is required. The corresponding electric power consumption is around 2.3 kW and the required water supply temperature is around 46°C. This can be observed in figures 7.3a, 7.3b, 7.3c and 7.3d, respectively. The corresponding COP and the speed of the heat pump are shown in Figure 7.3e.

When supporting the power system by reducing the indoor temperature to 15°C, it is noticed that there is a period without electric power consumption for almost 8 hours. Here, a flexibility of 100% is offered for a duration of 8 hours.

Later, when the heating is again started to maintain the indoor temperature at 15°C, it is observed that the heat pump turns on and off like a traditional fixed speed heat pump. This is due to the operational limitations of the heat pump. Observing Figure 4.2, it is noticed that the minimum speed of the heat pump corresponding to an evaporating temperature of -13°C (the outdoor ambient temperature is -5°C, considering 8°C drop between the evaporator and the source, results in an evaporating temperature of -13°C) and the condensing temperature varying between 33°C and 36°C is 1800 RPM. The heat delivered by the heat pump at this speed is greater than the desired

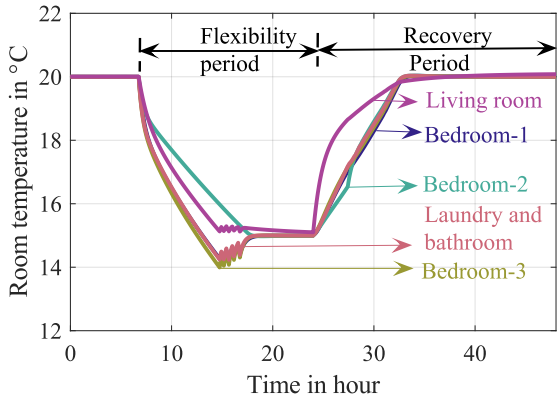


**(a)** Indoor temperature

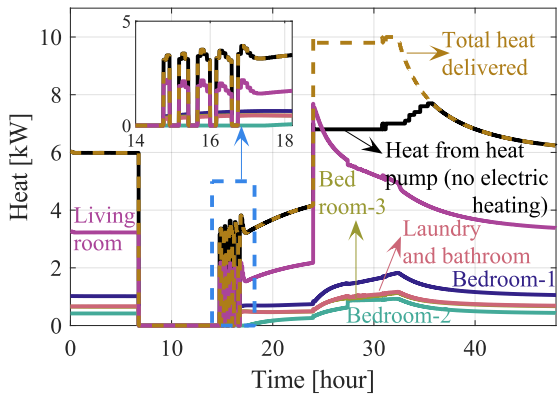


**(b)** Heat power consumption

**Figure 7.3:** Thermodynamics in the house under study, equipped with the variable speed air source heat pump when reducing the indoor temperature to 15°C in the entire house, at an outdoor ambient temperature of -5°C.

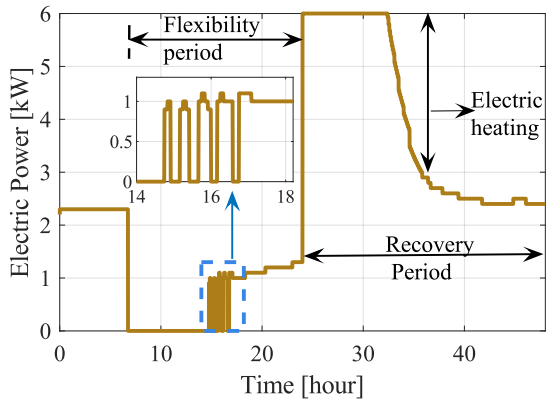


**(c)** Electric power consumption

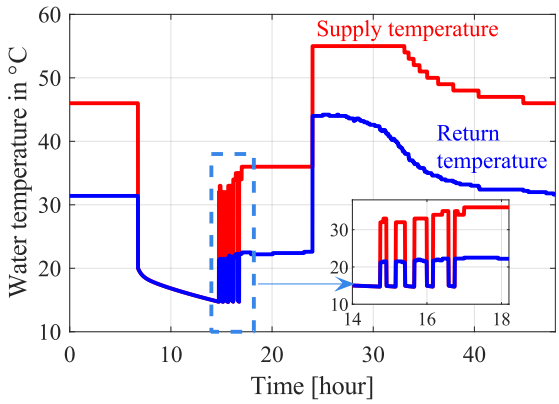


**(d)** Water supply and return temperature

**Figure 7.3:** Thermodynamics in the house under study, equipped with the variable speed air source heat pump when reducing the indoor temperature to 15°C in the entire house, at an outdoor ambient temperature of -5°C (continued).

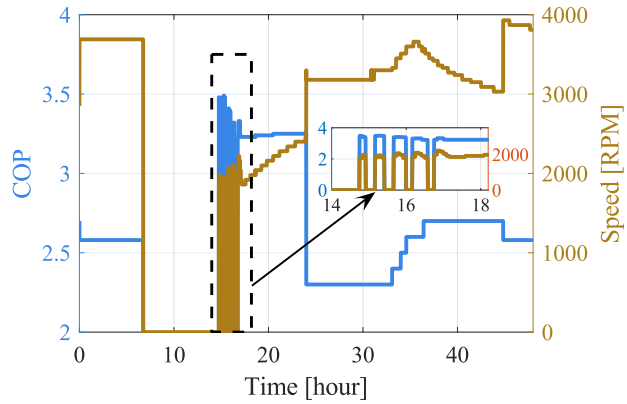


**(e)** COP (excluding the electric heating) and speed

**Figure 7.3:** Thermodynamics in the house under study, equipped with the variable speed air source heat pump when reducing the indoor temperature to 15°C in the entire house, at an outdoor ambient temperature of -5°C (continued).

value, and hence the heat pump behaves like a fixed-speed heat pump for some time. Here, the average electric power consumption is 1.0 kW and the corresponding flexibility is reduced from 100% to 57%.

During the recovery of indoor temperature in all rooms, it is observed that as the heating demand in the rooms increases, additional electric heating is used, as seen in figures 7.3b and 7.3c. Consequently, the electric power consumption also increases and then gradually decreases as the target indoor temperatures are achieved. In this case, the maximum electric power consumption of 6 kW lasts for a duration of about 8.4 hours.

It is interesting to observe that the flexibility of 100% can be offered for 8 hours, with the consequence of the indoor temperatures dropping to 15°C. Later, for the next 9 hours, the flexibility offered gradually reduces to 57%.

## Case 2: 20°C in the living room

To support the grid during severe power deficit conditions, the heating of all rooms except the living room is turned off, based on the interview results.

In this case, the objective is to provide heating only to the living room to maintain its temperature at 20°C.

In Figure 7.4b, it is observed that the heating demand is highest in the living room, followed by Bedroom 1, Laundry and bathroom, Bedroom 3 and Bedroom 2. It can be inferred that the higher the heated floor area, the greater the heating demand. However, although the area of Bedroom 2 and Bedroom 3 is the same, the heating requirement is slightly lower in Bedroom 2. This is because Bedroom 2 is better insulated as its external wall area is lower compared to Bedroom 3.

During the flexibility period, when the heating is turned off in all rooms except the living room, the heating demand in the living room is observed to gradually increase to maintain the temperature at 20°C. This is due to the drop in indoor temperature in the other rooms. As Bedroom 2 is better insulated, it takes longer for the temperature to drop compared to the other rooms. This can be observed in Figure 7.4a.

The electric power consumption reduces to 1.2 kW for a duration of 6 hours, which corresponds to a flexibility of about 48%. This value gradually reduces to about 39% due to the increase in heating demand, as the temperature reduces in the other rooms. This can be observed in Figure 7.4c. The average consumption of electric power during the flexibility period is 1.28 kW.

During the recovery period, the peak electric power consumption of 6 kW occurs for a duration of about 4.3 hours and gradually reduces as the target indoor temperatures are achieved.

In this case, a flexibility of 44% is provided for 17.25 hours.

## Case 3: 17.5°C in Bedroom 2

The indoor temperature of Bedroom 2 is reduced to 17.5°C from 20°C and in all other rooms the objective is to maintain a minimum indoor temperature of 10°C, to support the power grid with severe power deficit conditions.

Figure 7.5 shows the indoor temperatures, the heating demand in different rooms of the house, followed by the electric power consumption.

During the flexibility period, it is observed that in rooms other than Bedroom 2, the indoor temperature is not maintained at a minimum value of 10°C. This is because the minimum value of the heat delivered by the heat pump to maintain the indoor temperature at 17.5°C in Bedroom 2 is much higher than the desired value (between 0.25 kW and 0.4 kW). Hence, excess

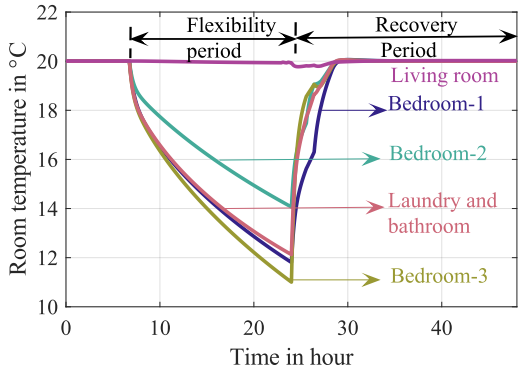


**(a)** Indoor temperature

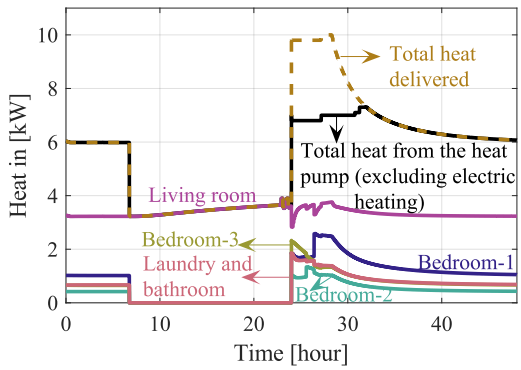


**(b)** Heat power consumption

**Figure 7.4:** Thermodynamics in the house under study, equipped with the variable speed air source heat pump when maintaining 20°C in the living room and shutting off heating in the other rooms, at an outdoor ambient temperature of -5°C.

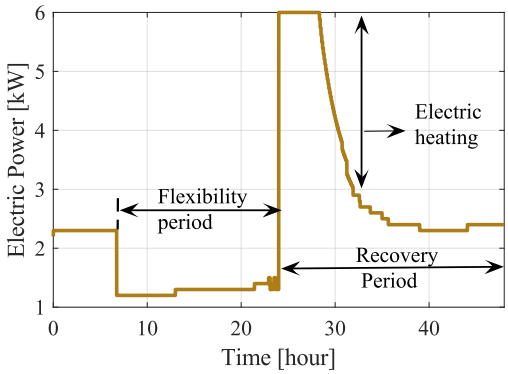


**(c)** Electric power consumption

**Figure 7.4:** Thermodynamics in the house under study, equipped with the variable speed air source heat pump when maintaining 20°C in the living room and shutting off heating in the other rooms, at an outdoor ambient temperature of -5°C (continued).

heat is instead delivered to other rooms to prevent the heat pump from cycling. Thus, the indoor temperatures in the other rooms are well above the value of 10°C.

In Figure 7.5c it is observed that there is a period without electric power consumption for five hours. Thus, a flexibility of 100% can be provided for five hours. Later, the flexibility reduces to 57%, as heating is required to maintain the indoor temperature of Bedroom 2 at 17.5°C.

During the recovery of indoor temperatures to 20°C, it is observed that the peak electric power consumption of 6 kW lasts for a duration of 7.74 hours.

In this case a flexibility of 100% can be offered for 5 hours, with the consequence that the indoor temperature in Bedroom 2 drops to 17.5°C. Later, for the next 12 hours, the flexibility offered is reduced to 57%.

## Case 4: Heating the entire house versus heating the smallest room versus heating the largest room

The main objective of this study is to investigate and quantify the flexibility potential by maintaining different temperatures in various rooms of the house.

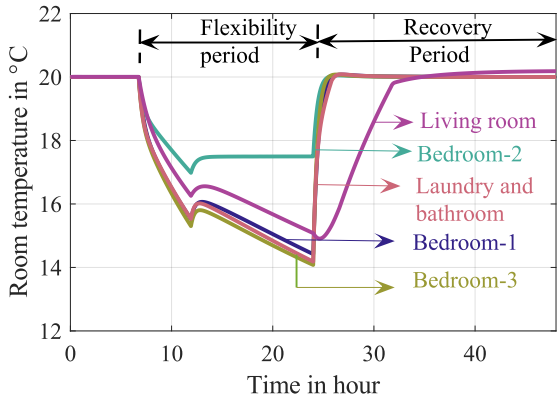


**(a)** Indoor temperature

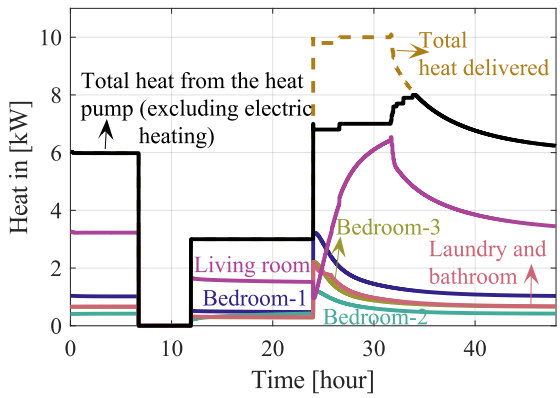


**(b)** Heat power consumption

**Figure 7.5:** Thermodynamic behaviour in the house under study, equipped with the variable speed air source heat pump when maintaining 17.5°C in the smallest well insulated room, at an outdoor ambient temperature of -5°C.

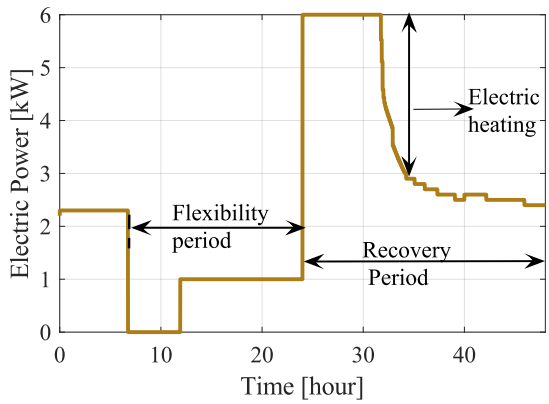


**(c)** Electric power consumption

**Figure 7.5:** Thermodynamic behaviour in the house under study, equipped with the variable speed air source heat pump when maintaining 17.5°C in the smallest well insulated room, at an outdoor ambient temperature of -5°C (continued).

Hence, flexibility is quantified by comparing three scenarios: uniformly heating the entire house, heating a well-insulated smaller room, and heating a larger room to various temperatures ranging between 19°C and 15°C, during the time of resilience activation.

The consolidated results of flexibility offered in the above three scenarios, by reducing indoor temperatures from 20°C and maintaining them between 19°C and 15°C is shown in Figure 7.6. Figure 7.6a shows the duration for which a flexibility of 100% can be provided, or, in other words, the duration without any consumption of electric power due to the thermal inertia of the house. As anticipated, the greater the thermal compromise, the longer the duration for which 100% flexibility can be provided. It is observed that in the second scenario, 100% flexibility can be provided for a longer duration compared to the other two scenarios. Furthermore, by comparing the three scenarios, it is observed that 100% flexibility can be provided for a similar duration while maintaining better thermal comfort in the smallest well-insulated room.

For example, a flexibility of 100% is provided for 5 hours, with the consequence that the indoor temperatures of the house drop to about 16°C, at an

outdoor temperature of -5°C. The same flexibility is provided by heating only a smaller area such as the better insulated Bedroom 2, which is 8% of the total floor area, to 17.5°C, while ensuring that the temperatures in the other rooms do not fall below 14°C as seen in Figure 7.5.

After some hours of offering a flexibility of 100% (as presented in Figure 7.6a), the flexibility reduces, as indoor temperatures should be kept at specified minimum values. The change in flexibility from 100% to various values in the three different scenarios is shown in Figure 7.6b. Here, it is observed that the flexibility level looks the same for different temperature reductions in the smallest room, which is Bedroom 2. This is because the minimum value of the heat delivered by the heat pump is much higher than the desired heating requirements in Bedroom 2, as seen in Figure 7.5. As a result, excess heat is delivered to other rooms. Consequently, the level of flexibility looks the same for various degrees of thermal compromise in Bedroom 2. For the other scenarios, it is inferred that the greater the degree of thermal compromise, the greater the flexibility provided.

Individual's preference or acceptance of personal comfort has a great impact on the flexibility provision from the house. The advantage of such a flexible resource is that the aggregated flexibility of multiple houses can be reshaped to a desired profile at the system level.

## Validation of the thermal model developed

The total coefficient of heat transfer (thermal resistances to outdoor temperature) of the house, including infiltration losses and heat recovery, is calculated to be 239.23 $\left(\frac{\mathrm{W}}{\mathrm{K}}\right)$.

Using the overall heat transfer coefficient, the heat required to maintain an indoor temperature of 20°C at an outdoor ambient temperature of -5° C is estimated to be 5.98 kW. Here, the proportion of heat losses due to mechanical ventilation including heat recovery in each room can be calculated using (3.6), neglecting infiltration. This is estimated to be 537 W, which is about 9% of the total heat demand in the house.

When 20°C is maintained throughout the house, there is no heat transfer between adjacent rooms. Thus, the heat requirement in each room can be estimated by calculating the heat transfer coefficient of each room with respect to the outdoor temperature. For each room, this can be calculated by determining the thermal equivalent of the parallel combination of ($R_{ventilation,infiltration}$)

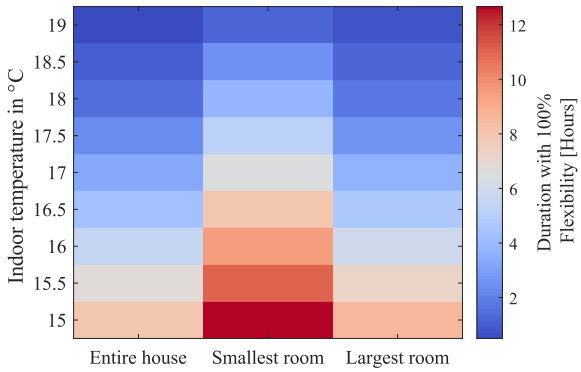


**(a)** Duration for which 100% flexibility is provided

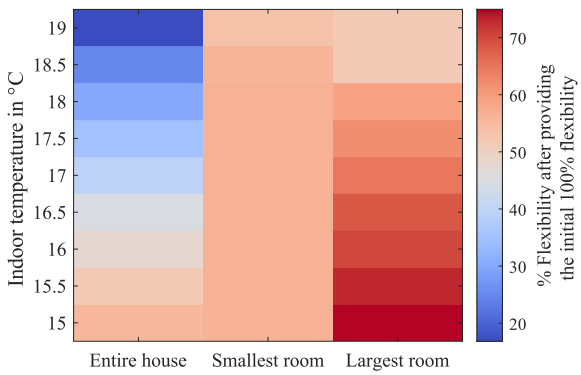


**(b)** Final flexibility after providing an initial flexibility of 100%

**Figure 7.6:** Flexibility quantification while maintaining different temperatures in various rooms of a house, at an outdoor ambient temperature of -5°C.

with ($R_{air,ext} + R_{ext} + R_{ext\ air,in}$). These values are estimated to be 1.02 kW, 0.42 kW and 0.65 kW for Bedroom-1, Bedroom-2, and Bedroom-3, respectively. Furthermore, for the living room followed by the laundry and bathroom, the heat requirements are estimated to be 3.23 kW and 0.67 kW, respectively. The total heat requirement in the house under study would be the summation of the heat requirement in each room and is estimated to be 5.99 kW. The total heat requirement and the heat requirement in each room to maintain 20°C at an outdoor ambient temperature of -5°C are well matched with the values obtained in the above three case studies, as seen in figures 7.3b, 7.4b and 7.5b. Thus, the thermal model of the house works as desired.

## 7.4 Conclusions

This study demonstrated the ability of single-family houses equipped with heat pumps to be used as flexible resources to support the power system in situations of severe power shortages.

In order to investigate the flexibility potential of maintaining different temperatures in various rooms in a house, a detailed model of a multi-room Swedish single-family house equipped with a variable-speed heat pump was developed. The model also includes the space heating controller to control the temperatures in different rooms of a house.

An initial indoor temperature of 20°C is considered for the analysis in all rooms and an outdoor ambient temperature of -5°C. In this study, flexibility is defined as a reduction in the electric power consumption of a heat pump, relative to the electric power consumption while maintaining 20°C in a house.

A flexibility of 100% is provided for 5 hours, when all rooms reduce thermal comfort equally to about 16°C, at an outdoor temperature of -5°C. The same flexibility can also be provided by heating only a smaller area, such as a better insulated bedroom, which is 8% of the total floor area, to 17.5°C, while ensuring that the temperatures in the other rooms do not fall below 10°C. After the first five hours, the flexibility decreases from 100% to 47% and 57%, respectively, in the above cases, for as long as the flexibility required. The impact of offering various levels of flexibility in relation to thermal comfort is demonstrated and quantified.

# CHAPTER 8

## Limiting the rebound effect of using flexibility

This chapter is based on the article

- **S. K. Nalini Ramakrishna**, T. Thiringer, P. Chen "Limiting the rebound effects when utilising flexibility from heat pumps using an adaptive heat pump controller," *Accepted, Energy Conversion and Management, 2025.*

## 8.1 Overview

In this chapter, the focus is on reducing the rebound effect associated with using flexibility of space heating systems equipped with heat pumps. The houses considered for analysis in this study are described in Case 3 of Table 4.4. The setup of the heat pumps is as described in Section 4.3. The heating of domestic water is blocked. Here, an outdoor ambient temperature of -5°C is considered.

## 8.2 Results and discussion

A typical house constructed during 1961-1975 is taken as an example to present an in-depth analysis on a component level, as they are high in number in comparison with other house categories.

The target indoor room temperature recovery from 15°C to 20°C, after providing flexibility by reducing the indoor temperature from 20°C to 15°C over a period of 17.25 hours, is chosen to represent an extreme situation with a severe power deficit condition. Similarly, a target recovery of indoor room temperature from 18°C to 20°C, after providing flexibility by reducing indoor temperature from 20°C to 18°C over a period of 3.25 hours, is chosen to represent a mild demand response condition.

The case with the standard heat pump controller refers to an advanced version of the standard weather-compensated heat pump control where $T_{supply}$ is changed to meet different heating requirements. This standard controller does not include the estimation of the heat pump's water supply temperature for providing maximum space heating via radiators, considering the limitations in heat pumps. However, this is included in the proposed controller.

### Recovery analysis during an extreme situation

To improve the resilience of the power system, the space heating is turned off until the indoor temperature reaches 15°C. Figure 8.1 shows the thermodynamics in the house before supporting the power system, then while supporting by reducing the electric power drawn, and finally during recovery of the indoor temperature to pre-disturbance conditions. The results obtained from the proposed controller are presented in bright colours, whereas those from the standard controller are represented in dark colours. The corresponding selected operating points are represented using green circles and pink diamonds, respectively.

The mapping of the selected operating points, considering the heat delivering capabilities of the heat pump and the installed radiators for the proposed and standard controller, are shown in Figure 8.2. Here, the desired heat value is represented using maroon circles.

In this study, the objective is to obtain the same recovery time for both the standard and the proposed controller, but with the proposed controller managing this without the electric heater.

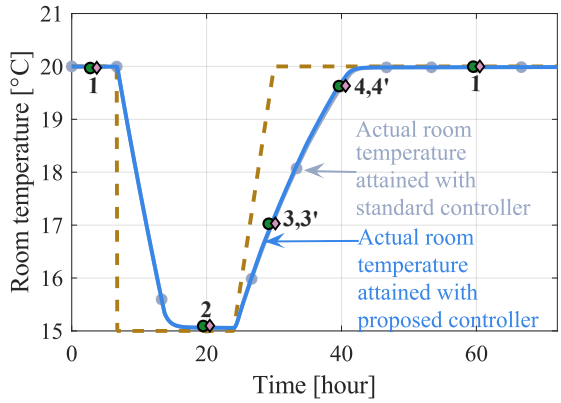


**(a)** Indoor temperature

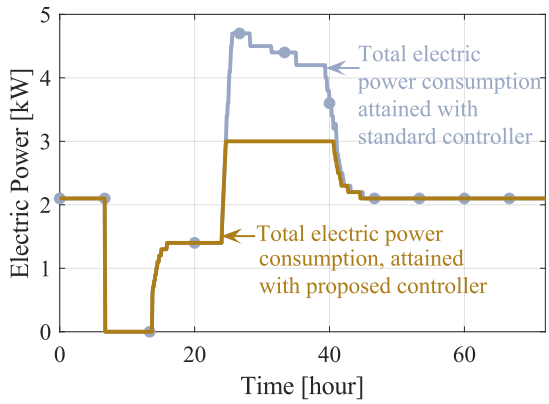


**(b)** Electric power consumption

**Figure 8.1:** Comparison of recovery analysis between the standard and the proposed controller, after providing flexibility during severe power deficit conditions in the house constructed during 1961-1975, at an outdoor ambient temperature of -5°C.

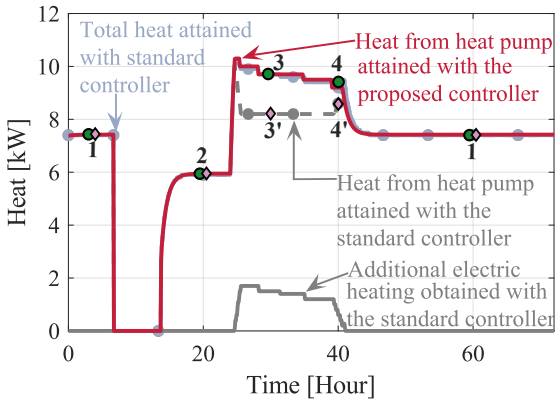


**(c)** Heat and additional electric heating

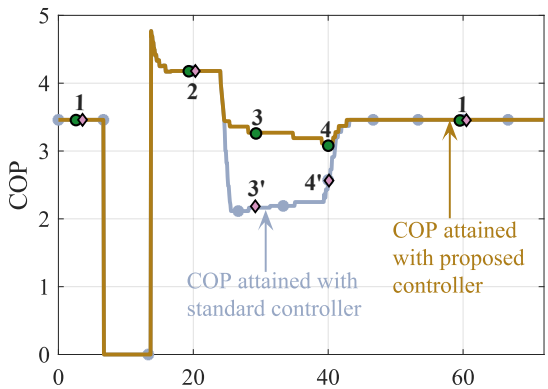


**(d)** COP of the heat pump

**Figure 8.1:** Comparison of recovery analysis between the standard and the proposed controller, after providing flexibility during severe power deficit conditions in the house constructed during 1961-1975, at an outdoor ambient temperature of -5°C (continued).

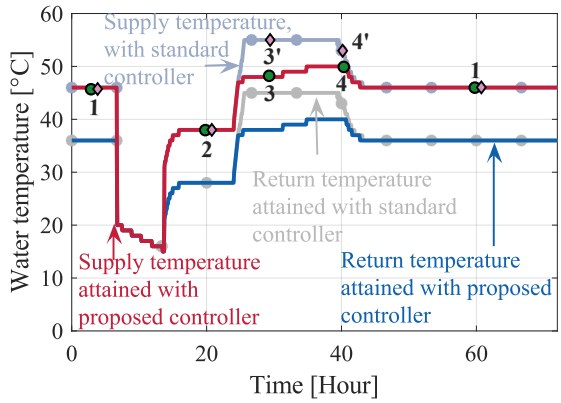


**(e)** Water supply and return temperature

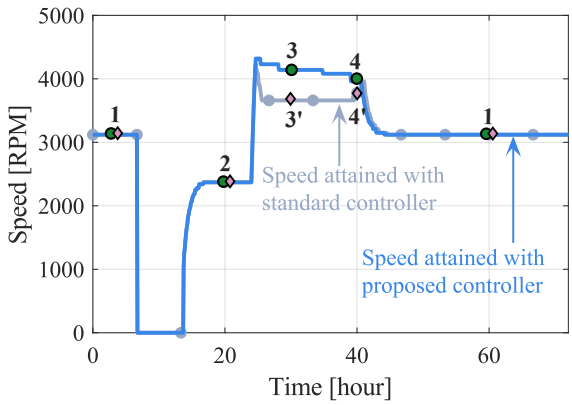


**(f)** Speed of the heat pump

**Figure 8.1:** Comparison of recovery analysis between the standard and the proposed controller, after providing flexibility during severe power deficit conditions in the house constructed during 1961-1975, at an outdoor ambient temperature of -5°C (continued).

It is observed that before providing support, the indoor temperature is maintained at 20°C. During the support time, the reference value of the indoor temperature is reduced to 15°C. As desired, there is a period without consumption of heat and electric power when the indoor temperature starts to decrease. The power system has now been relieved of 2.1 kW for some time. This is followed by a period with reduced heat and electric power consumption as the corresponding requirements are lower to maintain the indoor temperature at 15°C compared to maintaining it at 20°C. This can be seen in figures 8.1a, 8.1b and 8.1c. The corresponding COP, water supply and return temperature in the radiators, followed by the speed of the heat pump, is shown in figures 8.1d, 8.1e and 8.1f, respectively. During this period, in figures 8.1 and 8.2 it is observed that the actual and desired heat are the same using both the proposed and the standard controller.

During the recovery period, the reference value of the indoor temperature is ramped up starting at hour 24 to restore the indoor temperature by hour 30. From figures 8.1 and 8.2, during the recovery period, it is seen that there is a change in operating points when using the proposed and standard controller. Higher values of supply temperatures are chosen to deliver a high value of heat using the standard controller compared to the proposed controller. However, due to limitations in the heat delivering capability of the heat pump at these supply temperatures, additional electric heating is used to deliver the same heat as in the case of the proposed controller, which, of course, is strongly undesirable. Consequently, the COP is higher and the electric power consumption is lower using the proposed controller compared to the standard controller.

It does not help to have the electric heating blocked in the standard controller, as the indoor temperature recovery will now take a longer time due to limitations in the heat delivering capability of the heat pump at high supply temperatures and accordingly, the duration with 3 kW peak power consumption will be longer compared to the proposed controller.

The electric power consumption in houses constructed during 1976-1985 and 1986-1995 is shown in figures 8.3a and 8.3b, respectively. The evolution of indoor temperatures in these houses is shown in Figure 8.3c. From Table 4.4, for Case study 3 it is observed that the time constant in the above houses is high, and therefore recovery takes longer compared to the house built during 1961-1975. As the house constructed during 1986-1995 has the highest time

constant, indoor temperature recovery has a longer duration compared to the two previous types of house. It should be mentioned that during the flexibility period, the duration without electric power consumption increases with an increase in the time constant of the house, as witnessed in figures 8.3 and 8.1b. Furthermore, as indoor temperatures reach the target value of 20°C, the electric power consumption is reduced accordingly and eventually reaches a steady state value. From figures 8.3 and 8.1b, it is observed that

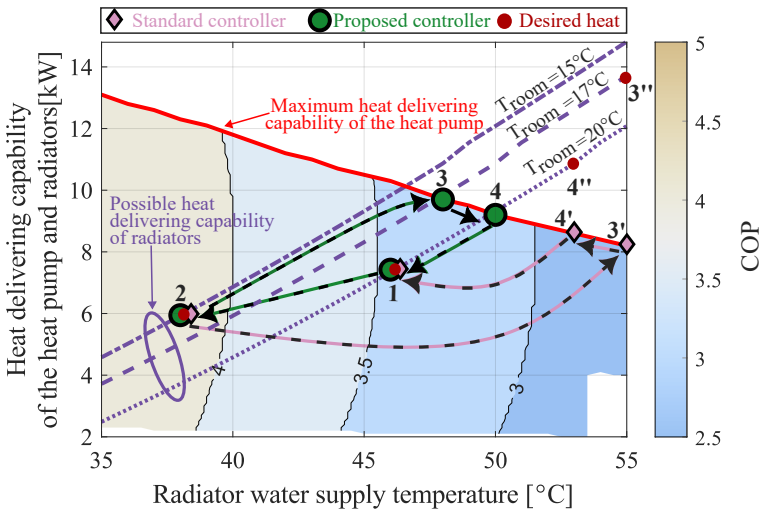


**Figure 8.2:** Operating points obtained using standard and the proposed controller, in a house constructed during 1961-1975.

with the proposed controller, in houses constructed during 1961-1975, 1976-1985 and 1986-1995, the peak power consumption is 1.7 kW and 1.3 kW lower, respectively, compared to the standard controller. Thus, achieving a reduction in rebound power consumption of approximately 36% and 30%, respectively compared to the standard controller. This clearly signifies the importance of matching the maximum heat delivered by the heat pump with the installed radiators, considering the limitations in the heat pump using the proposed controller.

Furthermore, it is observed that the performance in both the controllers matches exactly during pre-disturbance and flexibility periods, clearly emphasising the strength of the proposed controller during recovery periods.

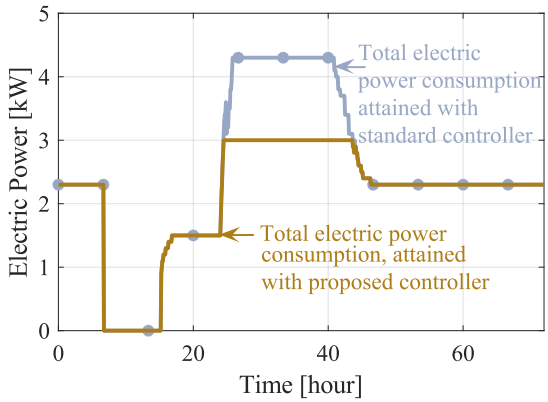


**(a)** Electric power consumption in a house constructed during 1976-1985

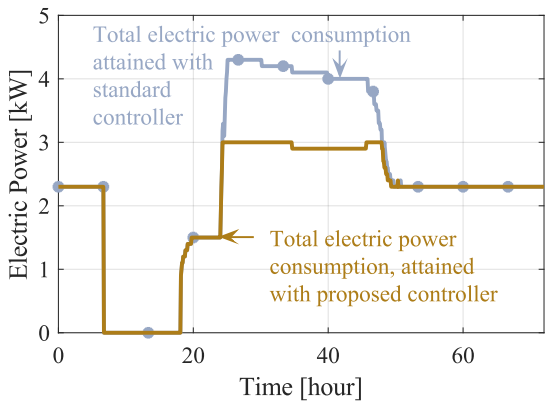


**(b)** Electric power consumption in a house constructed during 1986-1995

**Figure 8.3:** Indoor temperature and comparison of electric power consumption between the standard and the proposed controller after providing flexibility during severe power deficit conditions, in houses constructed during 1976-1985 and 1986-1995, at an outdoor ambient temperature of -5°C.

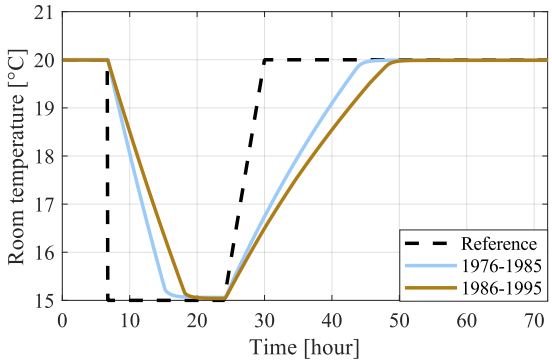


**(c)** Indoor temperature

**Figure 8.3:** Indoor temperature and comparison of electric power consumption between the standard and the proposed controller after providing flexibility during severe power deficit conditions, in houses constructed during 1976-1985 and 1986-1995, at an outdoor ambient temperature of -5°C (continued).

## Sensitivity analysis

### Variations in radiator number and infiltration rate

A sensitivity analysis is performed to test the performance of the proposed controller compared to the standard controller, considering a variation in the number of radiators and the infiltration rate.

As mentioned earlier, the objective of this study is to obtain the same recovery time for both the standard and the proposed controller, and, in addition, with the proposed controller managing this without the electric heater.

The time taken to recover indoor temperatures considering a variation of ±15% in the number of radiators and ±10% variation in infiltration rates, compared to the values in Case 3 in Table 4.4, is shown in Figure 8.4. The corresponding reduction in peak electric power consumption using the proposed controller compared to the standard controller is shown in Figure 8.5.

With a reduced number of radiators, higher supply temperatures are required to deliver the same heat as in the case with a high number of radiators. The heat delivering capacity of heat pumps at high supply temperatures is

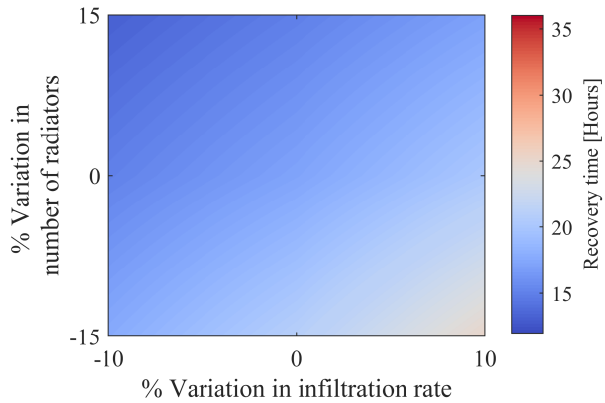


**(a)** Indoor temperature recovery time in a house constructed during 1961–1975

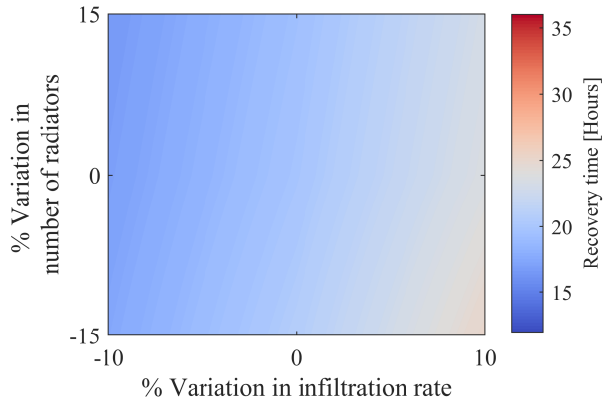


**(b)** Indoor temperature recovery time in a house constructed during 1976-1985

**Figure 8.4:** Sensitivity analysis on indoor temperature recovery time, considering variation in the number of radiators and infiltration rate.

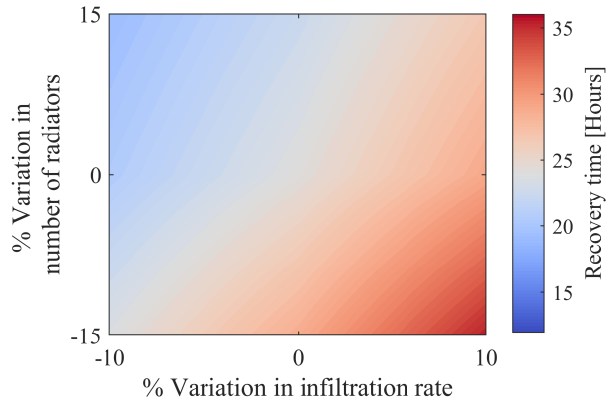


**(c)** Indoor temperature recovery time in a house constructed during 1986-1995

**Figure 8.4:** Sensitivity analysis on indoor temperature recovery time, considering variation in the number of radiators and infiltration rate (continued).

reduced as seen in Figure 8.2. Thus, as the heat capacity is limited at higher water supply temperatures, the recovery time increases. However, with a higher number of radiators, the recovery time is reduced because the heating capacity of the heat pumps is relatively higher at lower supply temperatures compared to the former case. This is observed in Figure 8.4.

Infiltration rates correspond to heat losses in houses. Thus, the lower the infiltration rate, the shorter the recovery time.

In Figure 8.5 it is observed that as the number of radiators increases, the reduction in peak electric power consumption compared to the standard controller increases. This is because the heat delivering capability of the radiators at lower supply temperatures increases with an increase in the number of radiators. This means that the maximum heat that can be provided during the recovery period using the proposed controller also increases. As the standard controller chooses a higher supply temperature where the heat pump's heating capability is limited, additional electric heating needed to deliver the same heat as in the case of the proposed controller increases.

The sensitivity analysis undertaken further demonstrates the strength of the proposed controller compared to the standard controller in reducing peak

electric power consumption.

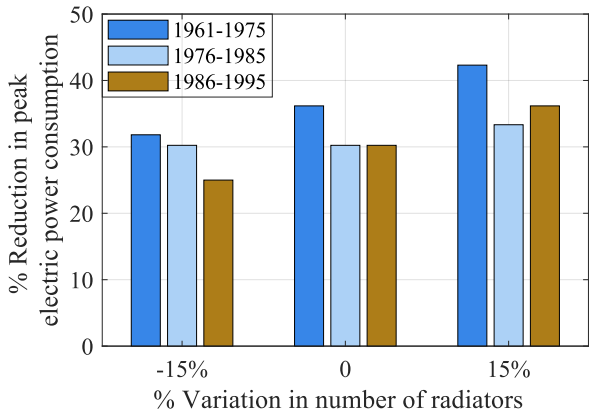


**Figure 8.5:** Sensitivity analysis on reduction in peak power consumption during recovery period, considering variation in the number of radiators, using the proposed controller compared to the standard controller, in the three house types.

### Variations in the difference between the supply and return water temperature in radiators

Sensitivity analysis considering the variation in the difference between $T_{supply}$ and $T_{return}$ in the radiators is performed to test the performance of the proposed controller. Based on references [70] [71], the difference between $T_{supply}$ and $T_{return}$ varies between 5°C and 10°C for space heating systems equipped with heat pumps. Hence, the same is considered for the sensitivity analysis. The other details of three houses are described in Table 4.4. The results of this sensitivity analysis are shown in Figure 8.6. In Figure 8.6, it is observed that the influence of the difference between $T_{supply}$ and $T_{return}$ in the radiators on the performance of the proposed controller is not significant.

## Recovery analysis during a mild situation

Figure 8.7 shows the consumption of electric power in the houses under study, while providing a mild demand response by reducing the indoor temperature

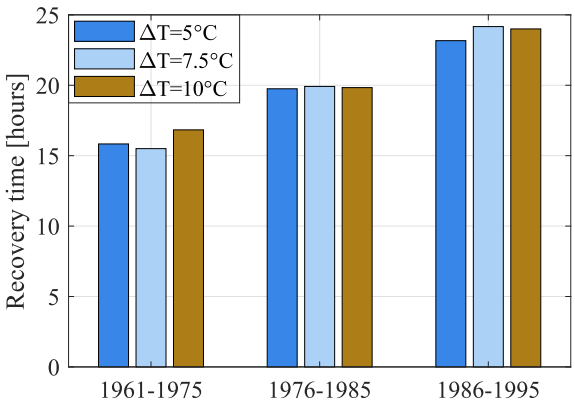


**Figure 8.6:** Sensitivity analysis on the recovery time considering variations in the difference between the supply and return water temperature in radiators, using the proposed controller, in the three house types.

from 20°C to 18°C over a period of 3.25 hours. In this case, a thought is that we perhaps only perform energy arbitrage. The analysis also includes the target indoor temperature recovery to 20°C in two hours, while ensuring a high COP. The results obtained with the proposed controller and the standard controller are represented in bright and dark colours, respectively. Here also, the objective is to ensure indoor temperature recovery at the same time using both controllers, and electric heating is disabled in the case of the proposed controller.

As witnessed previously, due to limitations in the heat pump's heat delivering capability at higher values of supply temperatures, additional electric heating is utilised in the case of the standard controller to deliver the same heat as in the case of the proposed controller. Thus, using the proposed controller, the rebound power is substantially lower. The key feature is that the proposed controller manages to have a higher COP compared to the standard controller.

Figures 8.7a, 8.7b and 8.7c reveal that during the recovery period, a reduction in peak electric power consumption by 31%, 30% and 29% is achieved in houses constructed during 1961-1975, 1976-1985 and 1986-1995, respectively, using the proposed controller compared to the standard controller.

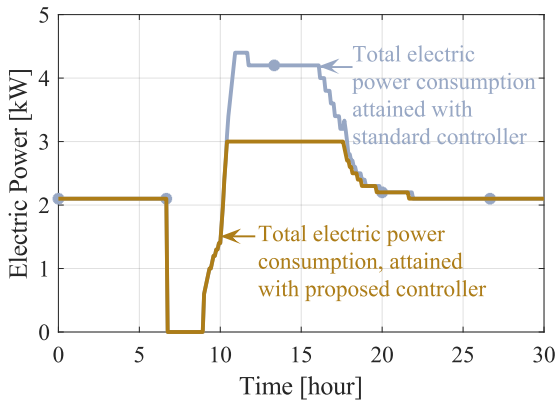


**(a)** Electric power consumption in a house constructed during 1961-1975

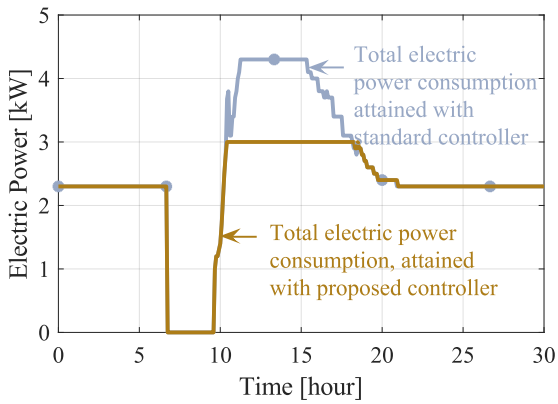


**(b)** Electric power consumption in a house constructed during 1976-1985

**Figure 8.7:** Indoor temperature and comparison of electric power consumption between the standard and the proposed controller after providing flexibility during mild demand response program, at an outdoor ambient temperature of -5°C.

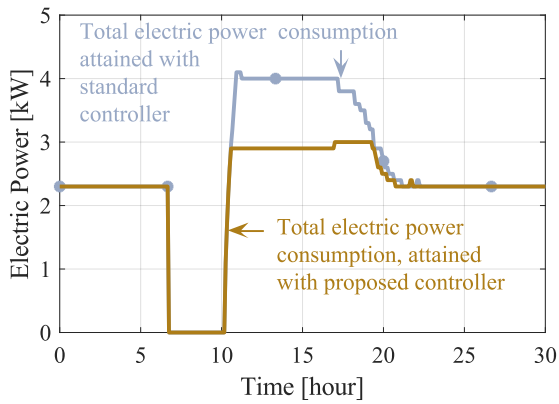


**(c)** Electric power consumption in a house constructed during 1986-1995

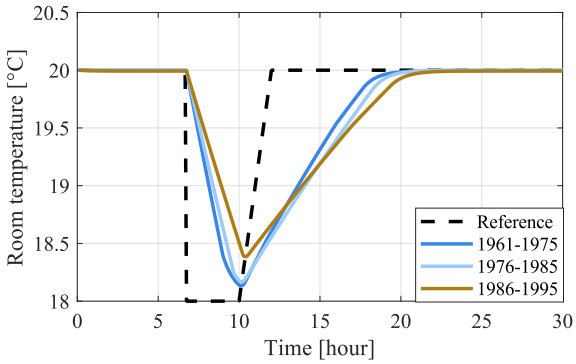


**(d)** Indoor temperature evolution in three house types

**Figure 8.7:** Indoor temperature and comparison of electric power consumption between the standard and the proposed controller after providing flexibility during mild demand response program, at an outdoor ambient temperature of -5°C (continued).

This clearly highlights the importance of the proposed controller in limiting the rebound effect of using heat pumps after participating in mild demand response programmes.

## Quantification of electric power consumption on a system level

The quantification of the electric power consumption by heat pumps on a system level, during the flexibility and recovery periods, is based on the following assumptions

- The initial indoor temperature in all the houses under study is 20°C.
- The signals for indoor temperature set points during flexibility and recovery periods in all the houses under study are synchronised.

### Recovery analysis during extreme situations

The quantification of electric power consumption as a function of time by 0.87 million heat pump equipped houses is shown in Figure 8.8. The details of these houses are indicated in Case 3 of Table 4.4, and the quantification is based on the results presented earlier during extreme situations.

It is observed that about 1.9 GW of electric power is required to maintain indoor temperatures at 20°C in 0.87 million houses. Consequently, the power system can be relieved of 1.9 GW, and in our example, this reduction is for 7 hours and then 650 MW for the next 10 hours, with the consequence of the indoor temperatures dropping to 15°C. During indoor temperature recovery to 20°C taking 20 hours, using the proposed controller, the maximum rebound power is limited to 2.6 GW compared to 3.9 GW using the standard controller. Thus, achieving a 33% reduction in peak power consumption.

This shows that the proposed controller helps to limit the CLPU effect by reducing the peak power consumption by the heat pumps after providing flexibility during extreme situations. These results help system operators during recovery periods, in taking informed decisions in load management while balancing power systems with limited generation and importing capacity, which is a key feature in increasing grid resilience.

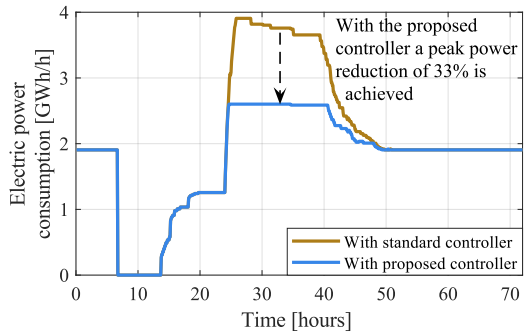


**Figure 8.8:** Quantification of electric power consumption by heat pumps prior to providing support to the power system, while supporting by reducing the indoor temperature from 20°C to 15°C and during recovering the indoor temperature to 20°C, using the standard and the proposed controller.

### Recovery analysis during mild situations

The quantification of electric power consumption as a function of time by 0.87 million heat pumps in the study, based on the results presented earlier during mild situations, is shown in Figure 8.9.

Here also the analysis remains the same as in the case of Figure 8.8. The power grid is relieved of 1.9 GW for about 2 hours. During the recovery period, the peak power reduction by 30% is obtained using the proposed controller compared to the standard controller. This emphasises the proposed controller's strength in limiting the CLPU effect witnessed after providing flexibility during mild situations as well.

## 8.3 Conclusions

The rebound effect of using flexibility of space heating systems equipped with heat pumps can have large negative CLPU effects, while restoring the indoor temperature to normal conditions. Furthermore, the fact that participation of TCLs in dynamic pricing schemes leads to substantial CLPU effects is confirmed in [12].

Today, modern variable speed heat pumps are dominating new installations

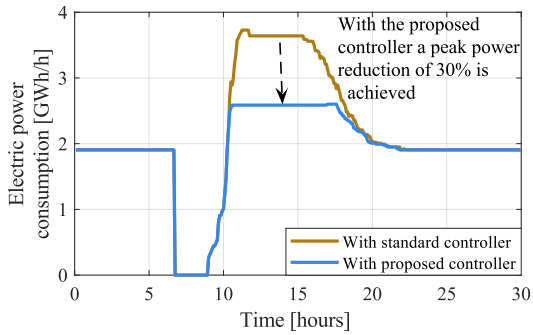


**Figure 8.9:** Quantification of electric power consumption by heat pumps prior to providing support to the power system, while supporting by reducing the indoor temperature from 20°C to 18°C and during recovering the indoor temperature to 20°C, using the standard and the proposed controller.

strongly, and they will soon dominate the accumulated installations. Thus, in this study, the possibility to limit the CLPU effects on a component level considering variable speed heat pumps is investigated i.e. a deeper analysis of the electric power consumption by heat pumps with the associated thermal effects is undertaken on a component level, which so far has been missing in scientific literature.

An adaptive heat pump controller is proposed to provide the maximum possible space heating during the recovery period, considering the limitations in heat pumps. The peak electric power required is much lower using the proposed controller compared to the standard heat pump controller while recovering the indoor temperature at the same time. This shows that the proposed controller helps to limit the CLPU effects by reducing the peak electric power consumption of the heat pumps during the recovery period.

Taking the southern half of Sweden as an example, at -5°C outside temperature, approximately 1.9 GW dedicated to heating is required to maintain indoor temperatures at 20°C, in 44% of single-family houses. The power system can be relieved of these 1.9 GW for 7 hours and 650 MW during 10 hours, with the consequence that indoor temperatures drop to 15°C. During an indoor temperature recovery to 20°C, over 20 hours using the proposed controller, the maximum rebound power is limited to 2.6 GW compared to

3.9 GW using the standard controller. Thus, achieving a 33% reduction in peak power.

During the same conditions, indoor temperatures are reduced from 20°C to 18°C over a duration of 3.25 hours, to represent a moderate demand response case. A target temperature recovery of 20°C is achieved in 10 hours and the recovery peak power is limited to 2.6 GW as opposed to 3.7 GW, which is approximately a 30% reduction compared to the standard controller. Thus, with the proposed controller, the CLPU effects are limited, thereby reducing the rebound effect during the recovery period, after participating in moderate demand response programmes.

In this study, the effectiveness of the proposed controller is clearly demonstrated. The proposed controller helps limit rebound effects of using flexibility from heat pumps, after supporting power systems during moderate situations and also during extreme events with severe power shortages.

# CHAPTER 9

# Conclusions and Future Work

## 9.1 Conclusions

In northern European countries such as Sweden, winter represents a challenging period for power systems, as it might operate close to its limits. During these periods, the loss of a major power plant combined with limitations in importing power or cyber and physical attacks on power systems can cause severe power shortage conditions that last several hours. In this context, improving the resilience of the power system becomes essential. Thus, in this thesis, the potential for load reduction using the flexibility of heating systems equipped with heat pumps in Swedish single-family houses is quantified. Single-family houses are chosen because their electric energy consumption is the highest in the residential sector.

In this study, flexibility is defined as a reduction in the electric power consumption of heat pumps, relative to the electric power consumption when maintaining 20°C throughout the houses.

For flexibility quantification, the houses built after the 1960's in southern half of Sweden, representing 54.25% of the total single-family houses, are considered. For the power system with a peak demand of 20-25 GW, the

flexibility estimation ranges between 2.1 GW and 0.5 GW, for outdoor ambient temperatures varying between -10°C and 10°C, respectively. These estimates are independent of the degree of thermal compromise. However, the duration for which the above flexibility can be provided is dependent on the degree of thermal compromise. By reducing indoor and water temperatures from 20°C and 55°C, to 15°C and 44°C, the power system is relieved of 2.1 GW for 5 hours and 0.8 GW as long as flexibility is required, at an outdoor temperature of -10°C.

It is shown that during the loss of a major generation in the modified Nordic-32 bus system with a high share of renewable power installations, active control of heating systems equipped with heat pumps provides great flexibility. It helps prevent the frequency nadir from becoming too low, causing undesirable load disconnections. Thus, a group of single-family houses that use the flexibility of heating systems has the potential to reinforce resilience in a large-scale power grid for a duration ranging from seconds to several hours.

To quantify the flexibility potential by maintaining different temperatures in a multi-room house, a detailed model of a house equipped with a variable speed heat pump is developed. A flexibility of 100% is provided for 5 hours, when all rooms reduce thermal comfort equally to about 16°C, at an outdoor temperature of -5°C. The same flexibility can also be provided by heating only a smaller area, such as a better insulated bedroom, which is 8% of the total floor area, to 17.5°C, while ensuring that the temperatures in the other rooms do not fall below 10°C. After the first five hours, the flexibility decreases from 100% to 47% and 57%, respectively, in the above cases, as long as flexibility is required.

The rebound effect of using flexibility from heat pumps can have large negative CLPU effects, while restoring the indoor temperature to normal conditions. Hence, an adaptive heat pump controller is proposed to limit the CLPU effects during the recovery period, considering the limitations in heat pumps. At -5°C outdoor temperature, approximately 1.9 GW is required to maintain indoor temperatures at 20°C, in 44% of single family houses. The power system can be relieved of 1.9 GW for 7 hours and 650 MW for the next 10 hours, with the consequence that the indoor temperatures drop to 15°C. During indoor temperature recovery to 20°C, over 20 hours using the proposed controller, the peak rebound power is limited to 2.6 GW compared to 3.9 GW using the standard controller. Thus, achieving a 33% reduction in

peak power. This shows that the proposed controller helps to limit the CLPU effects by reducing the peak power consumption of the heat pumps during the recovery period.

Furthermore, an important finding is that increasing emphasis on energy efficiency measures will eventually lead to replacement of fixed speed heat pumps by variable speed heat pumps, which have high controllability. Thus, variable speed heat pumps were considered for analysis. In this study, it is shown that the inclusion of traditional fixed speed heat pumps could result in an overestimation of the flexibility potential by approximately 19% compared to variable speed heat pumps.

## 9.2 Future Work

There are many further investigations that could follow on from this work. Some valuable efforts proposed are

- The impact of defrosting in air source heat pumps and the impact of reducing the ventilation rate on flexibility quantification and indoor temperature recovery, can be a value contribution.
- Experimental validation of the mathematical models proposed in this thesis. This helps in providing deeper insights that are not captured by simulations.
- Employing stochastic models to quantify flexibility on a system level to account for the uncertainty in the buildings' thermal properties and indoor temperature set points based on the occupants behaviour.
- Quantification of the rebound electric power consumption in a system with both space heating and water heating equipped with a heat pump, accounting for the withdrawal of hot water from the occupants during the recovery period.

# References


[1] Energinet, Fingrid, Statnett, Svenska kraftnät. "Nordic grid development perspective 2023." (2023).

[2] IEA. "Electricity security matters more than ever – power systems in transition – analysis." (2020), [Online]. Available: https://www.iea.org/reports/power-systems-in-transition/electricity-security-matters-more-than-ever (visited on 03/05/2023).

[3] Christine Große, Pär M. Olausson. "Is There Enough Power? Swedish Risk Governance and Emergency Response Planning in Case of a Power Shortage." (2023), [Online]. Available: https://snsse.cdn.triggerfish.cloud/uploads/2023/01/is-there-enough-power.pdf (visited on 06/13/2025).

[4] J. W. Busby, K. Baker, M. D. Bazilian, *et al.*, "Cascading risks: Understanding the 2021 winter blackout in Texas," *Energy Research & Social Science*, vol. 77, p. 102 106, 2021, ISSN: 2214-6296.

[5] Emergency information from Swedish authorities. "Reserve power and the "Styrel" system." (2024), [Online]. Available: www.krisinformation.se/en/hazards-and-risks/power-outages/reserve-power-and-the-styrel-system (visited on 06/13/2025).

[6] Swedish Energy Agency, "Energy in Sweden- An overview," *Energimyndigheten*, 2021.

[7] statista. "Final electricity consumption in households in Sweden from 2013 to 2019, by type." (2021), [Online]. Available: https://www.statista.com/statistics/1027100/final-consumption-of-electricity-in-households-in-sweden-by-type/ (visited on 04/13/2021).

[8] Chen, Huijuan, Ruud, Svein, and Markusson, Caroline, "Energy flexibility using thermal mass for Swedish single-family houses," *E3S Web of Conf.*, vol. 562, p. 04 003, 2024.

[9] Energimyndigheten. "Summary report: Use of heat pumps, thousands, by type of building, 2010-." (2025), [Online]. Available: https://pxexternal.energimyndigheten.se/pxweb/en/Energimyndighetens_statistikdatabas/Energimyndighetens_statistikdatabas___Officiell_energistatistik___Bostader_och_lokaler___Fritidshus/ (visited on 02/18/2025).

[10] T. Walfridson, M. Lindahl, N. Ericsson, *et al.*, "Large scale demand response of heat pumps to support the national power system," in *Proceedings of the 14$^{th}$ IEA Heat Pump Conference*, Chicago, Illinois, USA, 2023.

[11] F. Plaum, A. Rosin, and R. AhmadiAhangar, "Novel quantification method of aggregated energy flexibility based on power-duration curves," *IEEE Access*, vol. 12, pp. 132 825–132 837, 2024.

[12] K. McKenna and A. Keane, "Residential Load Modeling of Price-Based Demand Response for Network Impact Studies," *IEEE Transactions on Smart Grid*, vol. 7, no. 5, pp. 2285–2294, 2016.

[13] Evert Agneholm, "Cold load pick-up," in *PhD dissertation, Chalmers University of Technology, Sweden*, 1999.

[14] E. Vrettos and G. Andersson, "Scheduling and provision of secondary frequency reserves by aggregations of commercial buildings," *IEEE Transactions on Sustainable Energy*, vol. 7, no. 2, pp. 850–864, 2016.

[15] H. Gong, T. Rooney, O. M. Akeyo, B. T. Branecky, and D. M. Ionel, "Equivalent electric and heat-pump water heater models for aggregated community-level demand response virtual power plant controls," *IEEE Access*, vol. 9, pp. 141 233–141 244, 2021.

[16] T. B. H. Rasmussen, Q. Wu, J. G. Møller, and M. Zhang, "MPC coordinated primary frequency support of small- and large-scale heat pumps," *IEEE Transactions on Smart Grid*, vol. 13, no. 3, pp. 2000–2010, 2022.

[17] M. T. Muhssin, L. M. Cipcigan, N. Jenkins, S. Slater, M. Cheng, and Z. A. Obaid, "Dynamic frequency response from controlled domestic heat pumps," *IEEE Transactions on Power Systems*, vol. 33, no. 5, pp. 4948–4957, 2018.

[18] L. Zhang, N. Good, and P. Mancarella, "Building-to-grid flexibility: Modelling and assessment metrics for residential demand response from heat pump aggregations," *Applied Energy*, vol. 233-234, pp. 709–723, 2019, ISSN: 0306-2619.

[19] J. Hong, N. J. Kelly, I. Richardson, and M. Thomson, "Assessing heat pumps as flexible load," *Proceedings of the Institution of Mechanical Engineers, Part A: Journal of Power and Energy*, vol. 227, no. 1, pp. 30–42, 2013.

[20] G. Papaefthymiou, B. Hasche, and C. Nabe, "Potential of heat pumps for demand side management and wind power integration in the German electricity market," *IEEE Transactions on Sustainable Energy*, vol. 3, no. 4, pp. 636–642, 2012.

[21] J. Gasser, H. Cai, S. Karagiannopoulos, P. Heer, and G. Hug, "Predictive energy management of residential buildings while self-reporting flexibility envelope," *Applied Energy*, vol. 288, p. 116 653, 2021, ISSN: 0306-2619.

[22] D. Fischer, T. Wolf, J. Wapler, R. Hollinger, and H. Madani, "Model-based flexibility assessment of a residential heat pump pool," *Energy*, vol. 118, pp. 853–864, 2017, ISSN: 0360-5442.

[23] D. Papadaskalopoulos, G. Strbac, P. Mancarella, M. Aunedi, and V. Stanojevic, "Decentralized participation of flexible demand in electricity markets—part ii: Application with electric vehicles and heat pump systems," *IEEE Transactions on Power Systems*, vol. 28, no. 4, pp. 3667–3674, 2013.

[24] I. Diaz de Cerio Mendaza, I. G. Szczesny, J. R. Pillai, and B. Bak-Jensen, "Demand response control in low voltage grids for technical and commercial aggregation services," *IEEE Transactions on Smart Grid*, vol. 7, no. 6, pp. 2771–2780, 2016.

[25] W. Mendieta and C. A. Cañizares, "Primary frequency control in isolated microgrids using thermostatically controllable loads," *IEEE Transactions on Smart Grid*, vol. 12, no. 1, pp. 93–105, 2021.

[26] B. Baeten, F. Rogiers, and L. Helsen, "Reduction of heat pump induced peak electricity use and required generation capacity through thermal energy storage and demand response," *Applied Energy*, vol. 195, pp. 184–195, 2017, ISSN: 0306-2619.

[27] J. Vivian, E. Prataviera, F. Cunsolo, and M. Pau, "Demand side management of a pool of air source heat pumps for space heating and domestic hot water production in a residential district," *Energy Conversion and Management*, vol. 225, p. 113 457, 2020, ISSN: 0196-8904.

[28] T. Péan, R. Costa-Castelló, E. Fuentes, and J. Salom, "Experimental testing of variable speed heat pump control strategies for enhancing energy flexibility in buildings," *IEEE Access*, vol. 7, pp. 37 071–37 087, 2019.

[29] Y.-J. Kim, E. Fuentes, and L. K. Norford, "Experimental study of grid frequency regulation ancillary service of a variable speed heat pump," *IEEE Transactions on Power Systems*, vol. 31, no. 4, pp. 3090–3099, 2016.

[30] Y.-J. Kim, L. K. Norford, and J. L. Kirtley, "Modeling and analysis of a variable speed heat pump for frequency regulation through direct load control," *IEEE Transactions on Power Systems*, vol. 30, no. 1, pp. 397–408, 2015.

[31] Copeland$^{\mathrm{TM}}$, "Emerson Climate Technologies," in *Copeland$^{TM}$ Scroll Variable speed compressors for residential air conditioning applications*, (Accessed on 04/03/2022), Emerson Electric Co., 2020.

[32] T. Clarke, T. Slay, C. Eustis, and R. B. Bass, "Aggregation of residential water heaters for peak shifting and frequency response services," *IEEE Open Access Journal of Power and Energy*, vol. 7, pp. 22–30, 2020.

[33] M. A. Z. Alvarez, K. Agbossou, A. Cardenas, S. Kelouwani, and L. Boulon, "Demand response strategy applied to residential electric water heaters using dynamic programming and k-means clustering," *IEEE Transactions on Sustainable Energy*, vol. 11, no. 1, pp. 524–533, 2020.

[34] A. A. Farooq, A. Afram, N. Schulz, and F. Janabi-Sharifi, "Grey-box modeling of a low pressure electric boiler for domestic hot water system," *Applied Thermal Engineering*, vol. 84, pp. 257–267, 2015, ISSN: 1359-4311.

[35] R. Johnson, M. Royapoor, and M. Mayfield, "A multi-zone, fast solving, rapidly reconfigurable building and electrified heating system model for generation of control dependent heat pump power demand profiles," *Applied Energy*, vol. 304, p. 117 663, 2021, ISSN: 0306-2619.

[36] M. Khatibi, S. Rahnama, P. Vogler-Finck, J. Dimon Bendtsen, and A. Afshari, "Towards designing an aggregator to activate the energy flexibility of multi-zone buildings using a hierarchical model-based scheme," *Applied Energy*, vol. 333, p. 120 562, 2023, ISSN: 0306-2619.

[37] H. Golmohamadi, K. Guldstrand Larsen, P. Gjøl Jensen, and I. Riaz Hasrat, "Optimization of power-to-heat flexibility for residential buildings in response to day-ahead electricity price," *Energy and Buildings*, vol. 232, p. 110 665, 2021, ISSN: 0378-7788.

[38] H. Golmohamadi, K. G. Larsen, P. G. Jensen, and I. R. Hasrat, "Hierarchical flexibility potentials of residential buildings with responsive heat pumps: A case study of Denmark," *Journal of Building Engineering*, vol. 41, p. 102 425, 2021, ISSN: 2352-7102.

[39] J. Clauß, S. Stinner, I. Sartori, and L. Georges, "Predictive rule-based control to activate the energy flexibility of Norwegian residential buildings: Case of an air-source heat pump and direct electric heating," *Applied Energy*, vol. 237, pp. 500–518, 2019, ISSN: 0306-2619.

[40] A. Saleem and C. E. Ugalde-Loo, "Thermal performance analysis of a heat pump-based energy system to meet heating and cooling demand of residential buildings," *Applied Energy*, vol. 383, p. 125 306, 2025, ISSN: 0306-2619.

[41] P. Hua, H. Wang, Z. Xie, and R. Lahdelma, "Integrated demand response method for heating multiple rooms based on fuzzy logic considering dynamic price," *Energy*, vol. 307, p. 132 577, 2024, ISSN: 0360-5442.

[42] E. Biyik and A. Kahraman, "A predictive control strategy for optimal management of peak load, thermal comfort, energy storage and renewables in multi-zone buildings," *Journal of Building Engineering*, vol. 25, p. 100 826, 2019, ISSN: 2352-7102.

[43] F. Langner, M. Frahm, W. Wang, J. Matthes, and V. Hagenmeyer, "Hierarchical-stochastic model predictive control for a grid-interactive multi-zone residential building with distributed energy resources," *Journal of Building Engineering*, vol. 89, p. 109 401, 2024, ISSN: 2352-7102.

[44] M. Frahm, T. Dengiz, P. Zwickel, H. Maaß, J. Matthes, and V. Hagenmeyer, "Occupant-oriented demand response with multi-zone thermal building control," *Applied Energy*, vol. 347, p. 121 454, 2023, ISSN: 0306-2619.

[45] P. Verdugo, C. Cañizares, and M. Pirnia, "Modeling and energy management of hangar thermo-electrical microgrid for electric plane charging considering multiple zones and resources," *Applied Energy*, vol. 379, p. 124 951, 2025, ISSN: 0306-2619.

[46] K. P. Schneider, E. Sortomme, S. S. Venkata, M. T. Miller, and L. Ponder, "Evaluating the magnitude and duration of cold load pick-up on residential distribution using multi-state load models," *IEEE Transactions on Power Systems*, vol. 31, no. 5, pp. 3765–3774, 2016.

[47] F. Bu, K. Dehghanpour, Z. Wang, and Y. Yuan, "A data-driven framework for assessing cold load pick-up demand in service restoration," *IEEE Transactions on Power Systems*, vol. 34, no. 6, pp. 4739–4750, 2019.

[48] W. W. Lang, M. D. Anderson, and D. R. Fannin, "An analytical method for quantifying the electrical space heating component of a cold load pick up," *IEEE Transactions on Power Apparatus and Systems*, vol. PAS-101, no. 4, pp. 924–932, 1982.

[49] R. Benato, S. Dambone Sessa, G. M. Giannuzzi, C. Pisani, M. Poli, and F. Sanniti, "A novel dynamic load modeling for power systems restoration: An experimental validation on active distribution networks," *IEEE Access*, vol. 10, pp. 89 861–89 875, 2022.

[50] R. Mortensen and K. Haggerty, "Dynamics of heating and cooling loads: Models, simulation, and actual utility data," *IEEE Transactions on Power Systems*, vol. 5, no. 1, pp. 243–249, 1990.

[51] M. Song, R. R. nejad, and W. Sun, "Robust distribution system load restoration with time-dependent cold load pickup," *IEEE Transactions on Power Systems*, vol. 36, no. 4, pp. 3204–3215, 2021.

[52] C. Ucak and A. Pahwa, "An analytical approach for step-by-step restoration of distribution systems following extended outages," *IEEE Transactions on Power Delivery*, vol. 9, no. 3, pp. 1717–1723, 1994.

[53] A. Al-Nujaimi, M. A. Abido, and M. Al-Muhaini, "Distribution power system reliability assessment considering cold load pickup events," *IEEE Transactions on Power Systems*, vol. 33, no. 4, pp. 4197–4206, 2018.

[54] Y. L. Li, W. Sun, W. Yin, S. Lei, and Y. Hou, "Restoration strategy for active distribution systems considering endogenous uncertainty in cold load pickup," *IEEE Transactions on Smart Grid*, vol. 13, no. 4, pp. 2690–2702, 2022.

[55] Y. Wang, X. Su, M. Song, W. Jiang, M. Shahidehpour, and Q. Xu, "Sequential load restoration with soft open points and time-dependent cold load pickup for resilient distribution systems," *IEEE Transactions on Smart Grid*, vol. 14, no. 5, pp. 3427–3438, 2023.

[56] M. Wang, Z. Fan, J. Zhou, and S. Shi, "Research on urban load rapid recovery strategy based on improved weighted power flow entropy," *IEEE Access*, vol. 9, pp. 10 634–10 644, 2021.

[57] M. Menazzi, C. Qin, and A. K. Srivastava, "Enabling resiliency through outage management and data-driven real-time aggregated ders," *IEEE Transactions on Industry Applications*, vol. 59, no. 5, pp. 5728–5738, 2023.

[58] C. Qin, L. Jia, S. Bajagain, S. Pannala, A. K. Srivastava, and A. Dubey, "An integrated situational awareness tool for resilience-driven restoration with sustainable energy resources," *IEEE Transactions on Sustainable Energy*, vol. 14, no. 2, pp. 1099–1111, 2023.

[59] Ohio University. "P-h diagram for R134a refrigerant." (2022), [Online]. Available: https://www.ohio.edu/mechanical/thermo/property_tables/R134a/ph_r134a.html (visited on 02/25/2022).

[60] N. Kocyigit, H. Bulgurcu, and C.-X. Lin, "Fault diagnosis of a vapor compression refrigeration system with hermetic reciprocating compressor based on p-h diagram," *International Journal of Refrigeration*, vol. 45, pp. 44–54, 2014, ISSN: 0140-7007.

[61] Emerson Climate Technologies, "Economized Vapor Injection (EVI) for ZF*KVE and ZF*K5E Compressors," in *Application Engineering Bulletin*, Emerson Climate Technologies, 2019, pp. 1–29.

[62] N. Park, J. Y. Shin, and B. Y. Chung, "A new dynamic heat pump simulation model with variable speed compressors under frosting conditions," in *8th International Conference on Compressors and their Systems*, ScienceDirect, 2013, pp. 681–696.

[63] Emerson Climate Technologies. "Scroll compressors with vapour injection for dedicated heat pumps." (2004), [Online]. Available: http://www.sklep-klimatyzacja.pl/dokumentacje/COPELAND_dok_2006/EN_C060217_AGL_ZHEVI.pdf (visited on 02/25/2022).

[64] T. W. Moesch, A. M. Bahman, and E. A. Groll, "Performance Testing of a Vapor Injection Scroll Compressor with R407C," in *International Compressor Engineering Conference*, Purdue University, 2016, pp. 1–10.

[65] Swedish Energy agency. "Exhaust and supply air ventilation with heat recovery." (2023), [Online]. Available: https://www.energimyndigheten.se/en/sustainability/households/other-energy-consumption-in-your-home/ventilation/exhaust-and-supply-air-ventilation-with-heat-recovery-ftx-system/ (visited on 11/10/2023).

[66] Purmo. "Technical catalogue, panel radiators." (2022), [Online]. Available: https://www.purmo.com/docs/Purmo-technical-catalogue-full-panel-radiators-10_2021_EN.pdf (visited on 05/01/2022).

[67] EnergyPlus: Energy Simulation Program. "Water thermal tanks." (Accessed on 15/08/2022). (2022), [Online]. Available: https://bigladdersoftware.com/epx/docs/8-1/engineering-reference/page-106.html (visited on 08/15/2022).

[68] Energy Stats UK. "Vaillant arotherm weather curve information." (2025), [Online]. Available: https://energy-stats.uk/vaillant-arotherm-weather-curve-information/ (visited on 05/01/2025).

[69] M. Maivel and J. Kurnitski, "Heating system return temperature effect on heat pump performance," *Energy and Buildings*, vol. 94, pp. 71–79, 2015.

[70] Daikin. "Daikin altherma 3 geo, installer reference guide." (2025), [Online]. Available: https://www.daikin.eu/content/dam/document-library/Installer-reference-guide/heat/ground-to-water-heat-pump/EGSAH-D9W.EGSAX-D9W%28G%29_Installer%20reference%20guide_4PEN569820-1E_English.pdf (visited on 11/18/2025).

[71] NIBE. "Sustainable heat pumps for all homes." (2025), [Online]. Available: https://www.nibe.eu/en-eu/products/heat-pumps (visited on 05/01/2025).

[72] SCB statistics Sweden. "Households by housing type and region, 31 december 2021." (2023), [Online]. Available: https://www.scb.se/en/finding-statistics/statistics-by-subject-area/household-finances/income-and-income-distribution/households-housing/ (visited on 08/19/2023).

[73] IEEE, Power System Dynamic Performance Committee. "Test systems for voltage stability analysis and security assessment." (PSS/E model, Accessed on 14/08/2023). (2015), (visited on 08/14/2023).

[74] T. Van Cutsem, M. Glavic, W. Rosehart, *et al.*, "Test systems for voltage stability studies," *IEEE Transactions on Power Systems*, vol. 35, no. 5, pp. 4078–4087, 2020.

[75] L. Saarinen, "A hydropower perspective on flexibility demand and grid frequency control," in *Uppsala universitet, Uppsala*, 2001.

[76] Pouyan Pourbeik. "Proposal for new features for the renewable energy system generic models." (2023), [Online]. Available: https://www.wecc.org/Administrative/Memo_RES_Modeling_Updates_010523_Rev25_Clean.pdf (visited on 10/10/2023).

[77] C. Haglund Stignor and T. Walfridson, "Nordsyn study on air-to-water heat pumps in humid nordic climate," in *Nordic Council of Ministers*, 2019.

[78] Emerson climate technologies. "Copeland scroll heating, heat pump optimized scroll technology." (2023), (visited on 08/15/2023).

[79] T. W. Moesch, A. M. Bahman, and E. A. Groll, "Performance testing of a vapor injection scroll compressor with R407c," in *International Compressor Engineering Conference*, Purdue University, 2016.

[80] E. K. Shungarov and S. A. Garanov, "Comparison of the characteristics of low-temperature scroll compressors for heat pump applications," *Chemical and Petroleum Engineering*, vol. 56, no. 5–6, pp. 378–384, 2020.

[81] S. Jain and C. W. Bullard, "Capacity and efficiency in variable speed, vapor injection and multi-compressor systems," Air Conditioning and Refrigeration Center, College of Engineering, University of Illinois at Urbana-Champaign, Tech. Rep. TR-227, May 2004.

[82] Engineering ToolBox, *Average overall heat transmission coefficients for fluid and surface combinations like water to air, water to water, air to air, steam to water and more*, Accessed: 2022-06-31, 2022.

[83] S. K. Nalini Ramakrishna and T. Thiringer, "Domestic hot water heat pump: Modelling, analysis and flexibility assessment," in *2023 IEEE PES 15th Asia-Pacific Power and Energy Engineering Conference*, 2023, pp. 1–5.

[84] M. Lundh, E. Wäckelgård, and K. Ellegård, "Design of hot water user profiles for swedish conditions," in *Proceedings of ISES World Congress 2007 (Vol. I – Vol. V)*, D. Y. Goswami and Y. Zhao, Eds., Berlin, Heidelberg: Springer Berlin Heidelberg, 2009, pp. 2074–2078, ISBN: 978-3-540-75997-3.

[85] Statistics Sweden, SCB. "Most children live in one- or two-dwelling buildings." (Accessed on 20/12/2023). (2023), (visited on 12/20/2023).

[86] Boverket. "Energi i bebyggelsen – tekniska egenskaper och beräkningar– resultat från projektet BETSI." (2010), [Online]. Available: https://www.boverket.se/sv/om-boverket/publicerat-av-boverket/publikationer/2011/energi-i-bebyggelsen---tekniska-egenskaper-och-berakningar/ (visited on 08/19/2022).

[87] Statistics Sweden, SCB. "Just over 4.9 million dwellings in Sweden." (2023), (visited on 12/20/2023).

[88] N. Blom, *Folkhälsomyndighetens allmänna råd om temperatur inomhus*, 2014.

[89] A. Hesaraki, E. Bourdakis, A. Ploskic, and S. Holmberg, "Experimental study of energy performance in low-temperature hydronic heating systems," *Energy and Buildings*, vol. 109, pp. 108–114, 2015, ISSN: 0378-7788.

[90] PURMO. "Heat output calculator." (2024), [Online]. Available: https://global.purmo.com/en/tools-and-services/item-selector (visited on 07/08/2024).

[91] J. Hedbrant, "On the thermal inertia and time constant of single-family houses," in *Licentiate dissertation, Linköpings universitet, Linköping, 2001*, 2001.

[92] A. Vadiee, A. Dodoo, and E. Jalilzadehazhari, "Heat supply comparison in a single-family house with radiator and floor heating systems," *Buildings*, vol. 10, no. 1, 2020, ISSN: 2075-5309.

[93] R. Kuniyoshi, M. Kramer, and M. Lindauer, "Validation of rc building models for applications in energy and demand side management," in *Proceedings of eSim 2018*, IBPSA Canada, 2018, 1–2-B-4.

[94] H. Johra and P. Heiselberg, "Influence of internal thermal mass on the indoor thermal dynamics and integration of phase change materials in furniture for building energy storage: A review," *Renewable and Sustainable Energy Reviews*, vol. 69, pp. 19–32, 2017, ISSN: 1364-0321.

[95] T. Hong and S. H. Lee, "Integrating physics-based models with sensor data: An inverse modeling approach," *Building and Environment*, vol. 154, pp. 23–31, 2019, ISSN: 0360-1323.

[96] Infineon. "Advanced semiconductor solutions for a hot future in heat pumps." (2022), [Online]. Available: https://www.digikey.my/en/pdf/i/infineon-technologies/advanced-semiconductor-solutions-for-a-hot-future-in-heat-pumps (visited on 05/15/2024).

[97] E. Mata and A. S. Kalagasidis, "Calculation of energy use in the swedish housing," *Chalmers Univeristy of Technology, Gothenburg, Sweden*, vol. 2009, p. 4, 2009.

[98] S. K. Nalini Ramakrishna, H. Björner Brauer, T. Thiringer, and M. Håkansson, "Social and technical potential of single family houses in increasing the resilience of the power grid during severe disturbances," *Energy Conversion and Management*, vol. 321, p. 119 077, 2024, ISSN: 0196-8904.

[99] S. F. Fux, A. Ashouri, M. J. Benz, and L. Guzzella, "EKF based self-adaptive thermal model for a passive house," *Energy and Buildings*, vol. 68, pp. 811–817, 2014, ISSN: 0378-7788.

[100] F. Amara, K. Agbossou, A. Cardenas, Y. Dubé, S. Kelouwani, *et al.*, "Comparison and simulation of building thermal models for effective energy management," *Smart Grid and renewable energy*, vol. 6, no. 04, p. 95, 2015.

[101] I. H. Bell, J. Wronski, S. Quoilin, and V. Lemort, "Pure and pseudo-pure fluid thermophysical property evaluation and the open-source thermophysical property library coolprop," *Industrial & Engineering Chemistry Research*, vol. 53, no. 6, pp. 2498–2508, 2014.

[102] BASH, CLI TOOLS AND CHEAT-SHEETS. "Heating curve." (2024), [Online]. Available: https://www.bashpi.org/?page_id=225 (visited on 05/15/2024).

[103] Z. You, M. Zade, B. Kumaran Nalini, and P. Tzscheutschler, "Flexibility estimation of residential heat pumps under heat demand uncertainty," *Energies*, vol. 14, no. 18, p. 5709, 2021.

[104] Swedish Energy Agency", "Energy in Sweden- An overview," *Energimyndigheten*, 2021.

[105] Svenska kraftnät, *Overview of the requirements for reserves*, 2022.